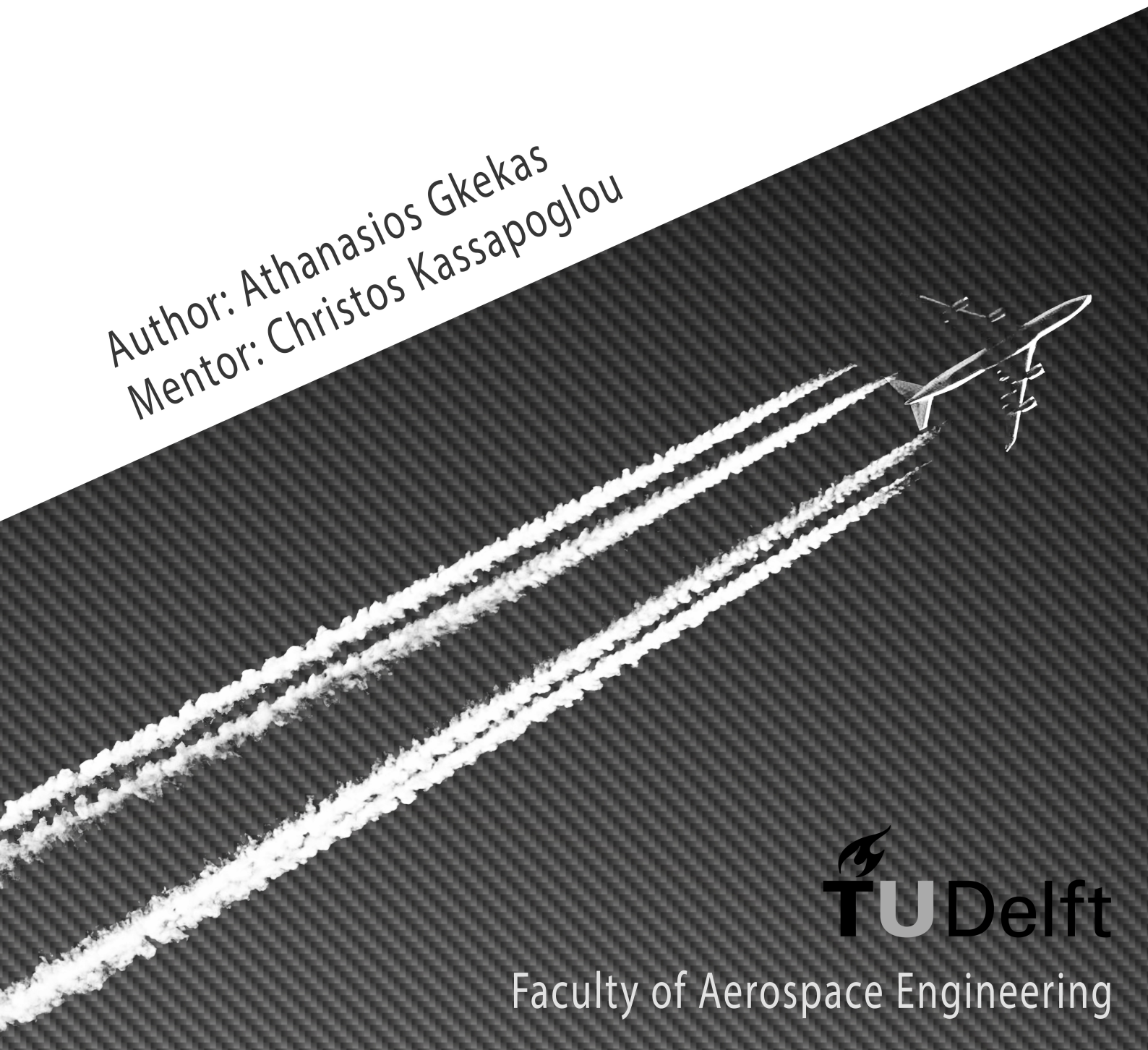


Development of a preliminary sizing tool, for strategic decision making in composite fuselages, using weight and cost optimization

Author: Athanasios Gkekas
Mentor: Christos Kassapoglou



**TU Delft**

Faculty of Aerospace Engineering

Development of a preliminary sizing tool for strategic decision making in composite fuselages using weight and cost optimization

by

Athanasios Gkekas

to obtain the Master of Science (MSc) degree
at the TU Delft University of Technology.

Student number: 5157978

Project duration:

November 15, 2020 – August 27, 2021

Thesis committee:

Prof. Dr. C. Kassapoglou, TU Delft, supervisor, chair

M. Schuurman, TU Delft

Dr. ir. D. Peeters, TU Delft

J. Waleson, GKN Fokker

An electronic version of this thesis is available at <http://repository.tudelft.nl/>.



Abstract

This study is an attempt to develop a preliminary composite fuselage sizing tool for the decision making process utilizing analytical structural analysis equations and a bottom-up cost approach to estimate weight and cost. Previous research by several authors and companies is reviewed in order to define the knowledge gaps that the project is going to fill. The objectives of this project are divided into two directions. The first one is the weight and cost fuselage design, and the second, is the weight and cost optimization process. After examining the existing literature both from academia and industry a different approach is proposed for each sector. In the structural design an analytical based model is proposed to assess the components integrity while cost equations for fully learned manufacturing processes are used based on the Advanced Composites Cost Estimation Manual (ACCCEM). An experience-driven optimization algorithm is proposed afterwards, taking into account manufacturing considerations and design rules of thumb. By combining these tools, a general tool for fuselage design that is completely suited for the preliminary design phase is proposed. The trade-off studies can provide important knowledge on the effect of different decisions and establish new design guidelines. The study concludes that an increase of the number of stiffeners and frames, in a fuselage structure, leads to a general decrease in weight and an increase in manufacturing cost. The addition of more stringers or frames after a certain level leads to an increase in weight, while the cost follows the same trend. The manufacturing constraints and the design rules-of-thumb applied lead to an increase in structural weight. Finally, the comparison between skin-stiffened and sandwich designs, shows that the weight saving potential is comparable for both configurations, and the cost saving potential is higher for the sandwich design.

Keywords: Trade-offs · Aircraft design · Composite fuselage design · Mass/weight estimation · Manufacturing Cost · Buckling · Skin buckling · Stiffener buckling · Composite structures

Acknowledgements

I will start my acknowledgments with a poem from K. Kavafis (1963), Ithaca.

"As you set out for Ithaca hope the voyage is a long one, full of adventure, full of discovery. Laistrygonians and Cyclops, angry Poseidon—don't be afraid of them: you'll never find things like that on your way as long as you keep your thoughts raised high, as long as a rare excitement stirs your spirit and your body. Laistrygonians and Cyclops, wild Poseidon—you won't encounter them unless you bring them along inside your soul, unless your soul sets them up in front of you.

Hope the voyage is a long one. May there be many a summer morning when, with what pleasure, what joy, you come into harbors seen for the first time; may you stop at Phoenician trading stations to buy fine things, mother of pearl and coral, amber and ebony, sensual perfume of every kind— as many sensual perfumes as you can; and may you visit many Egyptian cities to gather stores of knowledge from their scholars.

Keep Ithaca always in your mind. Arriving there is what you are destined for. But do not hurry the journey at all. Better if it lasts for years, so you are old by the time you reach the island, wealthy with all you have gained on the way, not expecting Ithaca to make you rich.

Ithaca gave you the marvelous journey. Without her you would not have set out. She has nothing left to give you now.

And if you find her poor, Ithaca won't have fooled you. Wise as you will have become, so full of experience, you will have understood by then what these Ithaca's mean.
"

By doing so, I would like to emphasize on the importance of this journey and the experiences it provided me with. Amid a global pandemic, and doing a master's was a difficult task. A chance to challenge yourself and test your limits, to find the motivation that made you start this journey without being in touch with family, friends, fellow students and professors. These people, are the ones I would like to thank for this experience. Their support and knowledge was crucial for carrying out this thesis.

First of all, I would like to thank my thesis supervisor, Christos Kassapoglou for the amazing collaboration during this thesis, his support and guidance, academic and professional experience. I gained a lot as an aerospace engineer working with him and I feel glad that I collaborated with him.

I would like to thank the members of the committee, Danil Peeters and Michiel Schuurman, for reviewing my thesis report and providing feedback about my work. I would also like to thank Andries Buitenhuis and Jan Waleson from GKN Fokker, for their interest in my work and the data they provided me with.

This master's degree would not have been possible without the support of my parents and family. To them I owe my gratitude, for helping me achieve my dreams.

Last but not least, i would like to thank my friends, old ones and new ones, from TU Delft, for the amazing experiences together. You will always be a part of life.

Finally, I would like to thank my partner, for supporting me throughout this thesis project and making me focus on my goal. It was a strange year, we made it beautiful.

Contents

| | |
|----------------------------------------------------------|-----|
| List of Figures | v |
| List of Tables | vii |
| Nomenclature | vii |
| 1 Introduction | 1 |
| 2 Literature Review | 3 |
| 2.1 Fuselage design, weight and cost analysis | 3 |
| 2.1.1 Knowledge gap | 5 |
| 2.2 Research Question, Objectives and Sub-goals | 6 |
| 2.2.1 Research Questions | 6 |
| 2.2.2 Research Objective | 6 |
| 3 Theoretical Content | 7 |
| 3.1 Geometry definition | 7 |
| 3.1.1 Structural idealization | 9 |
| 3.2 Material and layup definition | 11 |
| 3.3 Loading conditions | 11 |
| 3.3.1 Internal loads definition | 12 |
| 3.3.1.1 Bending | 12 |
| 3.3.1.2 Shear | 15 |
| 3.3.1.3 Torsion | 16 |
| 3.3.1.4 Pressure | 17 |
| 3.4 Margins of safety calculation | 17 |
| 3.4.1 Material strength | 18 |
| 3.4.1.1 Maximum stress | 18 |
| 3.4.1.2 Tsai-Hill | 18 |
| 3.4.1.3 Tsai-Wu | 18 |
| 3.4.2 Buckling | 19 |
| 3.4.2.1 Skin-stiffened structure | 19 |
| 3.4.2.2 Sandwich structure | 23 |
| 3.4.3 Interlaminar shear stress (ILSS) | 26 |
| 3.5 Flat/Curved Plates comparison | 27 |
| 3.6 Weight estimation | 28 |
| 3.6.1 Frames weight estimation method | 28 |
| 3.7 Cost estimation | 29 |
| 3.7.1 Advanced Composites Cost Estimation Manual (ACCEM) | 31 |
| 3.7.1.1 Skin Operations | 31 |
| 3.7.1.2 Stringer Operations | 32 |
| 3.7.1.3 Core Operations | 33 |
| 3.7.1.4 Curing Operations | 34 |
| 3.7.1.5 Post-processing Operations | 36 |

| | | |
|--------|---------------------------------------------------------------------------|----|
| 3.7.2 | Cost estimation limitations and suggestions | 37 |
| 3.7.3 | Aluminium design cost estimation | 37 |
| 3.8 | Trade off studies | 38 |
| 3.9 | Weight and Cost optimization. | 38 |
| 3.9.1 | Composite design rules of thumb | 39 |
| 3.10 | Programming language. | 39 |
| 4 | Software Description | 40 |
| 4.1 | Software Overview | 40 |
| 4.1.1 | Input files. | 41 |
| 4.1.2 | Output | 43 |
| 4.2 | Data flow and functions introduction | 45 |
| 4.3 | Key Functions | 47 |
| 4.3.1 | Fuselage geometry creation | 47 |
| 4.3.2 | Laminate properties calculation | 49 |
| 4.3.3 | Calculation of equivalent panel stiffness | 50 |
| 4.3.4 | Structural idealization | 50 |
| 4.3.5 | Load definition and distribution | 50 |
| 4.3.6 | Stress calculation | 53 |
| 4.3.7 | Failure strength calculation | 53 |
| 4.3.8 | Buckling/Crimping/Wrinkling strength calculation | 54 |
| 4.3.9 | ILSS strength calculation | 54 |
| 4.3.10 | Weight calculation | 54 |
| 4.3.11 | Cost calculation | 54 |
| 4.3.12 | Optimization. | 55 |
| 4.3.13 | Post-Processing | 57 |
| 5 | Trade off studies | 61 |
| 5.1 | Skin-Stiffened configuration-Composite | 61 |
| 5.1.1 | Investigation of the effect of stringer number | 61 |
| 5.2 | Skin-Stiffened configuration-Aluminium | 64 |
| 5.2.1 | Investigation of the effect of stringer number | 64 |
| 5.3 | Sandwich configuration-Composite | 64 |
| 5.4 | Comparison of different configurations. | 65 |
| 5.5 | Influence of the application of different lamination methods. | 65 |
| 5.6 | Investigation of the effect of frame number | 66 |
| 5.7 | Influence of the application of composite design rules-of-thumb | 67 |
| 5.8 | Case Study: Reference aircraft fuselage station | 71 |
| 5.9 | Run time analysis | 73 |
| 6 | Conclusions and Future Research Recommendations | 75 |
| 6.1 | Conclusions | 75 |
| 6.2 | Future Research Recommendations | 77 |

List of Figures

| | | |
|------|--------------------------------------------------------------------------------------------------------|----|
| 1.1 | Structural Concept of all-composite fuselage (Honda R& D technical review, 2004) | 1 |
| 3.1 | a) fuselage station design, b) example of stiffener dimensioning asked by the user | 7 |
| 3.2 | Stiffener types supported | 8 |
| 3.3 | Fuselage geometry definition | 8 |
| 3.4 | Panel geometry definition | 9 |
| 3.5 | Panel idealization(Megson,2007) | 9 |
| 3.6 | Fuselage idealized cross section | 10 |
| 3.7 | Layup definition according to CLT | 11 |
| 3.8 | Applied bending load on fuselage(Megson,2013) | 12 |
| 3.9 | Force distribution on fuselage cross section for bending (I. Sen, 2010) | 13 |
| 3.10 | Force distribution on panel's members (I. Sen, 2010) | 14 |
| 3.11 | Stringer cross-sectional characteristics (C. Kassapoglou, 2010) | 14 |
| 3.12 | Shear flow on fuselage's cross-section (I. Sen, 2010) | 16 |
| 3.13 | Hoop stress | 17 |
| 3.14 | Longitudinal stress | 17 |
| 3.15 | Failure modes of a skin-stiffened panel (Kassapoglou,2009) | 19 |
| 3.16 | Representative structure | 20 |
| 3.17 | Crippling of stiffener (Kassapoglou,2009) | 22 |
| 3.18 | OEF and NEF crippling of stiffener (Kassapoglou,2009) | 22 |
| 3.19 | Sandwich configuration (Kassapoglou,2009) | 23 |
| 3.20 | Honeycomb core deformations (Kassapoglou,2009) | 24 |
| 3.21 | Wrinkling failure modes: a), b) Symmetric, c) Anti-symmetric (Kassapoglou,2009) | 24 |
| 3.22 | Interaction curves for wrinkling under combination of loads (Kassapoglou,2009) | 25 |
| 3.23 | Sandwich crimping (Kassapoglou,2009) | 25 |
| 3.24 | Buckling coefficient grouped according to R/t values for curved plates ("Stress Analysis Manual" 1986) | 27 |
| 3.25 | Panel description including frames | 28 |
| 3.26 | Manufacturing Cost flowchart | 30 |
| 4.1 | Process flowchart for the approach presented | 41 |
| 4.2 | Code part of the (Input_def.m) file | 43 |
| 4.3 | Matlab command window output example | 45 |
| 4.4 | Fuselage geometry | 47 |
| 4.5 | Omega stringer geometry | 49 |
| 4.6 | Fuselage Upbending(GKN Fokker) | 51 |
| 4.7 | Fuselage Vertical Shear (Upbending)(GKN Fokker) | 52 |
| 4.8 | Fuselage Vertical Torsion(GKN Fokker) | 52 |
| 4.9 | Post processing plots for different values | 58 |
| 4.10 | Typical weight progression for the software | 58 |

| | | |
|------|--------------------------------------------------------------------------------------------------------------------|----|
| 4.11 | Maximum and Minimum margins of safety progression | 59 |
| 4.12 | Maximum and Minimum margins of safety progression | 60 |
| 4.13 | Maximum and Minimum margins of safety progression(satisfied) | 60 |
| 5.1 | Weight versus Cost trade study for stringer spacing (T stringer) | 62 |
| 5.2 | Weight versus Cost trade study for stringer spacing (C stringer) | 62 |
| 5.3 | Weight versus Cost trade study for stringer spacing (J stringer) | 63 |
| 5.4 | Weight versus Cost trade study for stringer spacing (aluminium design) | 64 |
| 5.5 | Weight versus Cost trade study for splits spacing (sandwich design) | 65 |
| 5.6 | Weight versus Cost trade study for stringer spacing under different lamination methods | 66 |
| 5.7 | Weight versus Cost trade study for frame spacing (T stringer) | 67 |
| 5.8 | Weight versus Cost trade study for stringer spacing under symmetric constraint (T stringer) | 68 |
| 5.9 | Weight versus Cost trade study for stringer spacing under balanced constraint (T stringer) | 69 |
| 5.10 | Weight versus Cost trade study for stringer spacing under balanced and symmetric constraint (T stringer) | 70 |
| 5.11 | Reference aircraft fuselage station (GKN Fokker) | 71 |
| 5.12 | Reference aircraft fuselage station thickness distribution provided by GKN Fokker | 72 |
| 5.13 | Reference aircraft fuselage station thickness distribution using the software | 73 |
| 5.14 | Run time versus iteration for the batch optimization process | 74 |

List of Tables

- 4.1 Material database structure 42
- 4.2 List of functions and their basic tasks 46
- 4.3 PID and GID matrices 48

- 5.1 Comparison of different configurations 65
- 5.2 Comparison of different design rules-of-thumb with the default software's rules 70

Introduction

In today's rapidly increasing world the aerospace field is always pushing for weight reduction in airframes. Composite materials have entered, grown fast and dominated the market over the past decades due to their strength-to-weight ratio. In the meantime great efforts have taken place in reducing their production cost and manufacturability through higher automation and mass production. Moreover, the continuous increasing trend for UAV's and small size, personal flying vehicles brought up the need for tools to quickly and accurately estimate projects' feasibility in the decision making process. Taking into account that high fidelity tools demand higher computational time, the use of low fidelity tools based on knowledge (KBE) or empirical data is gaining supporters in the early design phase (T. Führer et al.,2015) [25]. The high competitiveness of today's market leads to the need for designs providing overall capability and not only high performance. Thus new quicker tools for assessing the economic viability are needed (M. Lee et al., 2012) [50]. To achieve this, the design phase must focus not only on the structural requirements but incorporate cost estimation tools for different design decisions.

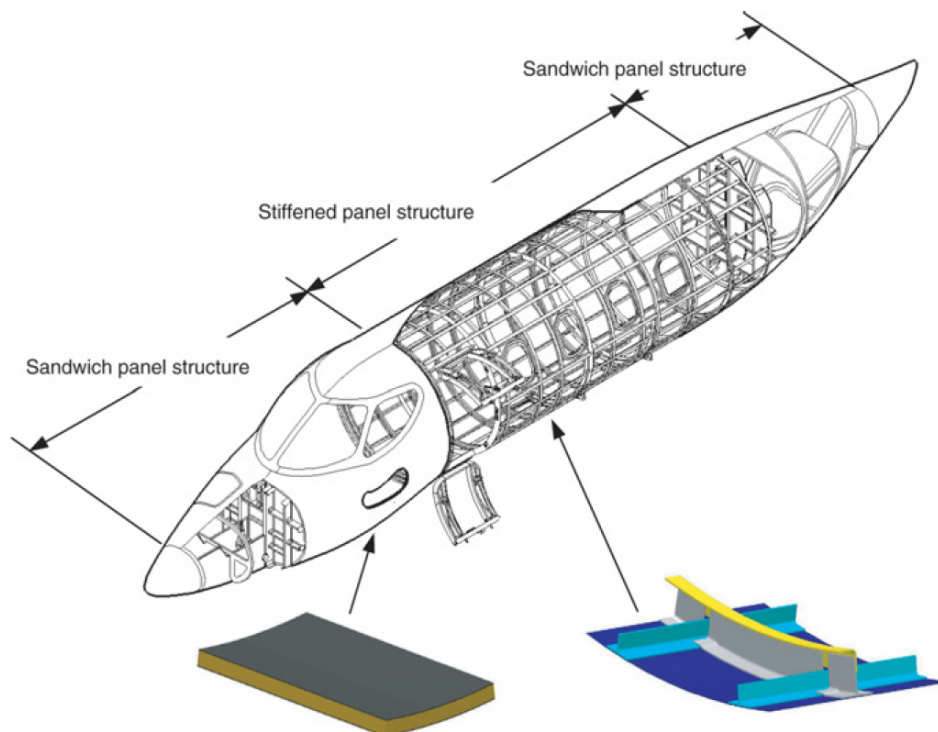


Figure 1.1: Structural Concept of all-composite fuselage (Honda R& D technical review, 2004)

The current study focuses on the development of a preliminary sizing tool for fuselage structural design, using a fully learned process (Advanced Composite Cost Estimating Manual, Northrop Corporation, 1976) [19], to assess the weight and cost of different configurations and layouts. Several trade studies will take place in order to define the effect of different configurations and an optimization will lead to the final preliminary design suggestion. Even though the amount of work and considerations are large it is quite promising, and achieving the proposed goal supports the belief that this type of tools will play a big role in strategic decision making in the years to come.

Literature Review

In this chapter the already existing approaches in relevant research areas are examined. Existing researches will be used in order to identify the methods used in academia and industry for the design of airframe components and specifically fuselages. Moreover, the approaches used in weight-cost estimation and optimization will be identified as well. Taking into account the high complexity of multi objective optimization methods and the large amount of algorithms used, the literature study for this purpose will not be presented in depth because the main target of the project in that field is a design of an optimization method based on knowledge data and driven by general design guidelines.

2.1. Fuselage design, weight and cost analysis

One of the first big attempts to establish tools for the design of fuselages for weight and cost was the Advanced Technology Composite Aircraft Structure (ATCAS) developed by Boeing for NASA's ACT program. The goal of the program was to achieve a 30-50 percent weight reduction and 20-25 percent reduction in cost. The ATCAS approach follows a three step phase. The first step sets a family of similar designs in terms of configurations and manufacturing constraints. The second step is a global evaluation of alternatives in terms of weight and cost and the last step is a local optimization with input design the one chosen from step two. Then several optimization cycles take place to gain the optimum design. Different configurations such as skin-stiffened or sandwich structures are generated during the first stage. A large amount of trade studies is conducted for different configurations resulting in achieving the project's goals in weight and cost reduction. In a study published under the ATCAS program a side panel is analyzed giving comparison charts about skin stiffened and sandwich structures as well as aluminum designs. The sandwich designs show the best performance in cost while having some weight penalties [20]. The ATCAS program utilized COSTADE [55] in order to calculate manufacturing costs of the components. This approach is examining the different parts of the fuselage in a separate way. The final remarks of the ATCAS program are that a combination of weight and cost in the optimization process leads to a more realistic final result. The stringer spacing in combination with minimum stiffness and buckling criteria are factors that mostly drive the cost optimization.

L. Krackers, 2009 [53] uses a Design and Engineering Engine (DEE) in combination with a multidisciplinary optimization (MDO) to make a comparison between skin-stiffened and sandwich structure. He utilizes high fidelity tools and finite element models to examine different configuration trade-offs. Several optimization algorithms are checked during the process. It is strongly advised to avoid singularities in finite element models because of

the errors they introduce. The author states that a genetic optimization tool provides a robust optimization while he notices that a two-step optimization increases accuracy by decreasing the design space. As a final remark, it is stated that an MDO approach does not lead to large improvements in comparison to the traditionally followed methods.

A similar approach was given by M. Lee et al., 2012 [50]. Using finite element models and Hypersizer as a structural optimizer and the software SEER-MFG (by Galorath) for a process-based cost analysis, the study tries to design a composite wing box. It is stated that design for manufacturing shows that not only the weight is a cost driving factor. Additionally, almost 80 percent of costs are defined during the preliminary design stage and for that reason taking into account several cost driving factors is of great significance. A multi objective optimization algorithm is used to optimize both for weight and unit cost. Case studies showed that the rib spacing has a significant impact both on weight and cost. As a final remark, the importance of a range of possible designs is noted in order to account for uncertainties introduced in the analysis due to assumptions in early stages. M. Kaufmann, 2008 [32, 33] proposes a cost/weight optimization taking into account manufacturing cost, non-destructive testing and lifetime fuel consumption. The author concludes that a combination of low-cost and low-weight design is the optimum and neither of them separately. It is also stated, once again, that cost related decisions in the early design stages play an important role in the following steps.

With the goal, to investigate different design decisions, regarding the wing box using lower fidelity tools G. Moors, 2019 [2] provides a big amount of trade-offs. The structural analysis is done through empirical and semi-empirical equations using an automated process. The software provides the possibility for finite element validation as an output. It has to be mentioned that no cost considerations take place in this approach. The structural optimization is based on an algorithm opting to achieve designs with positive margins of safety utilizing a self-written layup generator. The approach is based on weight trades for specific configurations under composite design guidelines. The design shows big divergence from the finite element model due to singularities. Moreover, the effect of different design decisions is depicted in charts and some analytical equations are derived from the trending lines. Another approach by T. Führer et al. [25] focuses on the automated model generation of aircraft structures. In the study published a wing box component is examined. The study utilizes a software called Delis for the generation of structural models of airframe structures. The evaluation of the results is again done through a finite element simulation. The proposed process provides a high flexibility in the decision making phase but again it encloses the high computational penalties of the finite element analysis.

An interesting analysis regarding the types of cost estimation processes is proposed by Ch. Hueber et al., 2016 [41]. In this study three categories of cost estimation methods are presented: analogous, parametric and bottom-up. Their positive and negative aspects are analyzed in depth as well. Furthermore, it provides information about cost estimation methods and software packages such as the ACCEM [19] and COSTADE [55]. It is mentioned that the ACCEM can provide sufficient results and is widely used in the industry. The study also describes a weight and cost optimization methods utilizing finite element analysis models. It is suggested that neither weight nor manufacturing cost should be the optimization's objective function, but the direct operating costs would provide a more realistic estimation.

Additionally, the authors refer to the discrepancies introduced in cost estimation, because of the difficulty to predict uncertain future situations. There are two situations where the problem gets solved easily. Either the part to be designed belongs to a family of products with a lot of cost data available, or the manufacturing route is well-known beforehand so that a bottom-up approach can be followed. It is of great importance that cost feedback is embedded in the conceptual design phase and/or trade off studies take place for different designs and manufacturing variants. The authors conclude that the success of cost estimation depends on two major factors: The possession of historical cost data or a high degree of experience to calculate a bottom-up process.

A combination of a knowledge based algorithm with the use of finite element analysis for the weight estimation is given in the paper of Choi et al., 2007 [16]. Cost estimation is done using ACCEM data and Nastran is used for the structural evaluation. The significance of trade studies in the early design phase is emphasized in the study. The research provides a tool using CAD, FEM and KBEs that can give sufficient results through trade-offs for the preliminary phase of the design. Even though, again the presence of finite elements is significant, there is no complex optimization algorithm and that reduces the time of the analysis. There is no reference to the design of bigger components using this method.

Finally, a significant amount of papers was published by C. Kassapoglou et al. regarding weight and cost optimization of composite structures. In the first two papers in chronological order [11, 12] a single stiffened panel is examined (either frame or standard panel) under a loading combination and checked for overall stability and strength taking into account cost considerations. The studies provide a solution with a multi objective (weight and cost) optimization algorithm where a Pareto set of designs is found. The high complexity of the analysis due to the optimization is noted from the author. Composite designs are once again considered more optimum than metal ones and a need for automation due to their nature is noted. As the author concludes: "Optimization of the fuselage as a whole becomes the goal. There is a need for an efficient, stable, and computationally very low cost (to be useful during all phases of the design) algorithm that can tackle this problem." (C. Kassapoglou, 1999) [11]. In the paper C. Kassapoglou and Dobyns, 2001 [12] a similar approach is followed but with the use of gradient based optimization algorithm for the post-buckling analysis of panels. It is considered to give more accurate results by the authors. Last but not least, P. Apostolopoulos and C. Kassapoglou, 2008 [7] following a similar process conclude that the minimization of cost leads to minimizing the number of stiffeners and the minimization of weight leads to the higher stiffener web height and flange width. Finally, I. Van Gent and Kassapoglou, 2013, [5] follow an approach of dynamic programming for the repetition of designs to be evaluated and use the ACCEM to incorporate a better tool for cost estimation. This method was applied to modular assemblies. Several trade-studies took place regarding weight and cost requirements.

2.1.1. Knowledge gap

Taking into consideration the current state-of-the-art researches in the field it is clear that the vast amount of them uses high fidelity tools that require high computational and set-up times. A minority of them uses low-fidelity tools but no paper is proposing a research for the study of whole fuselages. The gap of knowledge that results from the current analysis

is in the design of whole fuselage structures and the need for computationally efficient algorithms utilizing, knowledge based, cost estimation methods.

2.2. Research Question, Objectives and Sub-goals

2.2.1. Research Questions

According to the literature review many authors have tried to approach the problem of weight and cost optimization of composite parts. Most of them focus on local analysis of single panels (C. Kassapoglou, 1999a; P. Apostolopoulos, C. Kassapoglou, 2008) [7] using high fidelity tools. Attempts to approach the design of a wing box by G. Moors, C. Kassapoglou [2] and T. Führer [25] et al. focus only on the structural design of an assembly without taking into account the cost requirements. Moreover, the industry tends to follow sandwich structure designs providing ease of manufacturing but with significant penalties in weight. It is clear from the aforementioned that there are some small gaps in the body of knowledge regarding the design of a whole fuselage assembly incorporating cost requirements. Summing up all of the above, my main research question is:

Can a low fidelity, knowledge based preliminary sizing tool, provide realistic weight and cost optimization results, for composite fuselage assemblies, enabling the speed up of the decision making process?

2.2.2. Research Objective

Having already stated the research question above the main research objective to be answered is the following:

“To provide a new and quick preliminary sizing tool for the decision making process by developing a software for the design of composite fuselage assemblies utilizing low fidelity structural and cost analytical equations for selected manufacturing processes.”

To achieve this objective several sub-objectives are necessary. They are split into three sections trying to solve the issues of each chapter of the research. To begin with, there is a need to provide quick and accurate predictions. That is one of the biggest challenges this research faces. The use of knowledge based low fidelity tools and targeted optimization is a promising means to achieve that. The feasibility of the plan is yet to be evaluated by this research's outcomes. Secondly, a fuselage assembly model needs to be delivered taking into account a large amount of panels and configurations in the optimization process. To tackle this, automated load distribution changes and manufacturing feasibility constraints will take place to reduce design variables. Moreover, a flexible and user friendly software needs to be developed. The user will have the chance to choose between several configurations and layouts, set-up material and loading conditions' databases and also decide on different manufacturing processes. After that, trade off studies need to take place to assess the effect of different decisions in the design process.

Theoretical Content

In this chapter several theories and methods regarding the fuselage structural design, cost estimation and optimization will be analyzed. These theories and methods include the geometrical design considerations for the fuselage, the loading application, the structural analysis theories for composite materials such as the classical laminate theory to attain the mechanical properties and approximations for multiple failure modes found in fuselage structures (buckling, local buckling, strength, etc). Furthermore, regarding cost analysis, the Advanced Composite Cost Estimating Manual (ACCEM, Northrop Corporation, 1976) is used and a suggested optimization approach is analyzed.

3.1. Geometry definition

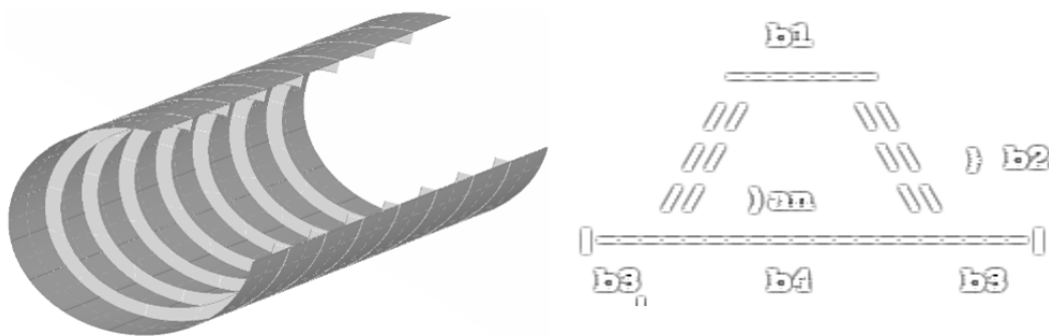


Figure 3.1: a) fuselage station design, b) example of stiffener dimensioning asked by the user

The chosen representative structure used in this thesis will be the fuselage of an airframe. Defining the weight and structural aspects of a whole fuselage is a big challenge in airframe design and that statement is based on the high complexity of the referred assembly. To tackle this problem in the preliminary design a representative cylinder is going to be split in different stations to account for the different radius sections of the structure. The user can choose the splits and dimensions both for radius and length of the fuselage stations. Then the stations can be split longitudinally and radially by the user to introduce stiffeners' and frames' locations in the initial skin-stiffened approach. A panel is defined by two frames and two stiffeners as pictured in 3.3. In future steps, the software can be modified to accommodate more complex cross sectional geometries.

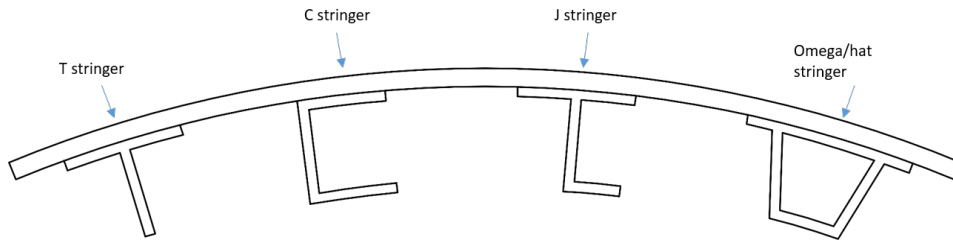


Figure 3.2: Stiffener types supported

As for the geometry of the stiffeners the software will ask for inputs from the user in order to define the type of stiffener (T, C, J, and Ω) as depicted in 3.2 respectively and the stiffener's dimensions. In the case of a sandwich design, the geometry is split again in the aforementioned way, without the addition of stiffeners to the calculations. It is assumed that the panels are attached to each other taking into account the additional joining area and assembly parts included. It has to be mentioned that the different stations, though split, have a continuation of load transfer and thus they are considered as a continuous structure.

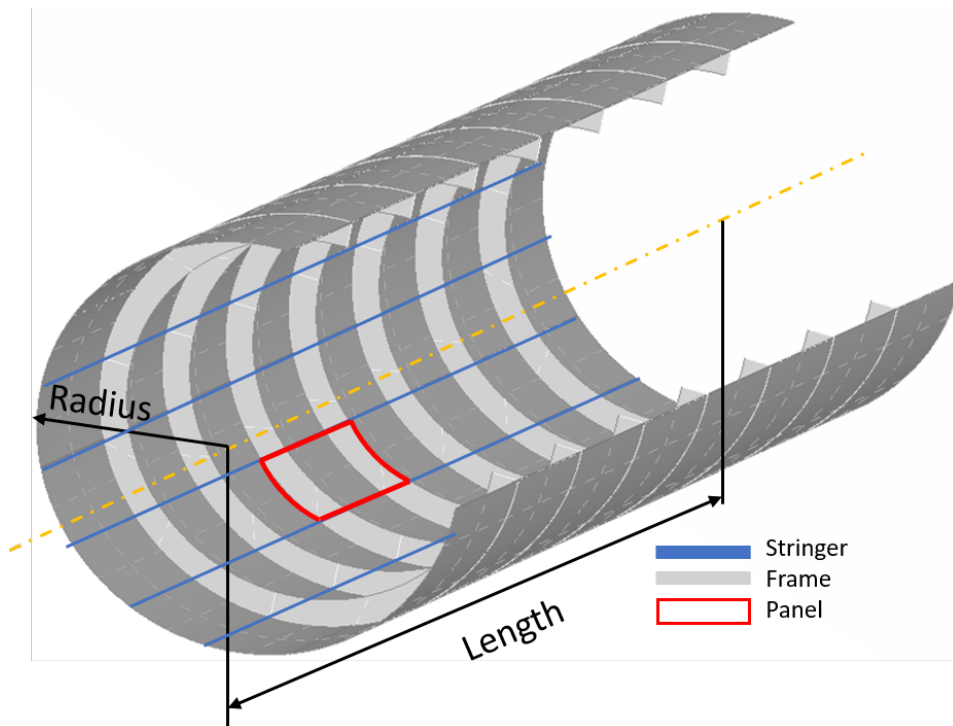


Figure 3.3: Fuselage geometry definition

The basic panels dimensions and notation are depicted below. The panel's length a lies on the longitudinal axis, z , and the panel's width on the radial dimension. The thickness of each panel is noted as t .

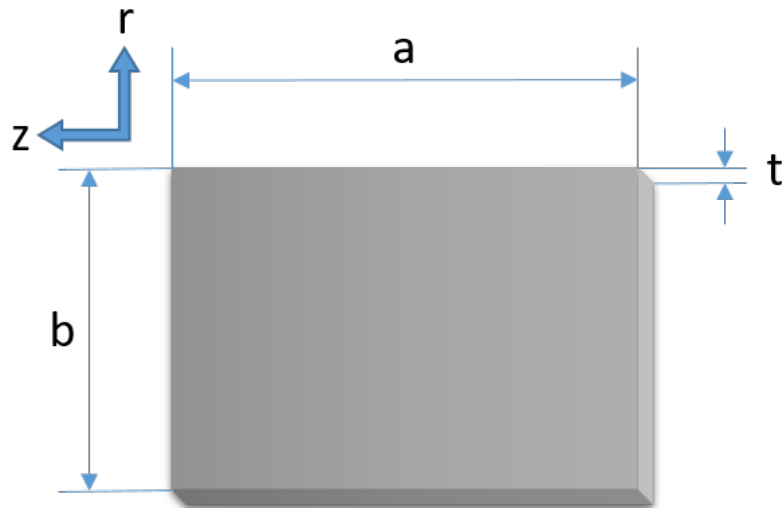


Figure 3.4: Panel geometry definition

3.1.1. Structural idealization

Following the geometry definition of the fuselage, a structural idealization needs to take place in order to simplify our geometry and appropriately distribute the internal loads applied due to several load cases. As presented in the book of Megson (4th Edition), chapter 20.2 [47], the structural idealization helps to represent complex structural sections with 'simpler mechanical models' which approximate the actual structure under given loading conditions. In 3.6 a cross section of the fuselage is depicted. Every red dot represents one boom consisting of a stringer and the skin attached to it. Thus, a structure consisting of direct stress carrying booms and shear stress carrying skins is created. The idealization logic for each panel can be seen in figure 3.5.

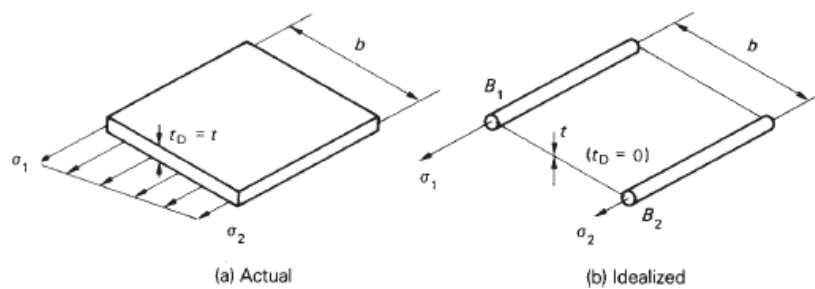


Figure 3.5: Panel idealization (Megson, 2007)

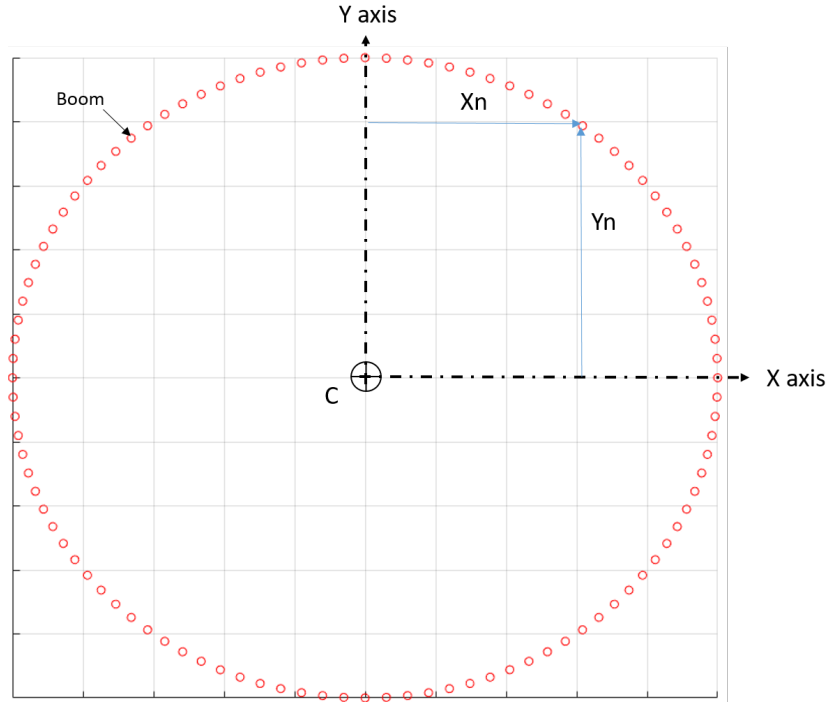


Figure 3.6: Fuselage idealized cross section

According to Megson [], a panel can be idealized using the following equation for booms:

$$B_1 = t_D \frac{b}{6} \left(2 + \frac{\sigma_2}{\sigma_1} \right) \quad (3.1)$$

$$B_2 = t_D \frac{b}{6} \left(2 + \frac{\sigma_1}{\sigma_2} \right) \quad (3.2)$$

Where, t_D : skin thickness, b : panel width, σ_1 : stress on stringer 1, σ_2 : stress on stringer 2. To account for a whole fuselage cross section, the cross section properties should be defined. First of all the center of gravity is calculated. Secondly, the booms properties and then the moments of inertia I_{xx} , I_{yy} and I_{xy} . The center of gravity can be calculated using the following formulas for x and y :

$$x_n = \sum_{n=1}^{\infty} \frac{(t_{sk} b_{sk} y_{sk} + (\frac{E_{str}}{E_{sk}}) A_{str} y_{sk})}{(t_{sk} b_{sk} + (\frac{E_{str}}{E_{sk}}) A_{str})}$$

$$y_n = \sum_{n=1}^{\infty} \frac{(t_{sk} b_{sk} x_{sk} + (\frac{E_{str}}{E_{sk}}) A_{str} x_{sk})}{(t_{sk} b_{sk} + (\frac{E_{str}}{E_{sk}}) A_{str})}$$

Where, t_{sk} : skin thickness, b_{sk} : panel width, E_{sk} : skin membrane stiffness along 1 axis, E_{str} : stringer stiffness along 1 axis, A_{str} : Stringer cross sectional area. The moments of inertia are given by:

$$I_{xx} = \sum_{n=1}^{\infty} (t_{sk} b_{sk} x_n^2 + (\frac{E_{str}}{E_{sk}}) A_{str} x_n^2)$$

$$I_{yy} = \sum_{n=1}^{\infty} (t_{sk} b_{sk} y_n^2 + (\frac{E_{str}}{E_{sk}}) A_{str} y_n^2)$$

$$I_{xy} = \sum_{n=1}^{\infty} (t_{sk} b_{sk} x_n y_n + (\frac{E_{str}}{E_{sk}}) A_{str} x_n y_n)$$

It has to be mentioned that, each panel has its own values regarding skin thickness, stiffeners' dimensions and members' thickness, stiffness E and area A. Using the equations above, the values are given as matrices containing the data for every single panel in order to calculate the final result for a whole fuselage section.

3.2. Material and layup definition

In the context of this thesis the materials used will be composite materials due to their high strength-to-weight ratio but with small changes in the software, isotropic materials could easily be used for the analysis. The initial design will be analyzed using a material database from literature [1] in order to be able to verify the results. In general the software gives the user the chance to enhance this database with desired materials. The approach will be versatile enough to deal with layups consisting of different types of materials in the same laminate. Then the governing equations of the Classical lamination Theory (CLT) will be used to attain the laminate properties (C. Kassapoglou, 2010) [1]. Finally, a choice to apply the appropriate knockdown factors will be given to the user regarding environmental, material scatter or effect of damage factors (C. Kassapoglou, 2010).

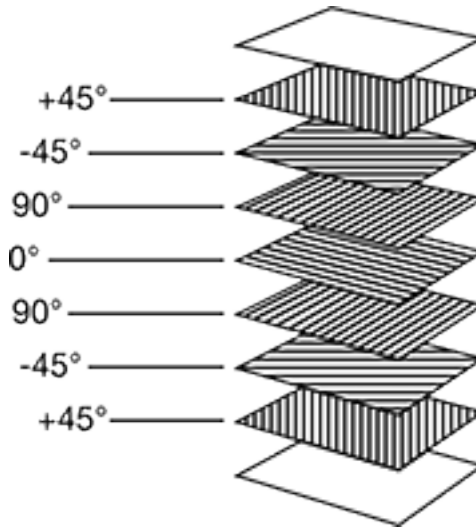


Figure 3.7: Layup definition according to CLT

3.3. Loading conditions

According to D. R. Polland et al., 1997 [57] critical loading conditions result from several ground and flight conditions. The software will give the possibility to the user to examine the desired critical loadcases either separately or in combination. The load case input will need to be in accordance with the guidelines given by the software. These guidelines will be described in detail in chapter 4.3.5. The load cases that will be used to validate the designs for the purpose of this project are: Cabin Pressurization, Negative bending, Positive

bending, Shear due to bending (Pitch maneuvers), Maximum axial tension and compression (Yaw maneuvers), and Combination of the above.

3.3.1. Internal loads definition

As mentioned above several loadcases will be examined by the software. Utilising the idealization of the fuselage cross-section described in section 3.1.1, the bending and shear strains throughout the fuselage structure can be calculated for each loading condition. The equations will be described in the following sections 3.3.1.1-3.3.1.4. Utilising the CLT the loading applied to each laminate comes in terms of load per unit width and in a vector form of:

$$\begin{Bmatrix} N_x \\ N_y \\ N_{xy} \\ m_x \\ m_y \\ m_{xy} \end{Bmatrix} = \begin{bmatrix} A_{11} & A_{12} & A_{16} & B_{11} & B_{12} & B_{16} \\ A_{12} & A_{22} & A_{26} & B_{12} & B_{22} & B_{26} \\ A_{16} & A_{26} & A_{66} & B_{16} & B_{26} & B_{66} \\ B_{11} & B_{12} & B_{16} & D_{11} & D_{12} & D_{16} \\ B_{12} & B_{22} & B_{26} & D_{12} & D_{22} & D_{26} \\ B_{16} & B_{26} & B_{66} & D_{16} & D_{26} & D_{66} \end{bmatrix} \begin{Bmatrix} \epsilon_{xb} \\ \epsilon_{yo} \\ \gamma_{xyo} \\ \kappa_x \\ \kappa_y \\ \kappa_{xy} \end{Bmatrix} \quad (3.3)$$

The left hand side of the equation is the load applied mentioned above. The loads per unit width N_x, N_y, N_{xy} are given in $[N/mm]$ and the moments per unit width m_x, m_y, m_{xy} are given in $[N]$.

3.3.1.1 Bending

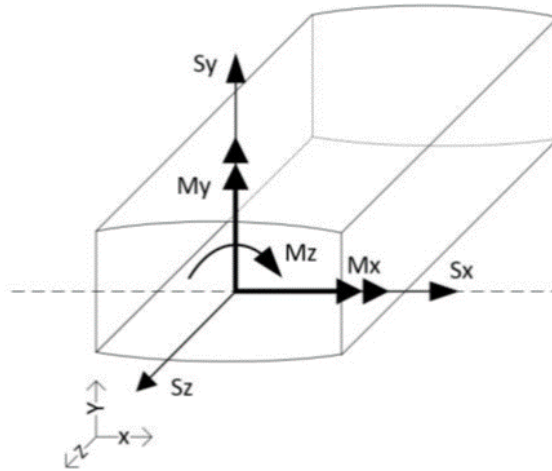


Figure 3.8: Applied bending load on fuselage(Megson,2013)

There are several forces and moments that can act on the fuselage due to different loading conditions. In figure 3.8 the more common ones are depicted. In the case of bending, there are two types of bending moments that act on the fuselage due to different conditions, M_y and M_z . For instance, in the upbending loading scenario, the upper part of the fuselage is subjected to compressive stresses while the lower part is subjected to tensile stresses. The position of the neutral axis is calculated by defining the center of gravity of the cross section and it passes through that point. The stresses applied on the fuselage can be derived from

the general equation:

$$\sigma_z = \frac{M_y I_{xx} - M_x I_{xy}}{I_{xx} I_{yy} - I_{xy}^2} x + \frac{M_x I_{yy} - M_y I_{xy}}{I_{xx} I_{yy} - I_{xy}^2} y \quad (3.4)$$

Where σ_z is the direct stress due to bending in a point of the cross-section, M_x and M_y are the bending moments around the x and y-axis respectively given in [Nmm], I_{xx} , I_{yy} and I_{xy} are the cross section's inertia terms and x and y are the x and y distances from the point on the section to the centroid of the cross-section. The above equation can be simplified for symmetrical fuselage shapes ($I_{xy} = 0$) to:

$$\sigma_z = \frac{M_y}{I_{xx}} x + \frac{M_x}{I_{yy}} y \quad (3.5)$$

However, the equation is valid for isotropic materials. In order to account for composite materials, Hooke's law ($\sigma = E\epsilon$) is utilised and the equation is written in terms of strain as given below:

$$\epsilon_z = \frac{M_y}{EI_{xx}} x + \frac{M_x}{EI_{yy}} y \quad (3.6)$$

The direct strain is calculated for each stringer and neighboring skin panels, so for each boom. The direct strain is then converted to applied force and finally the force is distributed to skins and stringers members according to their stiffness. The values of M_z and M_y used are typical bending moment values for fuselages of these dimensions and characteristics. They afterwards get converted to load input in the software. Further analysis will be done in chapter 4.

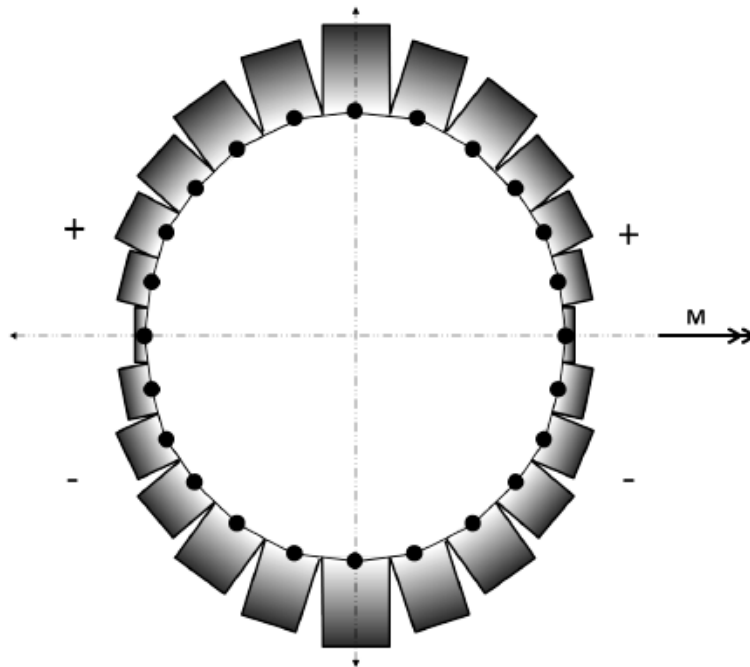


Figure 3.9: Force distribution on fuselage cross section for bending (I. Sen, 2010)

Given in the graph above is the distribution of force on the fuselage cross-section for a bending moment M . The top part experiences tension and the bottom part compression

with the higher positive and negative values on the upper-most and lower-most positions respectively.

Furthermore, the forces need to be distributed on the skin and stringers attached to each panel as shown in figure 3.10.

$$F_z = \epsilon_z EA_{panel} \tag{3.7}$$

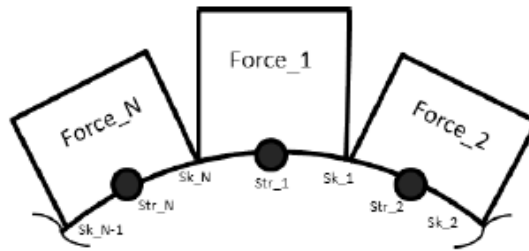


Figure 3.10: Force distribution on panel's members (I. Sen, 2010)

To do so, each stringer's stiffness needs to be calculated. A J stringer will be used to present the method below.

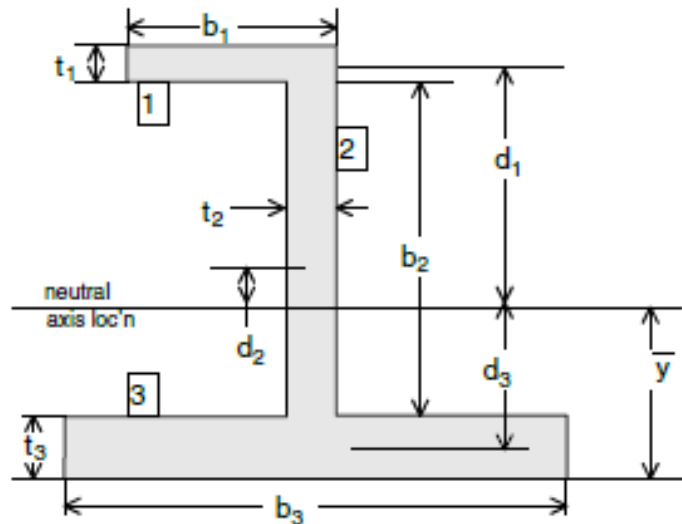


Figure 3.11: Stringer cross-sectional characteristics (C. Kassapoglou, 2010)

As depicted above, figure 3.11, the neutral axis is calculated using the equation:

$$\bar{y} = \frac{\sum(EAy)_j}{\sum(EA)_j} \tag{3.8}$$

It has to be mentioned that the E modulus is either the membrane or bending modulus of the laminate, depending on the loading condition tested. The force on each member can

be then calculated.

$$F_i = \frac{(EA)_i}{\sum_{j=1}^3 (EA)_j} F_{TOT} = \frac{E_i b_i t_i}{\sum_{j=1}^3 E_j b_j t_j} \quad (3.9)$$

The entire cross-section's equivalent axial stiffness is calculated by:

$$(EA)_{eq} = \sum_j (EA)_j \quad (3.10)$$

And finally, the bending stiffness for each member is given by:

$$(EI)_i = E_b \left[\frac{(\text{width})_i (\text{height})_i^3}{12} + A_i d_i^2 \right] \quad (3.11)$$

Thus the equivalent bending stiffness for the entire beam is:

$$(EI)_{eq} = \sum_j (EI)_j \quad (3.12)$$

Having calculated the properties of both skins and stringers for each panel, the force distribution can take place using the coefficient λ .

$$\lambda = \frac{\left(A_{11} + \frac{EA}{d_s} \right)}{A_{11}} \Rightarrow EA = A_{11} (\lambda - 1) d_s \quad (3.13)$$

Where, A_{11} is the skin's ABD matrix first element, EA is the stringer's stiffness and d_s equals to the width (b) for the current study (See figure 3.4).

Finally, the relationship between the total force applied on each panel and the forces acting on the skin and stiffeners is:

$$F_{\text{skin}} = \frac{A_{11}}{A_{11} + \frac{EA}{d_s}} F_{TOT} = \frac{1}{\lambda} F_{TOT} \quad (3.14)$$

$$F_{\text{stiffeners}} = \frac{(\lambda - 1)}{\lambda} F_{TOT} \quad (3.15)$$

Where F_{TOT} is:

$$F_{TOT} = b N_x \quad (3.16)$$

As the whole analysis is based on load per unit width (N_x) according to the Classical Laminate Theory (CLT) the load per unit width on the skin is:

$$N_{x\text{skin}} = \frac{F_{\text{skin}}}{b} = \frac{A_{11}}{A_{11} + \frac{EA}{d_s}} \frac{b N_x}{b} = \frac{1}{\lambda} N_x \quad (3.17)$$

3.3.1.2 Shear

In the case of shear, there are two types of loading that introduce shear flow, vertical forces due to bending and torsion. The shear flow is the gradient of a shear stress force through the body. The shear flow distribution is given by the following equation for closed section beams as mentioned in Megson[5]:

$$q_s = q_b + q_{s,0} = - \left(\frac{F_x I_{xx} - F_y I_{xy}}{I_{xx} I_{yy} - I_{xy}^2} \right) \sum_{r=1}^n B_r y_r - \left(\frac{F_y I_{yy} - F_x I_{xy}}{I_{xx} I_{yy} - I_{xy}^2} \right) \sum_{r=1}^n B_r x_r + q_{s,0} \quad (3.18)$$

Where q_b is the open section shear flow, $q_{s,0}$ is the closing shear flow, F_x and F_y are the applied shear forces [N/mm] in x and y direction, x and y are the distances from a point on the section to the shear centre, and B_r is the boom's area in mm^2 . For a symmetrical cross-section the equation reduces to:

$$q_s = -\frac{S_y}{I_{xx}} \sum_{r=1}^n B_r y_r + q_{s,0} \quad (3.19)$$

The closing shear flow can be then calculated by:

$$0 = \oint p \cdot q_b ds + 2Aq_{s,0} \quad (3.20)$$

3.3.1.3 Torsion

Since the fuselage is a closed section beam, the shear flow produced by pure torsion can be calculated by:

$$q = \frac{T}{2A} \quad (3.21)$$

In the context of this study, the presence of a floor is not accounted for. That is the reason the equation 3.21 for a closed section beam can be used. Depending on the load case, the shear flow due to torsion can be added to the shear flow due to vertical forces. The highest values for shear are present on the sides of the cross-section and specifically in the center and the lower ones are present in the top and bottom parts.

The total shear flow on a fuselage cross section can be visualised in the graph below:

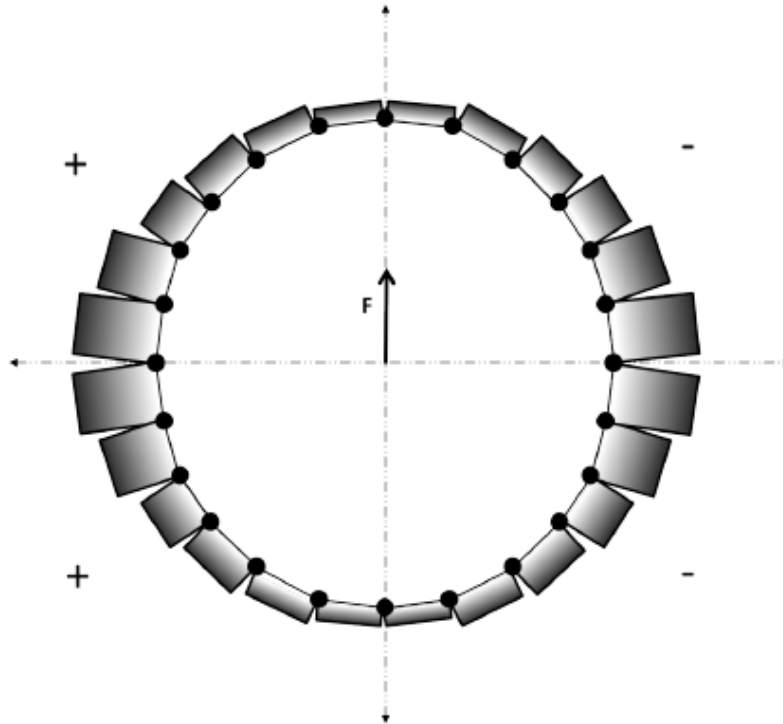


Figure 3.12: Shear flow on fuselage's cross-section (I. Sen, 2010)

3.3.1.4 Pressure

The last loadcase examined is the pressure loadcase. In pressurised fuselages there are forces introduced by pressure that lead to hoop and longitudinal stresses acting on the structure. The hoop stress is give by:

$$\sigma_{\text{circ}} = \frac{\Delta p R}{t} \quad (3.22)$$

Thus,

$$N_{\text{circ}} = \frac{\Delta p R}{t} b \quad (3.23)$$

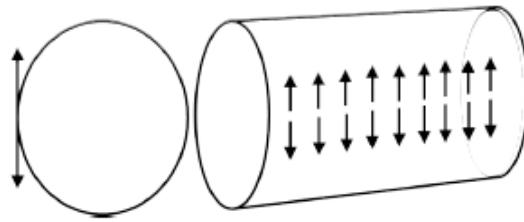


Figure 3.13: Hoop stress

And the longitudinal stress is given by:

$$\sigma_{\text{long}} = \frac{\Delta p R}{2t} \quad (3.24)$$

Thus,

$$N_{\text{long}} = \frac{\Delta p R}{2t} b \quad (3.25)$$

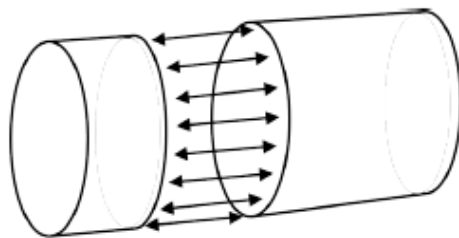


Figure 3.14: Longitudinal stress

The calculated loads per unit width acting on the fuselage due to pressure can be added to the overall loading depending on the loadcse examined.

3.4. Margins of safety calculation

For the scope of this research several margins of safety will be examined in order to assess failure of the composite structure. The examined margins of safety need to be split in

three categories: Material strength, Skin/Bay/Panel Buckling and Interlaminar shear. Furthermore, crippling will be added to the list for the skin-stiffened structure and wrinkling, crimping and dimpling for the sandwich design. The reader can refer to the book of Kassapoglou (2010), chapters 6,8,9 and 10 for a detailed analysis of these failure modes. First of all, the critical failure loads are calculated and then the reserve factor (RF), which is:

$$RF = \frac{N_{allowable}}{N_{applied}} \quad (3.26)$$

Finally the margin of safety (MS) for each scenario is calculated using the formula below:

$$MS = RF - 1 \quad (3.27)$$

3.4.1. Material strength

The material strength margins of safety will be estimated using several failure criteria as listed in the book by Kassapoglou, Chapter 4 (C. Kassapoglou, 2010). The user will have the chance to choose between three known criteria as Tsai-Wu, Tsai-Hill or Maximum Stress depending on his experience and the projects requirements. Other failure criteria, of the user's preference, can be added by appropriate changes of the respective section of the software.

3.4.1.1 Maximum stress

The maximum stress failure theory can be expressed as:

$$\sigma_x < X^t \text{ or } X^c \quad (3.28)$$

$$\sigma_y < Y^t \text{ or } Y^c \quad (3.29)$$

Either for tensile (t) or compressive (c) stress.

$$|\tau_{xy}| < S \quad (3.30)$$

If the values for stress in each direction exceed the maximum allowable, failure occurs.

3.4.1.2 Tsai-Hill

The final form of the Tsai-Hill criterion is given by:

$$\frac{\sigma_x}{X^2} - \frac{\sigma_x \sigma_y}{X^2} + \frac{\sigma_y}{Y^2} + \frac{\tau_{xy}}{S^2} = 1 \quad (3.31)$$

It has to be mentioned that this criterion and the Tsai-Wu criterion take into account the interaction of stresses and not only the individual comparison with the allowable in the direction of the applied stress. If the left hand side exceeds one then failure occurs. It has to be mentioned that the Tsai-Hill failure criterion is analogous to the Von Mises failure criterion for isotropic materials.

3.4.1.3 Tsai-Wu

Finally, the Tsai-Wu failure criterion is an attempt to generalize the Tsai-hill criterion using curve fitting. The form of the criterion used in the evaluation of failure strength is:

$$\frac{\sigma_y^2}{X^t X^c} + \frac{\sigma_x^2}{Y^t Y^c} - \sqrt{\frac{1}{X^t X^c Y^t Y^c}} \sigma_x \sigma_y + \left(\frac{1}{X^t} - \frac{1}{X^c}\right) \sigma_x + \left(\frac{1}{Y^t} - \frac{1}{Y^c}\right) \sigma_y + \frac{\tau_x y^2}{S^2} = 1 \quad (3.32)$$

3.4.2. Buckling

In the case of linear buckling the margins of safety to be calculated depend on the configuration. For that reason there are two separate categories: Skin-stiffened structure, Sandwich structure. A multiaxial approach proposed by Ueda et al. (1995)[35] will be followed. In that way every possible in-plane loading combination will be examined by the software. The critical buckling loads for separate cases of uniaxial buckling under compression and shear are given in the book of Kassapoglou, chapter 6[1].

3.4.2.1 Skin-stiffened structure

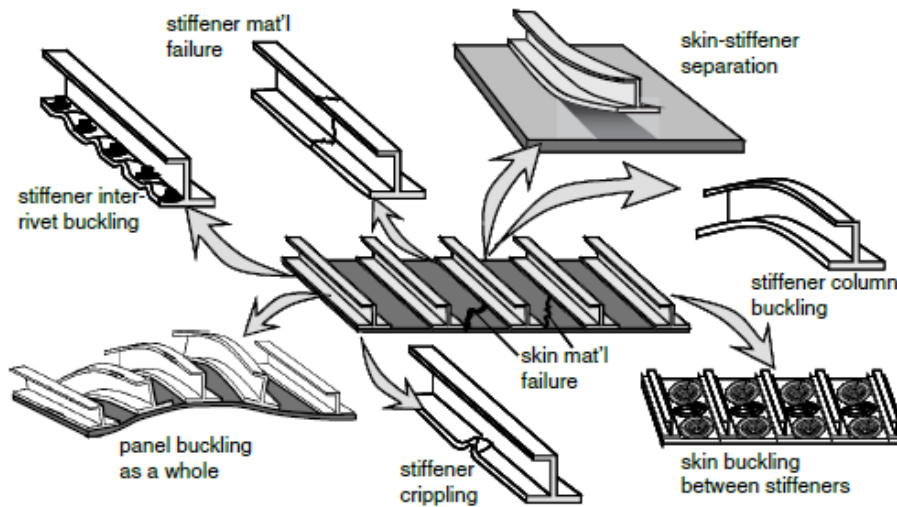


Figure 3.15: Failure modes of a skin-stiffened panel (Kassapoglou,2009)

Skin-stiffened structures require the calculation not only of skin referred margins of safety in failure but the ones for stiffeners and the panel as an assembly. Therefore, given below are the margins of safety that will be output of the software: Skin buckling, Panel buckling, Stiffener column buckling (according to the Euler buckling load as given by Kassapoglou, chapter 8), Stiffener flanges crippling (OEF or NEF), stiffener webs crippling (OEF or NEF), skin failure strength, Stiffeners' members failure strength. The above equations are calculated using chapter 9, Kassapoglou, 2010. Each panel consists of two stringers, two frames and the skin as depicted in 3.16. Where a is the panels length in the longitudinal direction and b is the width in the circumferential dimension. It has to be mentioned that simply supported boundary condition is assumed around the panel.

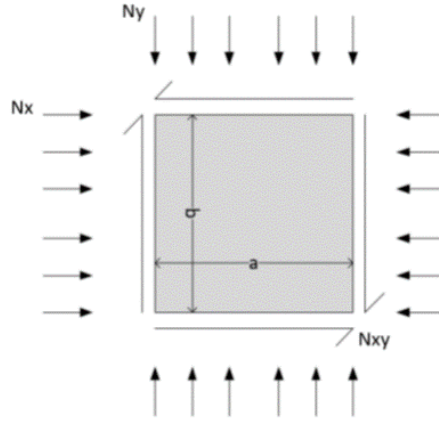


Figure 3.16: Representative structure

Skin and Panel Buckling In order to account for multiaxial loading conditions, including biaxial and shear loads, the formulas provided by Ueda et al.(1995)[35] are applied. Thus three scenarios are expected:

- When N_x is tensile and N_y is compressive

$$\frac{(m^2 + \beta^2)^2}{m^2(1 + \beta^2)^2} \frac{\sigma_x}{\sigma_{xcr}} + \frac{\sigma_y}{\sigma_{ycr}} + \left(\frac{\tau_{xy}}{\tau_{xycr}}\right)^2 = 1 \quad (3.33)$$

- When N_y is tensile and N_x is compressive

$$\frac{(1 + \beta^2)^2}{(m^2 + \beta^2)^2} \frac{\sigma_y}{\sigma_{ycr}} + \frac{\sigma_x}{\sigma_{xcr}} + \left(\frac{\tau_{xy}}{\tau_{xycr}}\right)^2 = 1 \quad (3.34)$$

- When both N_x and N_y are compressive

$$\left(\frac{\frac{\sigma_x}{\sigma_{xcr}}}{1 - \left(\frac{\tau_{xy}}{\tau_{xycr}}\right)^2}\right)^{e1} + \left(\frac{\frac{\sigma_y}{\sigma_{ycr}}}{1 - \left(\frac{\tau_{xy}}{\tau_{xycr}}\right)^2}\right)^{e2} = 1 \quad (3.35)$$

Where $\beta : a/b$, and for:

- $(\sqrt{2} < \beta < \sqrt{2}, e1=e2=1$
- $\beta > \sqrt{2}$

$$e1 = 0.0293\beta^3 - 0.3364\beta^2 + 1.5854\beta - 1.0596 \quad (3.36)$$

$$e2 = 0.0049\beta^3 - 0.1183\beta^2 + 0.6153\beta - 0.8522 \quad (3.37)$$

As mentioned above, the critical buckling loads are calculated using chapter 6 of the book of Kassapoglou (2009). The formulas for critical buckling loads in x, y and xy are given below:

$$N_x = \frac{\pi^2 [D_{11}m^4 + 2(D_{12} + 2D_{66})m^2\beta^2 + D_{22}\beta^4]}{a^2m^2} \quad (3.38)$$

$$N_y = \frac{\pi^2 [D_{22}m^4 + 2(D_{12} + 2D_{66})m^2(1/\beta)^2 + D_{11}(1/\beta)^4]}{b^2 m^2} \quad (3.39)$$

The critical buckling load in shear is calculated each time according to the panel's dimensions. A similar approach is followed by the book of Kassapoglou (2009) in sections 6.3 and 6.4. The reader can refer to this chapter for a detailed view of the approach. There are three cases examined, $a/b = 0$, $0 \leq a/b < 0.5$, $0.5 \leq a/b < 1$. For the second case a linear interpolation between the two other cases' results will give a good approximation.

For $0.5 \leq a/b < 1$ we get:

$$N_{xyEcr} = \frac{\frac{\pi^4 b}{a^3}}{\sqrt{\frac{14.28}{D1^2} + \frac{40.96}{D1D2} + \frac{40.96}{D1D3}}} \quad (3.40)$$

With,

$$\begin{aligned} D1 &= D_{11} + D_{22} \left(\frac{a}{b}\right)^4 + 2(D_{12} + 2D_{66}) \left(\frac{a}{b}\right)^2 \\ D2 &= D_{11} + 81D_{22} \left(\frac{a}{b}\right)^4 + 18(D_{12} + 2D_{66}) \left(\frac{a}{b}\right)^2 \\ D3 &= 81D_{11} + D_{22} \left(\frac{a}{b}\right)^4 + 18(D_{12} + 2D_{66}) \left(\frac{a}{b}\right)^2 \end{aligned} \quad (3.41)$$

For $a/b = 0$,

$$N_{xycrit} = \frac{\pi^2}{2AR^2 a^2 \tan \alpha} \left[\frac{D_{11} (1 + 6 \tan^2 \alpha AR^2 + \tan^4 \alpha AR^4) + 2(D_{12} + 2D_{66}) (AR^2 + AR^4 \tan^2 \alpha) + D_{22} AR^4}{2(D_{12} + 2D_{66}) (AR^2 + AR^4 \tan^2 \alpha) + D_{22} AR^4} \right] \quad (3.42)$$

To obtain the critical buckling load a minimization of the above equation takes place, by differentiating with respect to AR and $\tan \alpha$.

$$\frac{\partial N_{xycrit}}{\partial (AR)} = 0 \Rightarrow AR = \left[\frac{D_{11}}{D_{11} \tan^4 \alpha + 2(D_{12} + 2D_{66}) \tan^2 \alpha + D_{22}} \right]^{1/4}$$

and

$$\begin{aligned} \frac{\partial N_{xycrit}}{\partial (\tan \alpha)} = 0 \Rightarrow & 3D_{11}AR^4 \tan^4 \alpha + (6D_{11}AR^2 + 2(D_{12} + 2D_{66})AR^4) \tan^2 \alpha \\ & - (D_{11}2(D_{12} + 2D_{66})AR^2 + D_{22}AR^4) = 0 \end{aligned}$$

A similar approach is followed for the panel buckling allowables. In this case the whole panel's stiffness matrix has to be changed accordingly. Thus the stiffeners contribution is smeared to the skin to get the appropriate stiffness of the panel. The smearing equations are provided once again in the book of Kassapoglou, section 9.1. Thus the equivalent bending stiffness of the panel is given below:

$$D_{11equivalent} = D_{11skin} + \frac{EI_{xxstr}}{b} \quad (3.43)$$

$$D_{12equivalent} = D_{12skin} \quad (3.44)$$

$$D_{22equivalent} = D_{22skin} \quad (3.45)$$

$$D_{66equivalent} = D_{66skin} + \frac{GJ_{str}}{2b} \quad (3.46)$$

Where GJ_{str} is the polar moment of inertia of the stiffener, given by the equation below:

$$(GJ)_{eq} = \sum_j (GJ)_j \quad (3.47)$$

Stiffeners Buckling The stiffeners are designed to support direct stresses, tensile or compressive. When tensile loads are applied they are examined for material failure as mentioned above. On the other hand, when direct stresses are compressive a buckling analysis needs to take place as well.

The first failure mode mentioned above is column buckling of the stiffeners. Again considering a simply supported beam without the contribution of the skin helps to simplify the approach using the Euler buckling load. This approach, even though conservative, provides a sufficient result for the current study. The critical buckling load for column buckling of a beam with length L and stiffness $EI_{xx_{str}}$ is given by:

$$P_{cr} = \frac{\pi^2 EI_{xx_{str}}}{L^2} \quad (3.48)$$

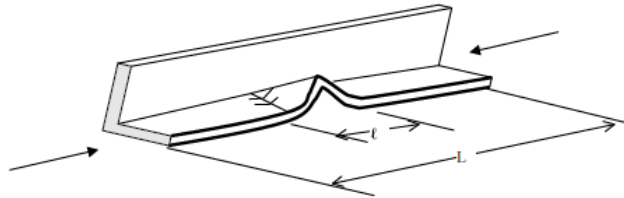


Figure 3.17: Crippling of stiffener (Kassapoglou,2009)

Stiffeners Crippling The second failure mode examined for stiffeners is the crippling failure mode. When crippling is the critical failure mode the flanges of the stringer buckle locally before the column buckling allowable is exceeded. There are two types of crippling, one-edge-free (OEF) and no-edge-free (NEF) as depicted below:

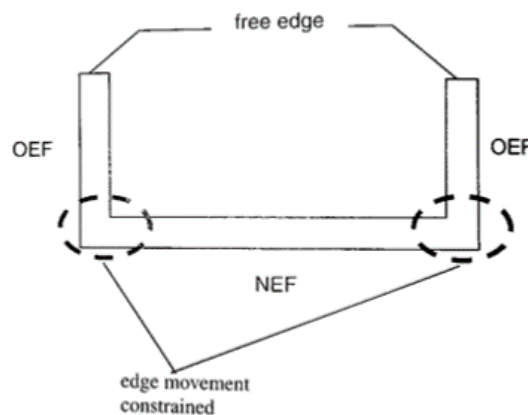


Figure 3.18: OEF and NEF crippling of stiffener (Kassapoglou,2009)

As given by the book of Kassapoglou [1], The critical crippling stresses for OEF and NEF, respectively, are:

$$\frac{\sigma_{crip}}{\sigma_{cu}} = \frac{1.63}{(b/t)^{0.717}} \quad (3.49)$$

$$\frac{\sigma_{crip}}{\sigma_{cu}} = \frac{11}{(b/t)^{1.124}} \quad (3.50)$$

Where σ_{crip} is the critical crippling stress, σ_{cu} is the ultimate failure strength of the laminate in compression, b is the width of the member and finally, t is the member's thickness. The aforementioned equations take into account the B-Basis values.

3.4.2.2 Sandwich structure

Sandwich structure designs require extra calculations about wrinkling, crimping and dimpling in addition to buckling and also the calculation of Interlaminar shear stresses acting on the core material. Therefore, the margins of safety for that case will be: Panel buckling, Panel wrinkling, Panel crimping, Core dimpling, Skins' failure strength. In that case the equations used will be taken from chapter 10, Kassapoglou, 2010.

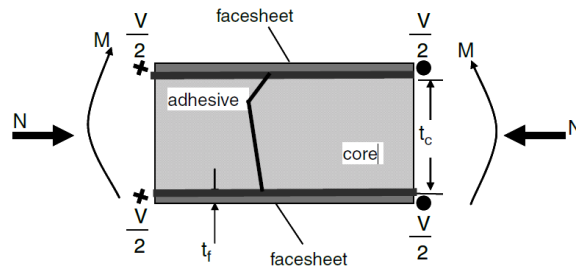


Figure 3.19: Sandwich configuration (Kassapoglou,2009)

In order to calculate the properties of the sandwich panel, the equivalent sandwich properties have to be calculated. The core is assumed to be a layer of the laminate plate with (near) zero in-plane stiffness and strength properties. To acquire the equivalent stiffness of the design, the following equation is used:

$$D_{ij} = 2 * (D_{ij})_f + 2 * (A_{ij})_f * \left(\frac{t_c + t_f}{2}\right)^2 \quad (3.51)$$

Where D_{ij} is the panel's equivalent bending stiffness matrix, $(D_{ij})_f$ and $(A_{ij})_f$ are the skins' membrane and bending stiffness matrices respectively, t_c is the core's thickness and t_f is the skin's thickness. Again, the same procedure is followed for each different panel.

Sandwich buckling The same procedure, mentioned above, about multiaxial buckling is followed for the sandwich panel. The buckling load under compression is given by:

$$N_{x_{crit}} / N_{y_{crit}} = \frac{N_{E_{crit}}}{1 + \frac{N_{E_{crit}}}{t_c * G_c}} \quad (3.52)$$

Where $N_{E_{crit}}$ is the critical load for the skin in the loading direction, t_c is the core thickness and G_c is the core shear modulus in the loading direction . The buckling load under shear is given by:

$$N_{xy_{crit}} = \frac{(G_{xz} + G_{yz}) * t_c}{\frac{(G_{xz} + G_{yz}) * t_c}{N_{xy_c}} + 2} \tag{3.53}$$

In this case, the values G_{xz} and G_{yz} are the shear moduli in the yz and xz direction as given in figure 3.20.

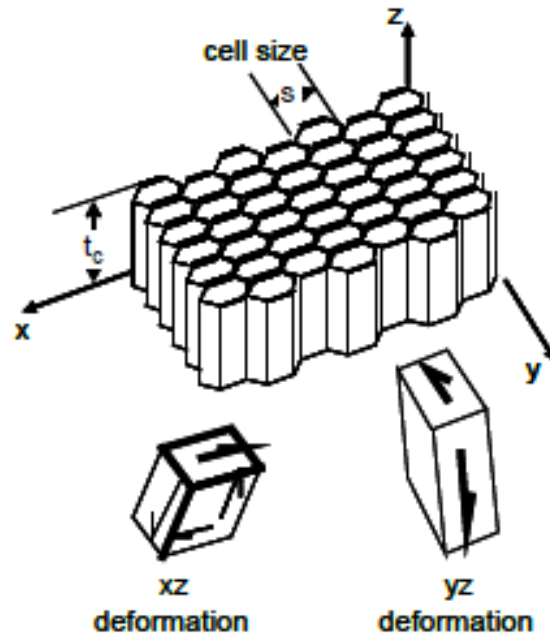


Figure 3.20: Honeycomb core deformations (Kassapoglou,2009)

Sandwich Wrinkling Wrinkling is a local buckling phenomenon where the facesheet of a sandwich buckles over a characteristic half-wavelength. There are two modes, symmetric, anti-symmetric that are examined in the current study (See fig. 3.21).

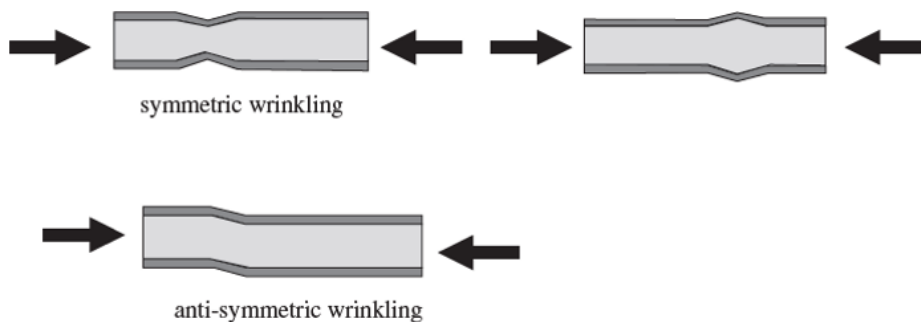


Figure 3.21: Wrinkling failure modes: a), b) Symmetric, c) Anti-symmetric (Kassapoglou,2009)

The equations for both types are provided in the book of Kassapoglou (2009) and given below:

$$N_{sym} = 0.43 * t_f * (E_f * E_c * G_{xz})^{(1/3)} \tag{3.54}$$

$$N_{antisym} = 0.33 * t_f * E_f * \sqrt{\frac{E_c * t_f}{E_f * t_c}} \tag{3.55}$$

In the case of wrinkling under a combination of loads the reserve factors and thus the margins of safety can be calculated using the interaction curves provided in the following table.

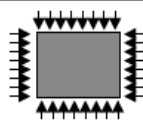
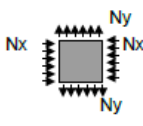
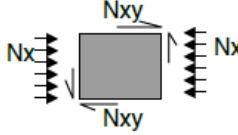
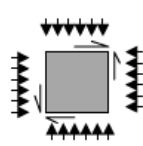
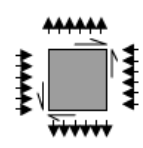
| Case | Loading | Design equation |
|---------------------------------------------------------------|-------------------------------------------------------------------------------------|-----------------------------------------------------------------------------------------------------------------------------------------------------------------------------------------------------------------|
| Biaxial compression |  | $N_x = \frac{N_{xwr}}{\left(1 + \left(\frac{N_y}{N_x}\right)^3\right)^{1/3}}$ |
| Compression in x direction and tension in y direction |  | $N_x = N_{xwr}$ |
| Combined compression and shear |  | $R_c + R_s^2 = 1$ |
| Biaxial compression and shear |  | $R_c + R_s^2 = 1$ $R_c = N_x / N_{xwr}$ $R_s = N_{xy} / N_{xywr}$ <p>N_{xwr} is wrinkling load in major core direction when biaxial compression acts alone (1st case in this table)</p> |
| Compression in x direction, tension in y direction, and shear |  | $R_c + R_s^2 = 1$ $R_c = N_x / N_{xwr}$ $R_s = N_{xy} / N_{xywr}$ <p>N_{xwr} is wrinkling load in x direction when compression acts alone.</p> |

Figure 3.22: Interaction curves for wrinkling under combination of loads (Kassapoglou,2009)

Sandwich Crimping Another failure mode, shown in figure 3.23, occurring when the core shear stiffness is very low, is crimping.

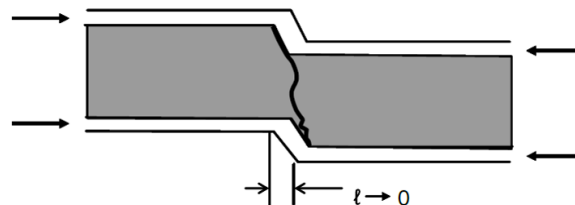


Figure 3.23: Sandwich crimping (Kassapoglou,2009)

The equations for sandwich crimping under compression and shear are given below as referred to in chapter 10.3 of the book of Kassapoglou (2010).

$$N_{crit_{compression}} = t_c * G_c \quad (3.56)$$

$$N_{crit_{shear}} = t_c * \sqrt{G_{xz} * G_{yz}} \quad (3.57)$$

Sandwich Dimpling Finally, the last failure mode examined for the sandwich design configuration is the sandwich dimpling. The critical buckling load is given below as referred to in chapter 10.5 of the book of Kassapoglou (2010).

$$N_{x_{dimp}} = 24 * \frac{D_{11f}}{s^2} \quad (3.58)$$

Where s is the core shell's size.

3.4.3. Interlaminar shear stress (ILSS)

The Interlaminar shear stress will be checked under the loading case of pressurization. Developing a software utilizing the analytical equations for panel deflection under pressure (C. Kassapoglou, chapter 5.3.2., 2010) the moments and shear forces on each panel can be calculated. By dividing the shear forces with the thickness of each panel the stresses are obtained and from them the ILSS criteria can be checked. The moments M_x , M_y and M_{xy} and the shear forces Q_x and Q_y , are calculated using the derivation of the deflection w of the panel. The equations for the aforementioned moments and shear forces are given below, as provided by the book of Kassapoglou (2009) [1]. It has to be mentioned, that the terms D_{16} and D_{26} are neglected due to the use of 45 and -45 plies at the appropriate positions.

$$M_x = \sum \sum (D_{11}(\frac{m\pi^2}{a})^2 + D_{12}(\frac{n\pi^2}{b})^2) A_{mn} \sin \frac{m\pi x}{a} \sin \frac{n\pi y}{b} \quad (3.59)$$

$$M_y = \sum \sum (D_{12}(\frac{m\pi^2}{a})^2 + D_{22}(\frac{n\pi^2}{b})^2) A_{mn} \sin \frac{m\pi x}{a} \sin \frac{n\pi y}{b} \quad (3.60)$$

$$M_{xy} = - \sum \sum 2D_{66} \frac{mn\pi^2}{ab} A_{mn} \cos \frac{m\pi x}{a} \cos \frac{n\pi y}{b} \quad (3.61)$$

$$Q_x = \sum \sum (D_{11}(\frac{m\pi^2}{a})^3 + D_{12}(\frac{n\pi^2}{b})^2(\frac{m\pi}{a}) + 2D_{66} \frac{mn^2\pi^3}{ab^3}) A_{mn} \cos \frac{m\pi x}{a} \sin \frac{n\pi y}{b} \quad (3.62)$$

$$Q_y = \sum \sum (D_{12}(\frac{m\pi^2}{a})^2 + D_{22}(\frac{n\pi^2}{b})^3(\frac{m\pi}{a}) + 2D_{66} \frac{m^2n\pi^3}{a^2b}) A_{mn} \sin \frac{m\pi x}{a} \cos \frac{n\pi y}{b} \quad (3.63)$$

Where, for a given pressure load p_0 the A_{mn} is:

$$A_{mn} = \frac{\frac{16p_0}{\pi^2 mn}}{D_{11}(\frac{m\pi}{a})^4 + 2(D_{12} + 2D_{66})\frac{m^2n^2\pi^4}{a^2b^2} + D_{22}\frac{n^4\pi^4}{b^4}} \sin \frac{m\pi}{2} \sin \frac{n\pi}{2} \quad (3.64)$$

In order to calculate the shear stresses acting on the laminate the shear forces are divided by the thickness and thus the ILSS allowable can be compared to the result calculated. The shear stresses in a laminate with thickness t_s are calculated using the equations below.

$$\tau_{xz} = \frac{Q_{xmax}}{t_s} \quad (3.65)$$

$$\tau_{yz} = \frac{Q_{ymax}}{t_s} \quad (3.66)$$

3.5. Flat/Curved Plates comparison

In order to avoid using high fidelity models for the analysis of curved plates it is assumed that the panels are divided by the stiffeners into sub-panels and the sub-panels' structural integrity is examined assuming they are flat. In that way, every panel consists of two stiffeners, two frames and the adjacent skin. In order to neglect curvature the ratio of radius over thickness, should be taken into account so that the deviation between flat panels' and curved panels' critical buckling stress is minimized. This will set a design limitation to the software because only a given range of radius over thickness and number of stiffeners configurations will be available to the user. Nevertheless, as the axial compression and shear buckling coefficients, K_c and K_s , are higher for curved plates than flat ones (E. F. Bruhn, 1973) [9], the design of configurations outside the suggested range, will be possible with a slight weight penalty due to the overestimation of the critical buckling stress. As stated in the "Stress Analysis Manual", 1986, [24] curved plates can be analysed as flat plates in buckling when the following requirement is satisfied:

$$\frac{b^2}{(R * t)} < 1 \quad (3.67)$$

Where b is the plate's width, R the radius of curvature and t is the plate's thickness. Assuming that a typical composite plate's thickness for a skin is around 2 mm, a range of width over radius could give the desired range for our design. Additionally, in order to account for manufacturability and feasibility of a skin stiffened design, a range of [50,200] mm for panel width is chosen. It is then clear that for values of b near the upper limit the radius has to be significantly large.

For panels with $(b^2/(Rt) > 1)$, figure 3.24 can be used to determine the buckling coefficient.

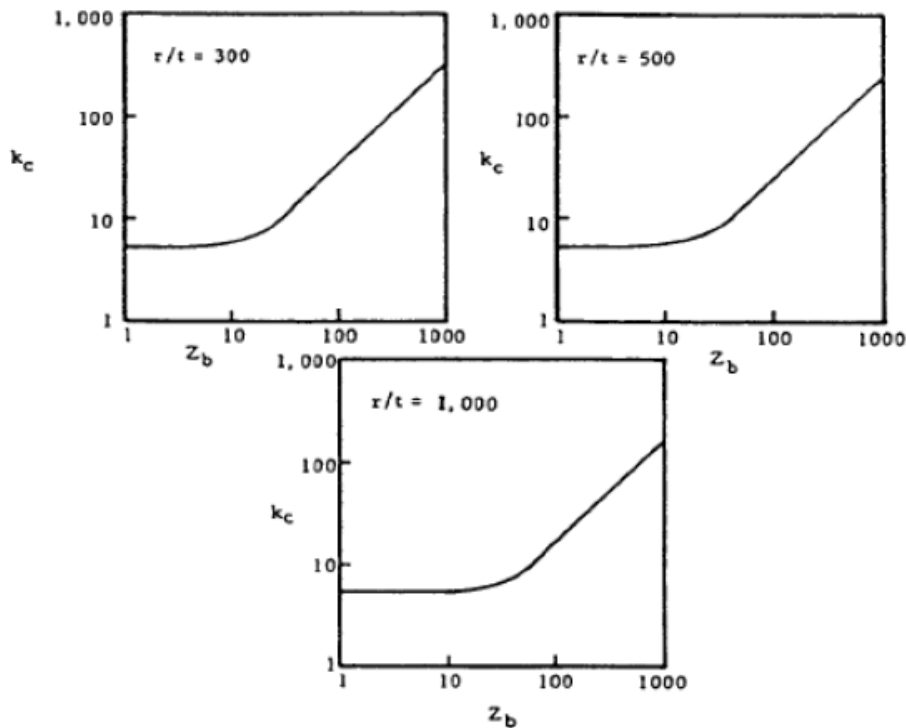


Figure 3.24: Buckling coefficient grouped according to R/t values for curved plates ("Stress Analysis Manual" 1986)

Where $Z_b = b^2 / (Rt) \sqrt{1 - \nu^2}$ and ν is the equivalent Poisson's ratio. Thus a correction factor would help improve accuracy in the critical buckling stress calculations. It has to be mentioned that most small size aircrafts have a radius of at least 1000 mm. Given the aforementioned, the assumption of flat panels in the buckling analysis will not introduce large errors in the structural analysis for the majority of configurations. The categories of aircrafts that will result in a weight overestimation are small UAV's or single person vehicles having a small fuselage radius and that can be balanced by the use of a correction factor based on figure 3.24.

3.6. Weight estimation

Several authors use detailed calculation formulas for the estimation of the max take-off weight. In this study, only the structural weight of the fuselage will be used and that will need to be optimized. According to the definition of the panels from the user the calculation will be done panel wise according to dimensions and layup data. Additionally, a weight error factor is introduced in order to account for extra weight in each configuration due to assumptions made at an early stage about fuselage characteristics not included in the analysis. Such characteristics are the cut-outs reinforcements (cargo and landing gear hatches, doors, and windows), the fuselage-to-wing and vertical stabilizer joining areas, fuselage floor and keel structures. In each configuration the total weight will be given by the following formulas:

$$W_{skin-stiffened} = W_{skins} + W_{stiffeners} + W_{error} \quad (3.68)$$

$$W_{sandwich} = W_{skins} + W_{cores} + W_{adhesive} + W_{error} + W_{rampdown} \quad (3.69)$$

It is up to the user to generate the weight error depending on the application. In the context of this thesis the weight error is not included in the estimation of the total fuselage weight.

3.6.1. Frames weight estimation method

The method described above does not take into account the frames in the design of the fuselage. In order to gain higher accuracy in the results of the weight estimation, a method to obtain the minimum frame dimensions to achieve positive margins of safety is developed.

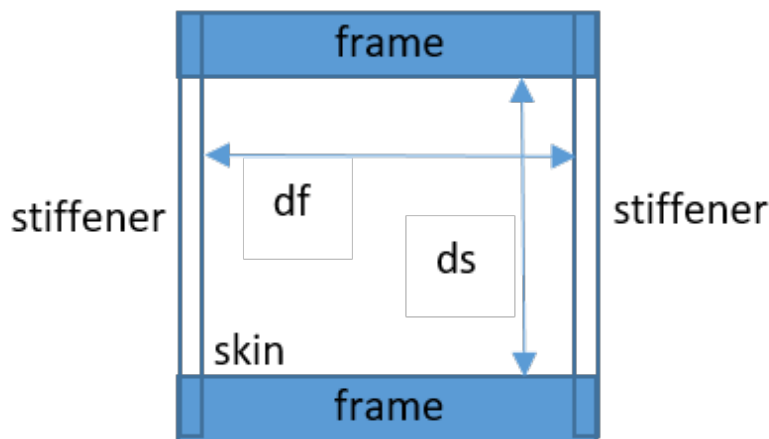


Figure 3.25: Panel description including frames

In 3.25 a single panel is depicted including the frames. In that case, a panel consists of two frames, two stringers and the skin. The skin thickness is noted as t_s , the frame spacing as d_f and the stringer spacing as d_s . From Bruhn (eq. C 7.8) and multiplying by E_f , we get:

$$2.73 \frac{E_f I_f}{d_f t_s^3} - \frac{E_f A_f}{t_s d_f} \geq 5E_f \quad (3.70)$$

Where E_f is Young's modulus of frame in the 1 (horizontal) direction, I_f is the moment of inertia of the frame and A_f is the area of the frame.

if the above structure were to buckle as a column, with skin and frames together, that buckling load would equal the load of the skin buckling alone as a simply supported plate between the frames, when the applied load is horizontal. Thus:

$$\frac{\pi^2 (E_s I_s + 2E_f I_f)}{d_s^2} = \frac{\pi^2 \left(D_{11} m^2 + 2(D_{12} + 2D_{66}) AR^2 + \frac{D_{22}}{m^2} AR^4 \right) d_f}{d_s^2} \quad (3.71)$$

The right hand side of the equation is multiplied by d_f in the numerator to get the right units (force per width). Differentiating the right hand side with respect to m and setting equal to zero we then substitute the result in the right hand side and solve for $E_f I_f$ and get:

$$E_f I_f = \frac{d_s^2}{d_f} \left(\sqrt{D_{11} D_{22} + D_{12} + 2D_{66}} \right) - \frac{E_s d_f t_s^3}{24} \quad (3.72)$$

It has to be mentioned, that in both equations above the D matrix is rotated by 90 degrees to get the D_{11} value aligned with the horizontal axis. The above equation gives the minimum value for $E_f I_f$. Substituting in the first equation and solving for A_f we can calculate the area of the frame and thus by knowing the local circumference, the volume and density, the weight of the frame can be calculated.

$$A_f \leq 2.73 \frac{E_f I_f}{E_f t_s^3} - 5t_s d_f \quad (3.73)$$

The only unknown in the equation is the E_f of the frame. Considering that, typically, frames consist of approximately 30 percent of 0 degrees plies in the circumferential direction (close to quasi-isotropic), a lower bound for the value of E_f will be about 50 GPa. Using this value we can calculate the minimum A_f . Nevertheless, the value of E_f can be an input from the user if more data about the frames are available. The final frames' weight for N_{frames} the number of frames as a total is then:

$$Weight_{frames} = \rho A_f d_f N_{frames} \quad (3.74)$$

3.7. Cost estimation

Cost estimation is the second of the two important aspects examined in this study. In order to attain accurate and comparatively fast results in manufacturing time estimation, a process based cost estimation approach will be used as the one presented in the ACCEM, (Northrop Corporation, 1976) [19]. As mentioned in Ch. Hueber et al., 2016: "The ACCEM method is widely used in the aerospace industry and considered to give reasonable results. Due to the relative age of the system one has to carefully judge possible changes affecting

the manufacturing steps before using the ACCEM time dependencies.” It is thoroughly understood that to use the aforementioned tool, some slight changes in processes have to be implemented in the design. The ACCEM uses mostly simple equations including the setup time and a parts dimension to the power of a constant to calculate the manufacturing time. [19]

In this part of the software the user will be asked to input the parameters of their design. A general flowchart of the process is depicted in the figure below ,3.26.

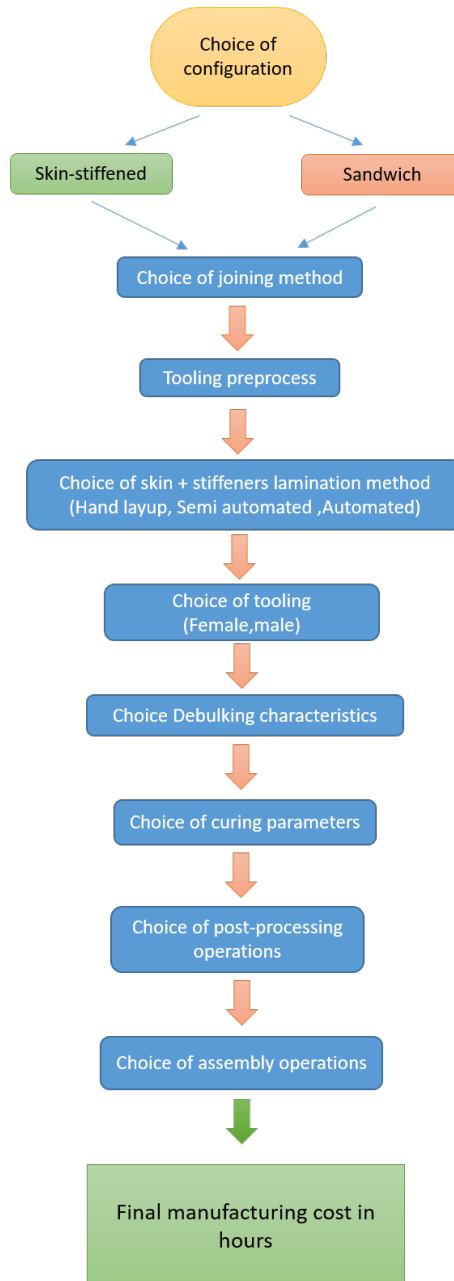


Figure 3.26: Manufacturing Cost flowchart

3.7.1. Advanced Composites Cost Estimation Manual (ACCEM)

In this section the characteristics of the cost estimation according to ACCEM will be analyzed, both for skin-stiffened and sandwich configurations. The sets of equations used are split in four categories. First of all, the appropriate skin's operations, secondly the stiffeners' or core's operations, thirdly the curing operations and finally the post-processing ones. The cost estimation process takes into consideration all the panels and stiffeners of the design in combination with different manufacturing configuration choices and comes up with a final summation of the separate manufacturing costs in terms of processing hours.

First of all, a choice about the joining method needs to take place. The skin and stiffeners can be joined by the following methods:

1. Co-curing of preformed stringers and skin
2. Separate adhesive bonding of cured skin and stringers
3. Co-bonding of cured stringers and un-cured skin
4. Fastening of cured skin and stringers

3.7.1.1 Skin Operations

The skin operations are split in two categories, pre-processing and lamination. The pre-processing phase includes the tool clean-up, application of release agent, trimming and positioning templates required. The lamination phase consists of the choice of lamination method (Hand layup, Semi-automated and automated placement), the increments due to curvature and the debulking time. All the units mentioned in this chapter are in inches so a conversion in mm need to be done in the software. The post-processing time is:

$$(0.000018) A_{part} + (0.00011) P_{part} \quad (3.75)$$

Where P_{part} is the perimeter and A_{part} is the area of the panel. Then the positioning with the use of templates depends on the number of templates (N_{temp}) used in the process.

$$[0.000107(A_{part})^{0.77}](N_{temp}) \quad (3.76)$$

For each of the lamination methods chosen by the user there are three options of material, 3 in tape, 12 in tape and woven for the hand layup only.

- Hand-layup
 - 3 in tape: $0.05 + 0.0014L^{0.6018}$
 - 12 in tape: $0.05 + 0.001454L^{0.8245}$
 - woven: $0.05 + 0.000751A_{ply}^{0.6295}$
- Semi-automated
 - 3 in tape: $0.1 + 0.000368L^{0.8446}$
 - 12 in tape: $0.1 + 0.001585L^{0.558}$
- Automated

- 3 in tape: $0.15 + 0.00063L^{0.4942}$
- 12 in tape: $0.15 + 0.00058L^{0.5776}$

Where, L is the longest ply dimension and A_{ply} is the ply's area. The increment due to curvature has three options as well, tape on male tool, tape on a female tool and woven on tool. The parameter L_b refers to the length of the panel in the longitudinal direction and R is the fuselage's radius of curvature.

- Tape on male tool: $\frac{(0.01)}{R^{0.5932}} L_b$
- Tape on female tool: $\frac{0.0064}{R^{0.5739}} L_b$
- Fabric on tool: $0.0007 + \frac{0.00444}{R^{0.5958}}$

Finally, the debulking time is calculated for either a disposable or a reusable vacuum bag and a choice is made by the user about the number of plies after which debulking takes place.

- Disposable bag: $0.02 + 0.00175A_{part}^{0.6914}$
- Reusable bag: $0.02 + 0.000557A_{part}^{0.815}$

3.7.1.2 Stringer Operations

For the case of stringer manufacturing costs, two can be distinguished regarding the layup technique.

1. Layup is done in a layup tool and then transferred to the curing tool
2. Layup is done directly on curing tool

The lamination choices mentioned above for the skin operations are exactly the same with the ones followed for stiffeners lamination and will not be mentioned again in this section. Additionally, for the stiffeners' operations the following manufacturing costs are included.

- Positioning template: $0.000107(Aply)^{0.77}$
- Transfer ply from template to cure tool: $0.000145(Aply)^{0.6711}$
- Transfer stack to cure tool: $0.000145(Amaxply)^{0.6711}$
- Clean curing tool: $0.000018(Apart)$
- Aply release agent: $0.000018(Apart)$
- Transfer layup to curing tool: $0.000145(Amaxply)^{0.6711}$

The variable $Apart$ refers to the area of the part, while the variable $Amaxply$ refers to the area of the biggest ply in the part. The last four operations are omitted if the layup is done directly on the curing tool.

An extra amount of manufacturing time is added if the plies are bent over corners increasing complexity. The distinction is done between four options.

1. Around sharp male corner: $0.00007L_b$
2. Into sharp female corner: $0.00016L_b$
3. Over gradual male radius: $0.0007L_b$
4. Into gradual female radius:
 - $0.00016L_b$ for $R < 2$ in
 - $\frac{0.00047}{R^{1.3585}} L_b$ for $R > 2$ in

In the case that the layup lies on a curved surface an additional time penalty is added to the cost for tape/fabric stretching or shrinking and .

- Tape stretch $\frac{0.01}{R^{0.5532}} L_b F^{0.7456}$
- Tape shrink $\frac{0.0064}{R^{0.5379}} L_b F^{0.5178}$
- Fabric stretch or shrink $[\frac{0.00494}{R^{0.5958}} + 0.0007] L_b$

Where F is the flange width.

For the debulking process the same equations are used as for the skin operations. the only difference here is that the A_{part} parameter is equal to $(w + h)L_b$, with w the width of the stiffener's flange and h the height of the web.

3.7.1.3 Core Operations

The core operations refer to all the processes that need to take place in the manufacturing phase of the sandwich structure. The process is exactly the same for the skin part of the structure but the core needs additional handling in order to make it ready for assembly with the laminated skin. The core operations used as mentioned by the ACCEM are the following:

- Sawing
 - Handling: $0.0004543A^{0.3810}$
 - Sawing: $0.05 + (0.000663T^{0.423})L$
- Machining
 - Handling: $0.002657A^{0.5051}$
 - Flat: $0.5 + 0.0002(w/1.5)(L + 6)$
 - Contour: $0.6 + 0.00005(4w)(L + 6)$
 - End mill step: $0.11 + 0.0006wL$
 - End mill scarf: $0.11 + 0.0006wL$
 - End mill step: $0.11 + 0.0009L$
 - Cutout: $0.01 + 0.0120(N)$

- Forming
 - Hand: $0.05 + 0.000008A^{1.208}$
 - Power brake: $0.0008L^{0.5268}$
- Setup
 - Per die change: 0.12
 - Per die reposition: 0.03
- Liquid potting: $0.05+0.0105V$
- Tape foaming: $0.05+0.0257V$
- Cleaning: $0.05 + 0.00046V^{0.4257}$
- Splicing/Bonding
 - Apply Adhesive: $0.05 + 0.000055A_a$
 - Handling: $0.0015A^{0.6311}$

Where, A is the core area, T the core thickness, L the length of cut, w the maximum width of cut, N the number of cutouts, r the radius of curvature, V the volume to be potted, A_a the adhesive application area and A the part area.

3.7.1.4 Curing Operations

After the lamination phase, the curing takes place. Depending on the choice of joining method the curing can be done in one process or separately for each of the sub-components. The details of curing mentioned below are the same for the two options and the only difference is that the total cost is calculated for each part. Thus, for a single curing phase the following processes exist:

- Setup: 0.07
- Gather details and prefit: $0.001326(A_{part})^{0.5252}$
- Apply adhesive(if present): $0.000055A_{adh}$
- Assemble details: $0.000145(A_{part})^{0.6711}$
- Apply porous film and non porous film and vent cloth: $0.0000456(A_{part})$
- Apply bleeder ply: $0.00002(A_{part})$
- Install vacuum lines: $0.0062N_v$
- Install thermocouples: $0.0162N_t$
- Apply vacuum bag: $0.000018A_{part}$
- Apply double sided tape, seal and clamp edges: $0.0093P_{part}$

- Connect vacuum lines: $0.0061N_v$
- Smooth bag down: $0.00000072A_{part}$
- Check seals: $0.000017P_{part}$
- Disconnect vacuum lines: $0.0031N_v$
- Roll tray in Autoclave: 0.055
- Load part on tray: $0.000174(A_{part})^{0.6711}$
- Connect thermocouples: $0.0092N_t$
- Connect Vacuum lines: $0.0061N_v$
- Check bag: $0.0000072(A_{part}) + 0.00027P_{part} + 0.0088N_v$
- Check Autoclave, cure cycle, shutdown and open: 0.181

Where N_v is the number of vacuum lines, N_t the number of thermocouples, A_{part} the area of the part to be cured and P_{part} the perimeter. After the curing is finished there is a set of processes that take place in order to get the part out of the auxiliary materials and machinery. The cost for these processes is calculated by:

- Disconnect thermocouples: $0.0035N_t$
- Disconnect vacuum lines: $0.0031N_v$
- Roll tray out of Autoclave: 0.012
- Remove layup from tray: $0.000164(A_{part})^{0.6711}$
- Remove clamps: $0.00007P_{part}$
- Remove vacuum bag: $0.0000096A_{part}$
- Remove thermocouples: $0.0095N_t$
- Remove vacuum fittings: $0.0029N_v$
- Remove auxiliary materials: $0.000054A_{part}$

The summation of the above leads to the total cost for the aforementioned phases.

3.7.1.5 Post-processing Operations

The last part of the cost estimation method as described by the ACCEM consists of three parts, the trim and drill operations, the hole operations and the final part handling operations.

For the trim and drill phase the following operations add to the total cost:

- Hand routing: $0.05 + (0.0066t^{0.9219})L$
- Machine routing: $0.2 + 0.0015L$
- Hand sawing: $0.02 + (0.0046t^{0.6624})L$
- Machine sawing: $0.05 + (0.0022t^{0.6749})L$
- Hand sanding: $0.02 + 0.0005L$
- Portable tool sanding: $0.02 + (0.0012t)L$
- Machine sanding: $0.25 + (0.00046L)p_n$

Where, t is the average thickness of the laminate, L is the trim length and p_n is the number of passes done in the process.

For the hole operations the following options exist:

- Drilling: $0.05 + (0.01693D^{0.387}z^{0.4562} + 0.0006)Q$
- Reaming: $0.05 + (0.0218D^{0.2747}z^{0.8333} + 0.0006)Q$
- Counter boring: $0.05 + (0.01693D^{0.387}z^{0.4562} + 0.0006)Q$
- Counter sinking: $0.05 + (0.0006 + 0.0045D^{0.725})Q$
- Hole punching: $0.05 + 0.0036Q$
- Hole sawing: $0.05 + (0.01293z^{1.10151} + 0.0006)Q$

Where, D is the hole diameter, z is the hole depth and Q is the number of holes.

The last phase of the cost estimation is the final part handling taking into account the internal fixtures, clamps and inserts added to the assembly.

- Part, external fixture and templates handling: $0.000145(A_{part})^{0.6711} + 0.00777(A_{part})^{0.2894} + 0.000107(A_{part})^{0.7106}$
- Internal fixture handling: $0.00414(A_{part})^{0.03264}$
- Clamp handling: $0.000322P_{part}$
- Insert handling: $0.0007N_{inserts}$

In the case of fastening as a joining method the following equations are used:

- Fit-up included: $2.9 * 0.019N_{fasteners}$

- No fit-up: $0.019N_{fasteners}$

The number of fasteners $N_{fasteners}$ is defined by the fastener spacing and the panel's perimeter P_{panel} . The fastener spacing is calculated with the use of the hole diameter and for the current study it is set to be equal to six times the diameter according to the rules given by the book of Kassapoglou (2009), chapter 11. The number of fasteners is calculated with the following equation:

$$N_{fasteners} = \frac{P_{panel}}{6D} \quad (3.77)$$

The same procedure is followed for the stiffeners fastening to the skins, changing the panel perimeter variable with the stringer's length. Having all the required equations, the summation of the total cost in manufacturing hours can take place and the final result for the cost estimation is calculated.

3.7.2. Cost estimation limitations and suggestions

It has to be mentioned that in such an early stage of the design the cost would not approximate, accurately, the final cost and there is a risk of divergences. These discrepancies might occur due to various reasons that have to do with material, tooling, change in loading conditions or even changes in the already given design. For example, the material chosen in the beginning of the process might not be available in the future and the use of another material, inferior or superior in properties, will lead to higher weight and/or cost. Additionally, the stiffeners dimensioning might lead to manufacturing feasibility problems and changes in the tooling and process increasing the overall cost. Last but not least, assumptions made in early stages about loading conditions of a new aircraft design might be inaccurate and lead to changes in structural loads, thus influencing the weight and cost of structural parts and joining areas. In the context of this research, considering the intended use, and the bottom-up nature of the software, the aforementioned will not be a troubling factor. The comparative nature of the software will provide sufficient results for the decision making process. For verification purposes, though, the results of the software need to be cross-checked with similar projects' manufacturing costs. This process will clarify the discrepancies in the software and a cost error factor can be introduced to account for them.

3.7.3. Aluminium design cost estimation

The aforementioned procedure for the cost estimation based on the ACCEM refers to a composite design cost estimation method. In order to account for aluminium designs to do comparisons in the current study a separate procedure based on aluminium designs cost estimation takes place. The whole estimation is based on the fact that for an aluminium design, the assembly cost is about 60 percent of the total cost. Given in the ACCEM and with small corrections because we are dealing with metal design, the assembly cost using fasteners is:

$$A_{assmetal} = 0.1296 + 0.0124P_{part} + 0.000138A_{part} + 0.00011(A_{part})^{0.8586} + 0.127N_{fasteners} \quad (3.78)$$

Where P is perimeter of part, A is area of part and n is number of fasteners. P is in inches and A is in square inches. Suppose that we have an assembly with adhesive and assume that fasteners exist every 1 inch along the connection, the equation above is multiplied by

a factor of 0.8 to account for adhesive bonding. The final aluminium cost is given by:

$$Cost_{Al} = \frac{Cost_{Assembly}}{0.6} \quad (3.79)$$

3.8. Trade off studies

One of the goals to be achieved for this research is the evaluation of different scenarios and configurations. That is a separate step before the optimization process to assess the trends of different decisions in the design both in cost and weight. Such trade studies will be the effect of different configurations, the effect of changing stiffeners and frames spacing, the effect of changing stiffeners dimensions and type, the effect of changing core dimensions and also the effects different manufacturing decisions have in both weight and cost. The aforementioned are structural parameters influencing both weight and cost. Cost parameters that influence both are the choice of different bonding methods, the choice of different lamination methods (hand layup, Automated fiber placement, etc.), the curing parameters, assembly parameters and post processing. Several predefined designs will be tested in order to attain the desired trend curves. A similar method, focused on weight trade-offs for wing box design, is followed by G. Moors, 2019[2].

3.9. Weight and Cost optimization

The final step of the main process of this study is the weight and cost optimization of the desired design in order to be able to assess the viability of it. As mentioned in the literature study (Chapter 2) a lot of attempts to approach a weight and cost optimization have been done until today (T. Führer et al., 2015; C. Kassapoglou, 1999a; P. Apostolopoulos, C. Kassapoglou, 2008; M. Lee et al., 2012). Most of them rely on high fidelity models for single panels of airframe components. In the study presented, a more simplified approach will be followed for the optimization process. This approach, though simplified, aims to achieve realistic results in that phase of the design. The approach goes as follows in a stepwise configuration:

- Create initial design.
- Run weight and cost estimation software.
- Record panels with critical margins of safety.
- Reduce-Increase layers according to composite design 'rules of thumb' (C. Kassapoglou, chapter 11, 2010). For example, if the dominant load is buckling reduce of 45 degrees layers in forbidden. Symmetric and balanced laminates are always examined.
- Assign new layups to changed panels.
- Calculate load distribution due to changes.
- Record weight and cost.
- Repeat until optimum is reached (all margins of safety are between desired limits and convergence in weight is achieved).

3.9.1. Composite design rules of thumb

The laminate will be updated following the design rules of thumb presented in the book of Kassapoglou (2009) [1]. These rules are given below and they will be optional for the user to be applied in the design process. Several trade studies can come out of these designs helping understand the influence of each rule to the final weight and cost of the fuselage.

1. Laminates should be symmetric. This means that the stacking sequence, in which the plies are laid up should be mirrored with respect to the mid-plane. Using symmetric laminates leads to a B matrix equal to zero, thus eliminating membrane/bending coupling.
2. Laminates should be balanced. This means that for every θ ply there should be a same $-\theta$ ply, eliminating stretching/shearing coupling ($A_{16} = A_{26} = 0$).
3. Laminates should respect the 10 percent rule. This rule constraints the ply degrees percentage in each laminate. Thus, at least 10 percent of the plies should be in the principal directions 0, 45, -45, 90 degrees. The application of this rule helps in avoiding unwanted failure in secondary loadcases.
4. Laminates should contain no more than four unidirectional plies of the same direction next to each other. This rule helps in crack arresting.

The design rules of thumb mentioned above refer to the stacking sequence of the laminate. There are also some design rules of thumb mentioned in the book regarding the loading conditions and the performance of the structure. These rules will be followed by the software as well, depending on the user's choice.

1. Use of 0 degrees plies as far away from the neutral axis. This rule improves the bending stiffness of the laminate by maximizing the D_{11} component of the D matrix.
2. Use 45/-45 plies as far away from the neutral axis. This rule improves the crippling and buckling of a laminate by maximizing D_{66} .
3. Use fabric plies on the outer side of the laminate. This rule improves the damage resistance of the laminate.
4. The skins and stiffeners' webs, should be consisting mainly of 45/-45 degrees plies. This improves the shear stiffness and strength.

3.10. Programming language

It is clear from the methodology described that there is no physical experimental set-up used for this study. Nevertheless, the development of a software of this magnitude can be considered as an experimental set-up. The programming language used in the study is Matlab™ due to the experience of the researcher and the possibilities and freedom to the user it provides.

Software Description

In this chapter the theory's implementation, presented in chapter 3, into the MATLAB-code is explained in detail. The chapter consists of four sections. In the first section an overview of the program's logic is given, the user input files, the outputs and limitations of the software are explained. In the second section, the software's data flow is explained introducing the developed functions and their role in the software. In the next section the key functions and their usage are explained and in the final section the post processing capabilities of the software are being introduced.

4.1. Software Overview

The software's purpose is to provide the weight and cost for a given fuselage configuration by modifying the laminates layup and components' geometry or number. The various margins of safety, as described in chapter 3.3, are examined and kept in user specified ranges. To achieve that, the lay-up of the different sub-components is modified according to user specified laminate rules, either adding or removing plies to achieve the desired ranges. When this requirements are met, the software stops the iterative process and outputs the final result in terms of weight and cost. Additionally, the batch mode of the software gives the possibility to the user, to produce trade-offs and choose between several feasible designs. A set of functions is developed in order to achieve the goal of the study. The main program will provide all the required input data from the user and then separate functions will be used to calculate material properties, laminate properties, stringer properties, margins of safety, panel deflections and cost. Regarding cost, the main program will call a function where the user is asked for several input data or an input file can be given in the optimization process. The program will also use external input databases about material properties and/or loadcases. This program will run an iterative process in order to achieve the optimum results. In the flowchart below 4.1, the general process is depicted.

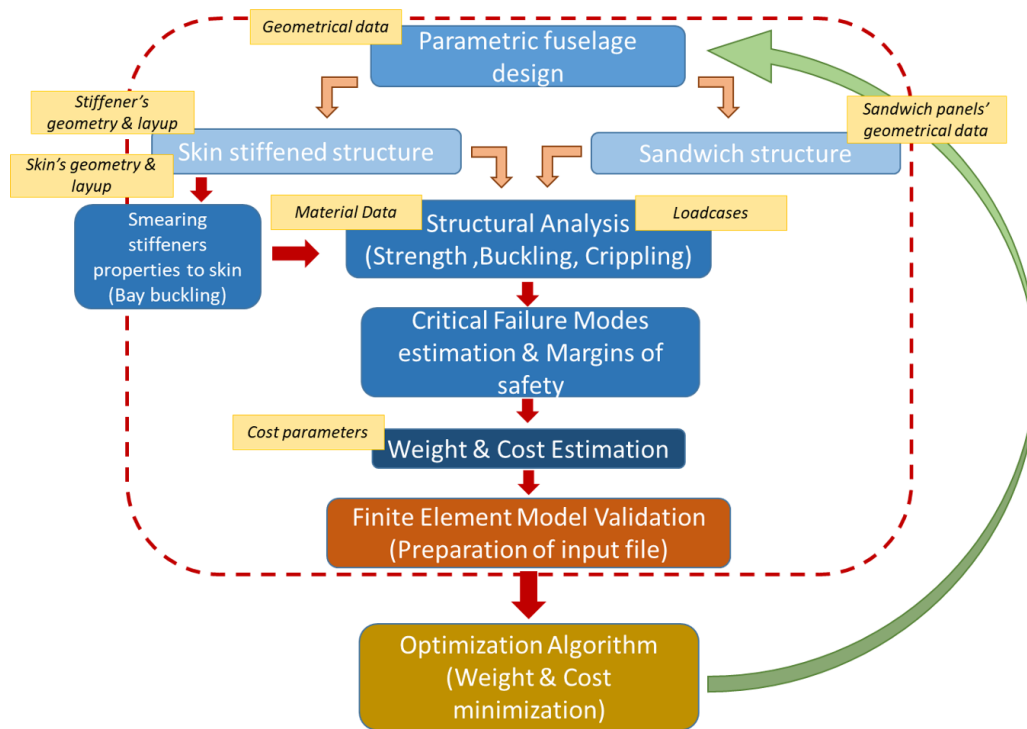


Figure 4.1: Process flowchart for the approach presented

4.1.1. Input files

There are multiple ways to introduce input in a software of this nature. Depending on the user's needs the software can be adapted to accommodate different input files or input the required parameters via a user interface. In the context of this study, several inputs were tested in order to conclude to a more user friendly and at the same time fast input. In the early stages, the software developed used to ask input from the user while the main program was running, including safety loops to account for non-applicable values, choices about input files from material and loading databases. This approach, though useful for one case study proved to be time consuming for the user. To improve that, and in order to run a large variety of designs and optimization loops, separate input files were introduced. These files can be found in the main folder of the software and modified by the user accordingly. The only input that is asked by the user when the main program is running is the configuration type. Thus, the parameter `conf` is either [1] for the skin-stiffened structure or [2] for the sandwich structure.

The aforementioned files are split in three types. The first one (`Input_def.m`) includes the decisions about the configuration (skin-stiffened or sandwich), the geometry of the fuselage (skins and stringers/cores dimensions and type) and the fuselage station's z coordinate, the layup and material information, the application of knockdown factors, the design rules of thumb applied and finally the type of loadcase and failure criteria used for the evaluation of the strength of the design.

The second input file (`Material_Database.xlsx`) is the material database created in an excel file. This file was created using several standard CFRP materials, both unidirectional and woven, core materials and aluminium. The user can modify this file, adding extra materials in the database, depending on the application. The interaction between the user and this input is done through the main input file described above (`Input_def.m`), where the user

can change the second column of the stacking sequence matrix (sts_s). Depending on the material's position in the .excel file each material gets a specific number. For instance, in the figure given above 4.2, the material with number 3 is a woven material and the material with number 4 is a unidirectional tape as given in the .excel file. The basic structure of the database is as follows.

Table 4.1: Material database structure

| Material Name (No.) | | AS4/3501-6(1) | Units |
|-----------------------------------|--------|---------------|----------|
| Longitudinal stiffness | E1 | 126000 | MPa |
| Transverse stiffness | E2 | 11000 | MPa |
| Shear modulus | G12 | 6600 | MPa |
| poisson's ratio | v12 | 0.28 | - |
| poisson's ratio | v21 | 0.024 | - |
| Tensile strength (1 direction) | Xt | 1950 | MPa |
| Compressive strength(1 direction) | Xc | 1480 | MPa |
| Tensile strength (2 direction) | Yt | 48 | MPa |
| Compressive strength(2 direction) | Yc | 200 | MPa |
| Shear strength (12 direction) | S12 | 79 | MPa |
| Shear strength (23 direction) | S23 | 79 | MPa |
| ply thickness | t | 0.14 | mm |
| density | ρ | 1.5 | kg/m^3 |

The third input file (Load_def1.m/Load_def2.m) provides the required loading data to the software. Again, the choice of the loading condition is done through the main input file (Input_def.m) in the last rows. Modifying the parameter nloads according to the desired loading condition the software loads the appropriate loadcase from the Load_def1.m or Load_def2.m files. There are several options for the user to select. With a numbering from 1 to 3 the user can choose between pressure alone (1), Upbending (2), Downbending (3). Furthermore, in order to run multiple loading conditions in one model, the user has the option to apply torsion and pressure to the already existing loading conditions. Thus, a combination of loads can be examined by the software. This is done by modifying parameters tor and pr. The value of [1] stands for YES and [2] for NO. It has to be mentioned that both input files for loading include the vertical shear introduced by the loading conditions of upbending and downbending. The loadcases data used for this study were provided by GKN Fokker for a reference aircraft project. The moment and force curves were then imported in the Load_upbending.m and Load_downbending.m functions. Further analysis of this functions will be done in section Key Functions.

The input files mentioned until now have to do mostly with the structural analysis of the fuselage. Two more input files were introduced to account for the cost required inputs, one for each different configuration. Thus, only one of them is used for each run. The cost input files for the two configurations are named Cost_stiff_input.m and Cost_Sand_input.m respectively. The cost input files include all the parameters mentioned in chapter 3.7.1 and the user has the freedom to choose between different manufacturing decisions.

```

%% Laminates rules of thumb
symmetric=1;
balanced=1;
ten_per=1; %10 percent rule
con4=1;     %4 continuous UD layers
%% Skin-Stiffened
if conf==1
    R=1500; %radius
    L=5000; %length
    n_str=28; %number of stringers
    n_fr=5; %number of stringers
    sts_s=[45,0,-45,90,90,-45,0,45]';%quasi-isotropic composite
    sts_s=[sts_s,[3,4,4,4,4,4,4,3]'];
    Knock_choice=1; %Knockdown [1]YES,[2]NO
    str_type=2;%[1]T,[2]C,[3]J,[4]Hat stringer type
    b1=10; %upper flange width
    b2=20; %web height
    b3=10; %lower flange width
    an=45; %angle if stringer is hat
    geom_opt=2;%[1]YES,[2]NO
    sts_f=[45,-45,0,90,0,90,0,-45,45]';%quasi-isotropic composite
    sts_f=[sts_f,[4,4,4,4,4,4,4,4,4]'];
    sts_w=[45,-45,0,90,0,90,0,-45,45]';%quasi-isotropic composite
    sts_w=[sts_w,[4,4,4,4,4,4,4,4,4]'];
    FC_type_s=3; %[1]Tsai Wu,[2]Tsai-Hill,[3]Max Stress,[4]Puck
    pz=18;pz=-0.00689475729*pz; %Pressure in psi
    nloads=2; %[1]Pressure only,[2]up bending,[3]Down bending
    tor=2; %Apply torsion [1]YES,[2]NO
    pr=2; %Apply pressure [1]YES,[2]NO

```

Figure 4.2: Code part of the (Input_def.m) file

4.1.2. Output

Since the purpose of this software is to provide the minimum weight and cost for a given design, the desired outputs are two, the final weight and cost of each design. The software makes an attempt to minimize weight and afterwards it calculates the associated cost. Nevertheless, there are also other output data that are helpful for diagnostic purposes or post processing and this data need to be saved so that they could be accessed and used afterwards. While the main optimization file is running there are several outputs displayed in the command window.

First of all, the current time is displayed and the software asks for the configuration type. Then the time for each of the process of the sequence is displayed. As depicted in the figure above 4.3 the input is loaded first, then the layup and stringers properties and loading conditions. Secondly, running the basic structural analysis functions for the initial file, the failure strength and buckling margins of safety are calculated. Afterwards, having calculated the structural aspects, the weight is calculated and the cost of the design and their processing time is displayed. In the following step, the optimization starts and that is stated in the display. The number of each iteration is displayed as well until a final solution is obtained. Then an indication about the program's end is given and the final weight and cost are displayed along with the end time and the total run time of the program.

In the case of solving a batch of possible designs the required data for post processing are being saved in Matlab database files. The variables that are saved as structured variables are:

- MS: Margins of safety for every failure type examined
- skin: Skin properties and characteristics
- stringer: Stringers properties and characteristics
- core: Core properties and characteristics
- R: Radius of design
- L: Length of design
- n_str: Number of stringers
- n_fr: Number of frames
- a: Panel's length
- b: Panel's width
- Load: Applied loadcase data
- RunTime: Total run time of the process
- result: The weight and cost results for each iteration
- it: Iterations number
- PID: Panel identification matrix consisting of nodes for each panel
- panel_num: The number of total panels
- Askin: Skin's area used in cost calculation
- Pskin: Skin's perimeter used in cost calculation
- conf: Type of configuration

An example of the Matlab command window is given below.

```

Current Time: 21:22:34
-----
Please choose the configuration type: [1] Skin-stiffened structure, [2] Sandwich structure1
Input loaded: 2.731 seconds
Layup loaded: 21.3526 seconds
Stringers loaded: 8.6573 seconds
Loading conditions loaded: 0.32227 seconds
Failure strength loaded: 2.2488 seconds
Buckling MS loaded: 8.0957 seconds
The initial cost is:882.3479hours
Cost loaded: 0.14351 seconds
The initial mass is:111.3838kg
Weight loaded: 0.089239 seconds
-----
Starting optimization process
Iteration number 1:2
Iteration number 1:3
|           |
Iteration number 1:16
Iteration number 1:17
Program ended
Final structural weight: 125.3081 kg
Final cost: 886.2718 hours
-----
End Time: 21:25:30
Total run time: 176 seconds

```

Figure 4.3: Matlab command window output example

4.2. Data flow and functions introduction

In this section, the basic data flow and software's tasks will be explained. The software provides two possibilities for the user, a single design analysis program and a batch design analysis program for the creation of trade studies. The differences between the two programs will be clarified in the following sections. Having setup the input files the main program can be executed. The usage of the main program is to call the separate functions created for the analysis and output the desired data to the user. The whole logic of the software is to be split in smaller functions for ease of use and debugging. In that way, the user can access each function and modify the code depending on the problems occurring or the updates that need to be done according to the user's needs and requirements. The basic functions tasks will be introduced here and a process flowchart is given in the end to understand the interaction between the functions and the data flow. Finally, the inputs and outputs of the functions will be explained as well. The inputs come both from the input file and other functions executed before the execution of the current function.

Table 4.2: List of functions and their basic tasks

| Function | Sub-Function | Task |
|-------------------|--------------------|----------------------------------------------------------------------------------------------------------|
| Geom_def | - | -Fuselage geometry creation -Panels definition |
| - | GPID | Creation of matrices including: -nodes' id -panels' nodes id -stringers' nodes id |
| Initial file | - | -Creation of the initial structural and cost characteristics |
| - | Mat_def_v2 | -Load materials database |
| - | Lam_def_v2 | -Creation of laminate |
| - | ABD_v2 | -Creation of ABD matrix -Laminate properties calculation |
| - | Stringer_props_v2 | -Stringer geometry creation -Stringer laminate properties calculation |
| - | Sandwich_props | -Calculation of sandwich properties matrix |
| - | Iyy_def | -Structural idealization and moment of inertia calculation |
| - | Pressure_loads | -Deflection, Moments and Shear forces, due to pressure, calculation at each panel |
| - | Load_def_1/2 | -Load loadcases data and distribute to structural elements |
| - | ILSS_def | -Calculation of Interlaminar shear stresses |
| - | RF_def_vs/vf/vw | -Calculation of stresses and strains -Calculation of margins of safety for laminate ultimate strength |
| - | Buckling_def_v1/v2 | -Calculation of margins of safety for buckling types |
| - | Crimping_def | -Calculation of margins of safety for crimping and dimpling |
| - | Wrinkling_def | -Calculation of margins of safety for wrinkling types |
| - | Weigth_def_s/sand | -Calculation of total weight of the structure |
| - | Cost_def_s/sand | -Calculation of total cost of the design |
| Optimistic12/3 | | -Optimize structure for given range of margins of safety |
| - | Feed_s1/f1/w1 | -Add layers according to laminate rules |
| - | Jenga_s1/f1/w1 | -Remove layers according to laminate rules |
| Optimization file | - | -Similar to the initial file. Calculation of all the parameters for updated designs. |

4.3. Key Functions

The key functions mentioned in section 4.2 will be explained in depth in this section. These functions make use of the theoretical basis explained in chapter 3 and as a whole they fulfill the goal of this study, the weight and cost analysis of a fuselage structure. The section starts by introducing the geometry creation for the fuselage and stringers. Following is the definition of the laminates and materials, structural idealization and properties. Then, the loading distribution according to different loadcases is described and the margins of safety calculation. The weight calculation and cost estimation comes next. Finally, the weight optimization functions are described and the logic behind the laminates updating to achieve optimum designs between specific margins of safety range.

4.3.1. Fuselage geometry creation

The first task of the software is to create the appropriate geometry for the fuselage and stringers or core (for sandwich structures). The function `Geom_def` is responsible for the creation of the basic dimensions. This function calls another function in order to create the matrices needed for the nodes representing the structure, the nodes of each panel and stringer. The creation of these matrices finds use both in the software and in future steps. Using these matrices would be useful for the creation of finite element models given the required file format. Furthermore, the function calculates the panels' area and perimeter and the whole parts' area and perimeter, values used in the cost estimation.

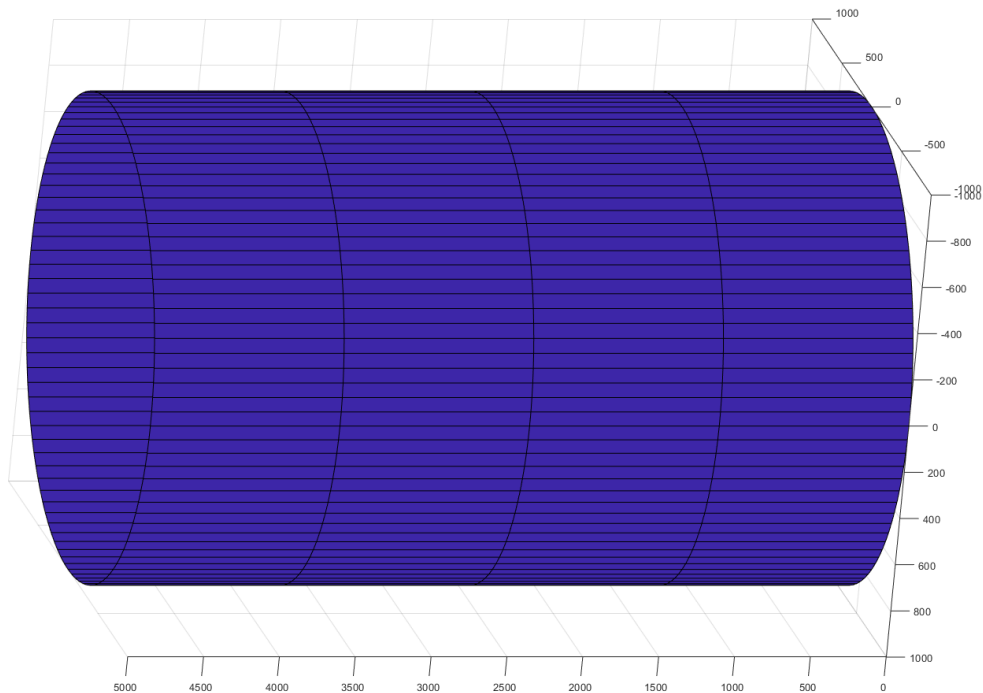


Figure 4.4: Fuselage geometry

In figure 4.4 the representation of the basic geometry is given. The geometry is split in

panels based on the number of frames and stringers defined by the user in the input file.

$$\text{Stringer_spacing} = \frac{2\pi R}{\text{Number_stringers}} = b \quad (4.1)$$

$$\text{Frame_spacing} = \frac{L}{\text{Number_frames} - 1} = a \quad (4.2)$$

Then, using function GPID.m the nodes are created and the required matrices mentioned above. The nodes matrix GID includes the nodes x,y and z coordinates in a Cartesian coordinate system after a transformation from the cylindrical system takes place. Afterwards the panel id matrix (PID) is created including the panel number and the four nodes enclosing it. Finally, the stringer id matrix (STRID) is created with the stringer number and the two nodes enclosing it. The following tables give an example of the representation of these matrices.

Table 4.3: PID and GID matrices

| PID | n1 | n2 | n3 | n4 |
|-----|-----|-----|-----|-----|
| 1 | 1 | 2 | 106 | 105 |
| . | . | . | . | . |
| . | . | . | . | . |
| n | 416 | 313 | 417 | 520 |

| GID | x | y | z |
|-----|--------|--------|-------|
| 1 | 0 | 1000 | 8128 |
| 2 | 60.37 | 998.17 | 8128 |
| . | . | . | . |
| n | -60.37 | 998.17 | 13128 |

The next step is the creation of the stringer's geometry. This is done with the use of function *Stringer_geom.m*. As mentioned in chapter 3, the user can choose between several stringer types (T, C, J, Ω) by modifying the input file accordingly. The variable responsible for the stringer type is named *str_type* and takes the values of 1-4 respectively. The dimensions of the stringers depending on their type are given in the input file by the user. In the case of an Ω stringer the angle of web is defined as well and the other dimensions are calculated by the software to achieve a feasible design. It has to be mentioned that the width of the flanges is the same for top and bottom flange in all stiffeners except the last one and there are several manufacturing limitations as well that will be explained in the following sections. In the following graph an example of the stiffeners dimensions is given.

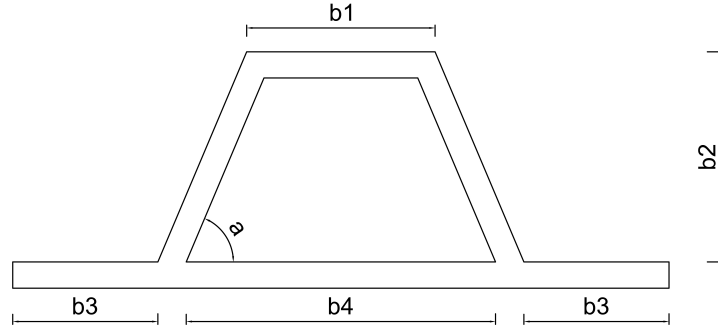


Figure 4.5: Omega stringer geometry

By defining the values for b_1 , b_2 , $b_3 = b_1$ and the angle a , the function calculates the value of b_4 using the orthogonal triangle enclosed by the geometry of the stiffener and the value of the web's height b_2 .

$$b_5 = \frac{b_2}{\tan a} \quad (4.3)$$

$$b_4 = b_1 + 2b_5 \quad (4.4)$$

If $a \neq 90$ then:

$$b_2 = \sqrt{b_5^2 + b_2^2} \quad (4.5)$$

In order to calculate the properties of the cross section the software uses the equations (3.8-3.12) mentioned in chapter 3.3.1.1 and thus the neutral axis $y_$, equivalent bending stiffnesses EI_{xx} , EI_{yy} and EI_{xy} , equivalent torsional stiffnesses GJ_{str} , equivalent stiffness EA and areas A_{str} required for the cost analysis are calculated. To calculate these values, the laminate properties of each member need to be calculated beforehand. This will be explained in the following subsection.

4.3.2. Laminate properties calculation

In this part, the calculation of the laminates' properties for both skins and stringers is explained. The approach will be versatile enough to deal with layups consisting of different types of materials in the same laminate. Then the governing equations of the Classical lamination Theory (CLT) will be used to attain the laminate properties (C. Kassapoglou, 2010) [1]. Finally, a choice to apply the appropriate knockdown factors will be given to the user regarding environmental, material scatter or effect of damage factors (C. Kassapoglou, 2010). This is done in the input file as well choosing [1] for YES and [2] for NO.

The functions responsible for the calculation of the laminate properties are :

- Lam_Def_v2.m, which sets up the laminates z matrices and calculates the thickness and mid-plane.
- ABD_v2.m, which calculates the ABD matrix and the membrane and bending stiffness for each laminate.

To include multiple materials in one laminate a function to calculate the components of the Q matrix for each ply ($Q_calc.m$) was developed. This is achieved by running an iteration for each ply with different material properties, getting the Q matrix and then calculating the ABD accordingly. The material properties matrices were also modified to include different

values for each ply. All the properties of the skins and stringers are assigned to classes in Matlab for ease of use named skin and stringer. In that way, all the data needed for each component can be accessed through these structures.

The results of the created functions for properties' calculation, were verified with the results given for multi-material laminates, in chapter 13 of the book of Kassapoglou (2010)[1]. Several laminates were examined to limit the risk of inconsistencies.

4.3.3. Calculation of equivalent panel stiffness

With all the data obtained from the aforementioned steps the software is able to calculate the equivalent stiffness of each panel, both for skin-stiffened and sandwich designs. This is done in the initial file. For the skin-stiffened scenario the equations 3.45-3.48 are used to calculate the equivalent D matrix. As for the sandwich structure the equation 3.53 is used as given in chapter 3. These matrices will be used in the failure strength and buckling margins of safety calculation.

$$D_{11_{equivalent}} = D_{11_{skin}} + \frac{EI_{xx_{str}}}{b} \quad (4.6)$$

$$D_{12_{equivalent}} = D_{12_{skin}} \quad (4.7)$$

$$D_{22_{equivalent}} = D_{22_{skin}} \quad (4.8)$$

$$D_{66_{equivalent}} = D_{66_{skin}} + \frac{GJ_{str}}{2b} \quad (4.9)$$

and:

$$D_{ij} = 2(D_{ij})_f + 2(A_{ij})_f \left(\frac{t_c + t_f}{2} \right)^2 \quad (4.10)$$

4.3.4. Structural idealization

Having defined the geometry and properties of the structure's components the structural idealization as explained in chapter 3.1.1 takes place. The function lyy_def.m is responsible for the creation of booms and moment of inertia calculation for each cross section of the fuselage's station analysed. The result is a matrix with length equal to the number of frames minus 1 containing all the moments of inertia. We also, output the values of booms in square mm and the y coordinate of each boom for further use in the load distribution.

4.3.5. Load definition and distribution

The load cases definition and application to the structure was one of the most trivial aspects of the study. There is always a big difficulty to access actual load data having the structural characteristics to verify your results afterwards. Additionally, different companies or organisations keep the data in different formats and need to convert them in order to use them in another software. In the context of this study, the loading data used came from a report provided to us by GKN Fokker containing the loads of the fuselage for a certain application. The loads were provided as curves so they had to be converted into equations and then the software was able to calculate the load at each point using the equation of the curve provided. This is done in the functions Load_Upbending and Load_Downbending. In this function the Moment-Z coordinate graphs were used for bending and the Vertical Force-Z coordinate graphs were used for shear calculation.

$$\sigma_x = \frac{M_x y}{I_i} \quad (4.11)$$

Additionally, having calculated the moments, the software calculates the stress at each boom and as a single panel is enclosed by four booms, an averaging of the stresses at them is assigned as the value of stress at the panel. That will be used afterwards in the force calculation as explained in chapter 3.3.1.1. An example of the curves imported into the software is given below in the graphs for upbending, shear due to upbending and torsion.

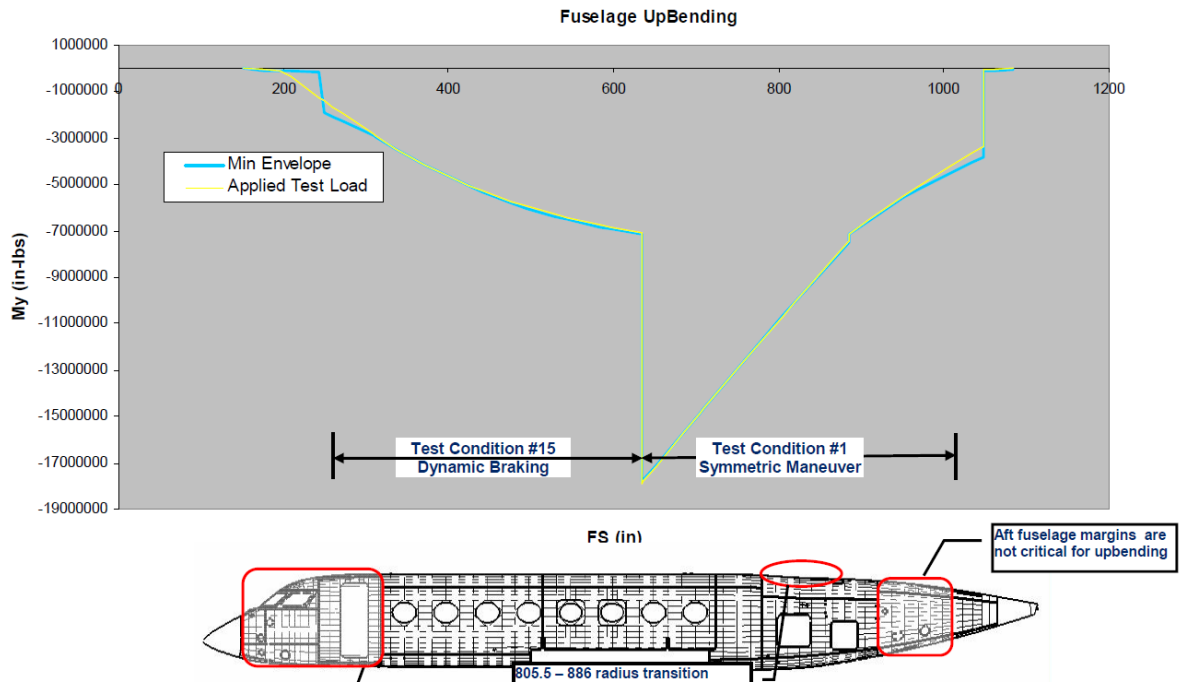


Figure 4.6: Fuselage Upbending(GKN Fokker)

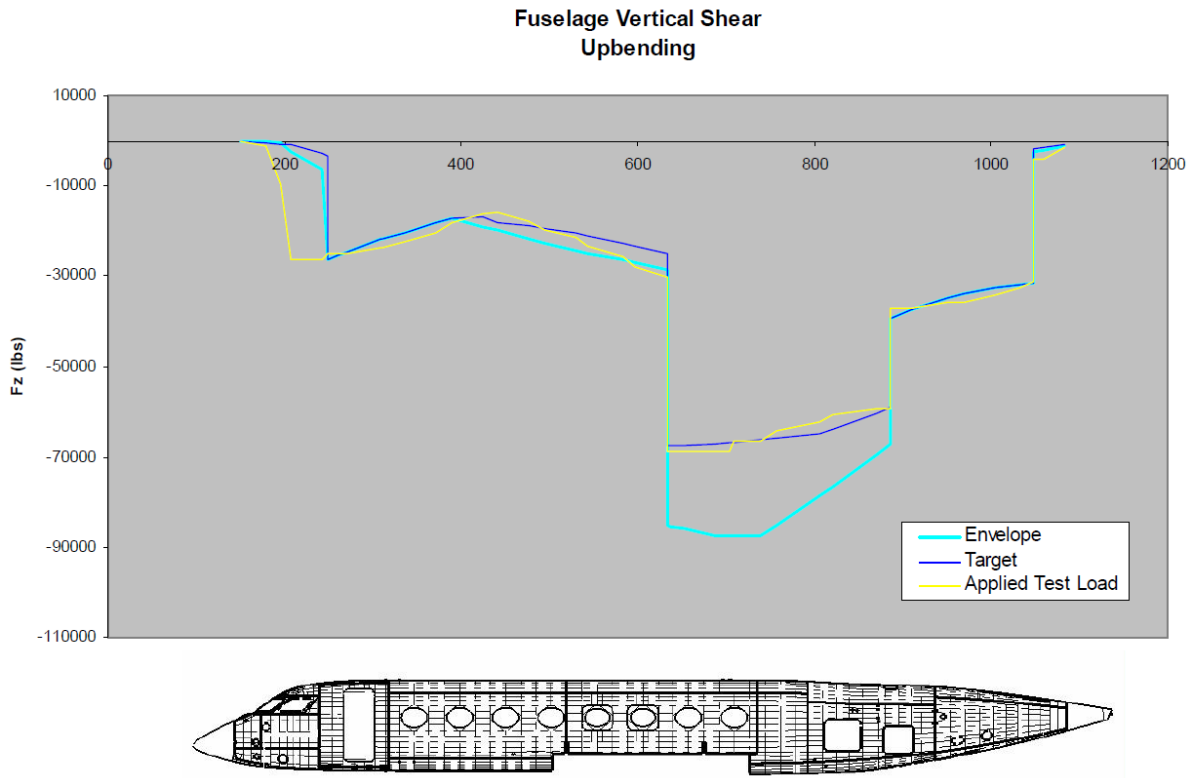


Figure 4.7: Fuselage Vertical Shear (Upbending)(GKN Fokker)

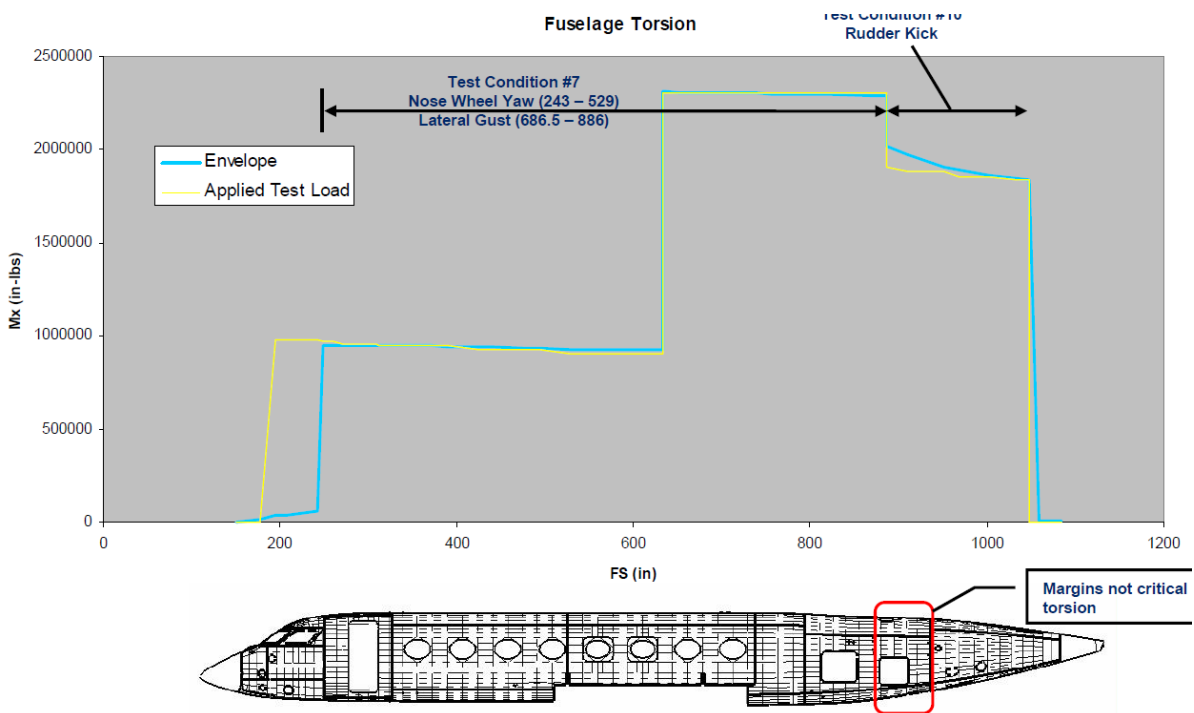


Figure 4.8: Fuselage Vertical Torsion(GKN Fokker)

It has to be mentioned that all the values in the graphs are given in inches and pounds, so a conversion to mm and Newton needs to be done in order to use them for our design.

An additional loadcase is calculated using the Pressureloads.m function. In this function the pressure given as an input in the input file is applied to each panel and the deflection along with the moments and shear forces acting on each panel are calculated. The pressure is given in psi so a unit conversion needs to take place. The desired output is calculated using equations 3.61 to 3.65 and saved in a separate matrix.

The next step is the distribution of the stress calculated as force per unit width to the structural components of the fuselage. This is done in the functions Load_def1.m and Load_def2.m for skin-stiffened and sandwich respectively.

These functions work with a set of options defined by the user in the input file depending on the desired loadcase. The logic goes as follows:

- If n=1: Only pressure load is applied
- If n=2: Only upbending and shear is applied
- If n=3: Only downbending and shear is applied
- If n=2 AND pr=1: A combination of upbending and pressure is applied
- If n=2 AND tor=1: A combination of upbending and torsion is applied
- If n=3 AND pr=1: A combination of downbending and pressure is applied
- If n=3 AND tor=1: A combination of downbending and torsion is applied
- If n=4: Only torsion is applied

With n being the loadcase option, pr the pressure addition option and tor, the torsion addition option defined by the user in the input file.

The software then distributes the forces in the panels and stringers or sandwich panels, for the second configuration, according to the methodology described in chapter 3.3 the final load format applied to each panel and member was described in 3.3.1 and is according to the CLT. However, for buckling, calculations and stringer crippling due to bending moments the loads applied to each stringer and member are saved in separate matrices as well. Finally, in order to avoid numeric errors a tolerance of 10^{-5} is used for the values of loads. If a load drops out of the range of $-10^{-5} < Load < 10^{-5}$ the value is set equal to zero.

4.3.6. Stress calculation

Having calculated the loads applied to the structure we are able to calculate the stresses and strains acting on it. To do so, the Stress_Calc_v2.m function is created. This function calculated the stresses and strains in global and principal axes utilizing the CLT. Again, a modification is made here to account for multiple materials in the laminate.

4.3.7. Failure strength calculation

The failure strength calculation for the laminates is done in the RF_def_vs.m type of functions. Taking into account, the user's choice for failure criteria given in the input file the software uses the failure criteria from 1 to 4, presented in chapter 3.4.1. The first ply failure loads are calculated as well and the ultimate laminate strength of the skins and stringer's members is derived. Finally, the reserve factors and margins of safety are given by the software as an output for their evaluation in the following steps.

4.3.8. Buckling/Crimping/Wrinkling strength calculation

Following the principles mentioned in chapter 3.4 the buckling strength for each buckling failure mode is calculated. More specifically, the software uses the load data in terms of force per unit width to calculate the critical buckling loads for each component. Then the reserve factors are calculated and the margins of safety for each panel. The software checks for skin buckling, panel buckling, column buckling of stringers and stringer OEF and NEF crippling, including the bending moments introduced by pressure loads at the stringers members. The required equations are again given in chapter 3.4. For the column buckling scenario the force is used in Newtons in contrary to the other failure modes. The function responsible for the above is named `Buckling_def.m`. To calculate the crimping and wrinkling strength the functions `Crimping_def.m` and `Wrinkling_def.m` are created. The margins of safety are saved in matrices to be evaluated later.

4.3.9. ILSS strength calculation

Having calculated the pressure loads and the shear stresses, the `ILSS_def.m` calculates the Failure strength for interlaminar shear strength and the reserve factor and margins of safety. The stresses are compared with the interlaminar shear strength provided by the datasheet.

4.3.10. Weight calculation

The goal of this software is to estimate the weight and cost of the fuselage design. The `Weight_def.m` function calculates the weight taking into account the skin and stringer laminates (thickness, density, number of plies) or cores of the structure in kilograms. An example of the calculation for a skin-stiffened design is given below:

$$weight_{skin} = \sum ab\rho_i t_i \quad (4.12)$$

$$weight_{stringer} = \sum 2b_f \rho_f t_f + \sum b_w \rho_w t_w \quad (4.13)$$

$$Weight_{fuselage} = weight_{skin} + weight_{stringer} \quad (4.14)$$

Where a is the panel length, b panel width, ρ the material density, t the ply thickness, the subscript f refers to flange and w to web of stringers. As mentioned in chapter 3.6 the additional weights are not included in the current weight calculation and it is up to the user to produce such an estimation.

4.3.11. Cost calculation

The cost calculation part is a separate part of the algorithm. There are two functions responsible for this task, one for the skin-stiffened and one for the sandwich design, `Cost-Def.m` and `CostDef_sand.m` respectively. The cost calculation follows the ACCEM as mentioned in chapter 3. The method is a sequential summation of manufacturing costs based on the users choices in the cost input file. For the calculation of the lamination cost each panel is taken into consideration, including the different layups of the laminates. The woven and unidirectional plies are split in order to calculate the different equations related to them. Two auxiliary functions are created in order to calculate cost for different joining methods, `Lam.m` and `Curing_cost.m`. The first one is responsible for the distinction between fabric and unidirectional and the lamination cost calculation. In that way, this function can be called for every laminate in the design, skins and stringers. The second

function is used in order to calculate the cost of different configurations. For example, if a joining method requires separate curing of skins and stringers the curing cost is calculated separately and multiplied by the number of the stringers to gain the total curing cost. All the equation mentioned in the theoretical content are used by the CostDef function to calculate the total cost of each configuration. Finally, a total cost in manufacturing hours is provided as an output.

4.3.12. Optimization

The basic logic of the optimization algorithm is given in chapter 3.9. In this part, the functions Optimistic2.m and Optimistic3.m will be explained. These functions call the functions feed.m and jenga.m in order to add or remove plies when needed, in order to achieve the desired margins of safety and minimize the total weight. Since all the margins of safety have been calculated, their values are added in a matrix called MS_sum. Each margin is assigned a number by the position in the matrix in order to evaluate them afterwards.

1. Skin strength
2. Flange strength
3. Web strength
4. Flange Crippling
5. Web Crippling
6. Skin buckling
7. Panel Buckling
8. Column buckling
9. ILSS x
10. ILSS y

The last two modes, 9 and 10, refer to the interlaminar shear strength in the x and y direction of the plate. As calculated in equations 3.64 and 3.65 the ILSS criterion is checked for both Qx and Qy values acting in the plate due to pressure loading.

Then, the minimum of each type for every panel is calculated and added in a matrix containing the minimum per panel. We come up with a matrix with a column containing the panel local minimum and a column giving the failure type from 1 to 9.

The next step is the evaluation of the margins for each panel. The user can define the desired range for the margins. For the current study the range is [0-1]. The evaluation is done by checking the type of the dominant stress condition (tensile, compressive, shear) and follows the following logic.

If the margin of safety is below zero, then:

- If $|\sigma_x| \geq |\sigma_y|$ AND $|\sigma_x| \geq |\sigma_{xy}|$
Add a 0 degree layer to the laminate

- If $|\sigma_y| \geq |\sigma_x|$ AND $|\sigma_y| \geq |\sigma_{xy}|$
Add a 90 degree layer to the laminate
- If $|\sigma_{xy}| \geq |\sigma_x|$ AND $|\sigma_{xy}| \geq |\sigma_y|$
Add a 45 degree layer to the laminate

If the margin of safety is above one, then:

- If $|\sigma_x| \geq |\sigma_y|$ AND $|\sigma_x| \geq |\sigma_{xy}|$
Remove a 0 degree layer from the laminate
- If $|\sigma_y| \geq |\sigma_x|$ AND $|\sigma_y| \geq |\sigma_{xy}|$
Remove a 90 degree layer from the laminate
- If $|\sigma_{xy}| \geq |\sigma_x|$ AND $|\sigma_{xy}| \geq |\sigma_y|$
Remove a 45 degree layer from the laminate

The same logic is followed for all the laminates, skins and stringers but they are applied for specific failure types in order to achieve the optimum solution based on design rules of thumb mentioned in chapter 3.9. the functions that add and remove plies will be explained later in this section.

Another method to achieve an optimum design is the change of the stringers geometry, a so called topography optimization method. In this part, the flanges width and webs height is changed in order to reduce the overall weight of the structure and improve the margins of safety. Nevertheless, this geometric changes cannot take place in an unlimited manner. The geometry needs to be limited according to manufacturing limitations in order to achieve a feasible and realistic design. Thus, the range of the flange width is:

$$10 \leq b_1 < \frac{b}{4} \quad (4.15)$$

These margins are based on experience in composite manufacturing, taking into account that flanges of lower than 10 mm cannot be manufactured easily nor connected to a skin and also a stiffener's flange cannot have an unlimited width compared to the skin's width. Regarding the web's height and core's thickness, and assuming that the stiffeners cannot interfere with the free volume of a fuselage for storage purposes, the height should be no more than 10 percent of fuselage radius and lo less than 20 mm. The last assumption has to do with manufacturability but also takes into account that the stringers are experiencing bending loads as well. Thus the range is:

$$20 \leq b_2 < 0.1R \quad (4.16)$$

The dimensions are changed at each loop by 1 mm for the current software, but that can be changed by the user to improve the software's functionality for the desired application.

The last part of the optimization algorithm that needs to be explained is the laminates updating functions, feed.m and jenga.m. The first one adds plies and the second one removes plies according to the evaluation's results mentioned above. These functions change the stacking and size of the laminates and recalculate their properties to return them for a new loop of evaluation to begin. However, that cannot be done randomly. The logic of these

functions is also based on the design rules of thumb mentioned above. The laminates provided in the first place include some rules of thumb, using 45 degrees fabric plies on the outer side and an almost quasi-isotropic laminate. According to the user's choice of rules, to be applied the functions add or remove plies trying not to violate them. For example, if balanced requirement is on, they cannot add or remove one layer from the stack, but add/remove a layer of opposite degrees in the stack as well. For instance, for every 0 degrees added a 90 degrees needs to be added. If the symmetry requirement is on there are two options given. The software can either add/remove a single ply in the center and use odd number of plies or follow the same logic with the balanced requirement. In that case, it cannot add or remove one layer from the stack, but add/remove a layer of the same degrees in the symmetric side of the stack. Moreover, there are some limitations regarding manufacturing constraints here as well. Thus, to avoid BVID problems, for example, the user can set a minimum amount of plies for the laminate. If that number is reached the software cannot remove more plies from the stack.

Taking into account, that not all the configurations can be feasible for such an automated process some termination variables need to be created. These variables (*term1*, *term2*) have a value that can be setup by the user and they are increased every time a result has not a big divergence from the last result, thus a tolerance is given by the user as well. After all the functions have been explained, the optimization's loop condition needs to be mentioned. The software runs in a 'while' loop until this conditions is satisfied and goes as follows:

WHILE

$$((MS_{min} \leq 0) OR (MS_{max} \geq 1)) AND ((term1 < 5) OR (term2 < 5)) \quad (4.17)$$

Run Optimistic12.m

Run Optimization_file.m

END

The limit value of 5 in equation 4.17 is also set by the user and can be changed accordingly. It has to be mentioned, that in each optimization loop, the load distribution is recalculated and redistributed to the structure, because the changes in layup and geometry lead to load distribution changes as well. This whole optimization process, based on empirical assumptions and logic, achieves feasible designs between desired margins of safety and leads to an almost optimum final result minimizing not only the weight and cost but the solving time in comparison to a high fidelity composite optimization. Keeping the margins of safety at such a range gives a very good approximation for the tool's functionality and purpose, to take strategic decisions in the preliminary phase of the design.

4.3.13. Post-Processing

With the vast amount of data calculated by the software and given as outputs there is a need to visualize the results and create diagnostic tools for the debugging process. In this section the available post-processing functions are explained.

The main post processing output of the software is the plot of different properties of each panel in a 2-D plane. The number of stringers lies on the vertical axis and the number of frames on the horizontal one. Running the function *Post_process* we get back the skin's, flange and web thickness, the stiffeners' EA, flanges' width and webs' height. In the following graph these values are visualized. The values are plotted with different colors starting

from blue and going to yellow for the highest values. In such a manner, the user can watch the results of the analysis and check the critical areas. Another advantage provided by this function, is the evaluation of the validity of the result. Thus, the software developer was able to check if the results provided were realistic based on the load case.

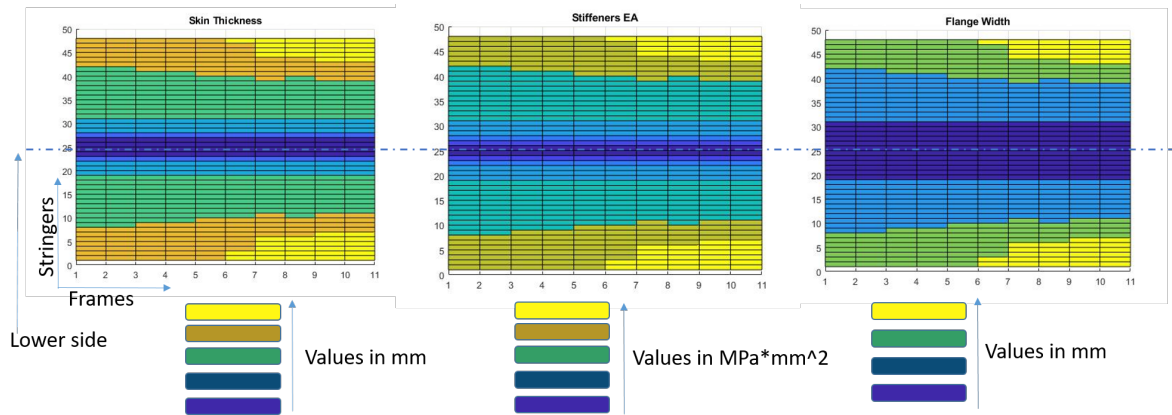


Figure 4.9: Post processing plots for different values

The next diagnostic tool shows the weight progression throughout the iterations to check that convergence is achieved. As the initial laminate is set relatively thin, the weight progression as shown in Figure 4.10 is typical for the software, as the weight increases rapidly at first until it reaches a level where no additional changes can be made. For that reason, a plateau is shown in the graph below from the fifth iteration and until the end. The weight result oscillates between two values until the variables term1 and term2 get their limit values.

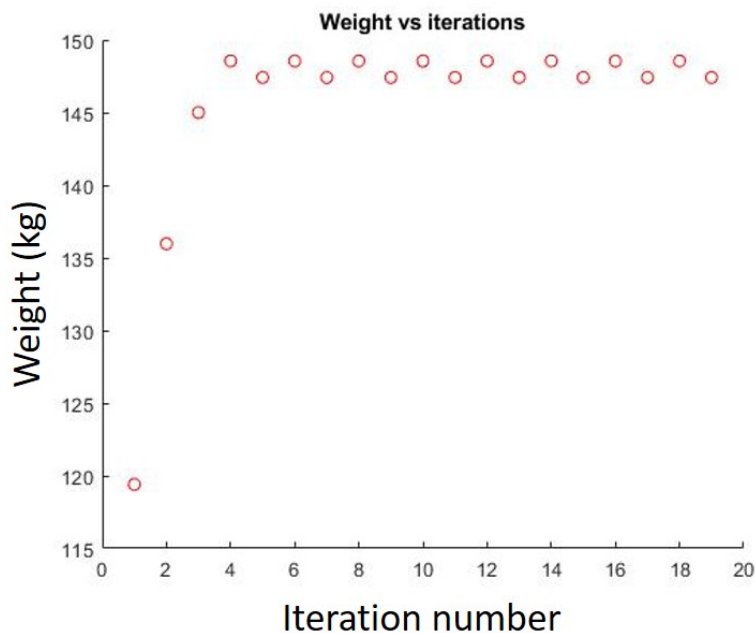


Figure 4.10: Typical weight progression for the software

A last check has to do with the optimization's effectiveness. Thus, the maximum and mini-

imum margins of safety over all the fuselage panels are plotted. In the example given below, it is clear that for some designs the software is not able to keep the margins of safety in the desired limits. That problem occurs due to the minimum manufacturing constraints applied in the design. For example, in the lower side of the fuselage and in a low loaded area of the fuselage for upbending, given the minimum dimensions of the stringers and the number of stringers being high, the margin cannot be reduced more than the value of approximately 3. This result was cross-checked by plotting the margins of safety over the fuselage area. In this plot 4.13, we can watch the 'problematic' area has a local margin of safety of 3, while in all the other parts of the fuselage the margins are kept in the desired range.

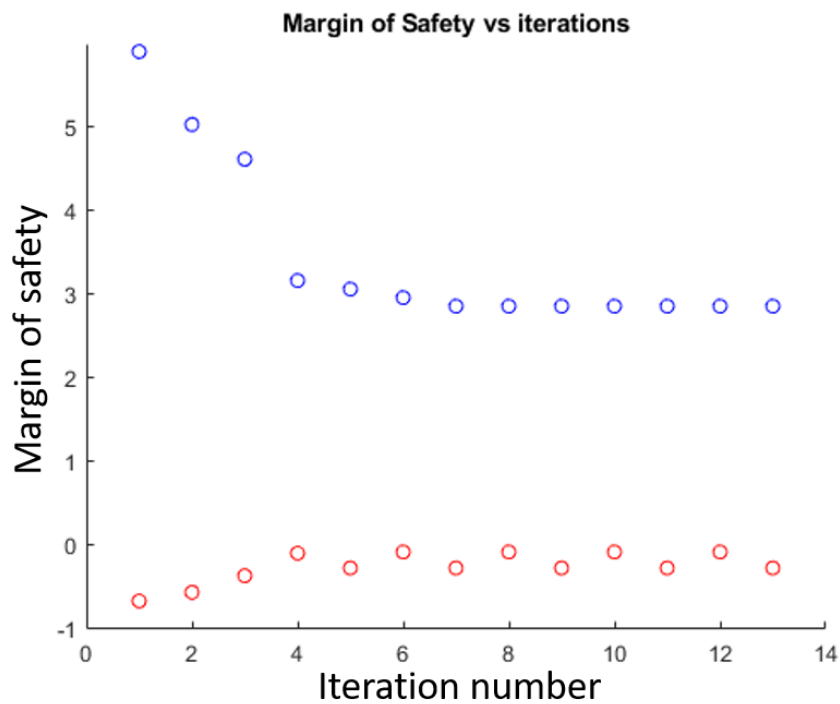


Figure 4.11: Maximum and Minimum margins of safety progression

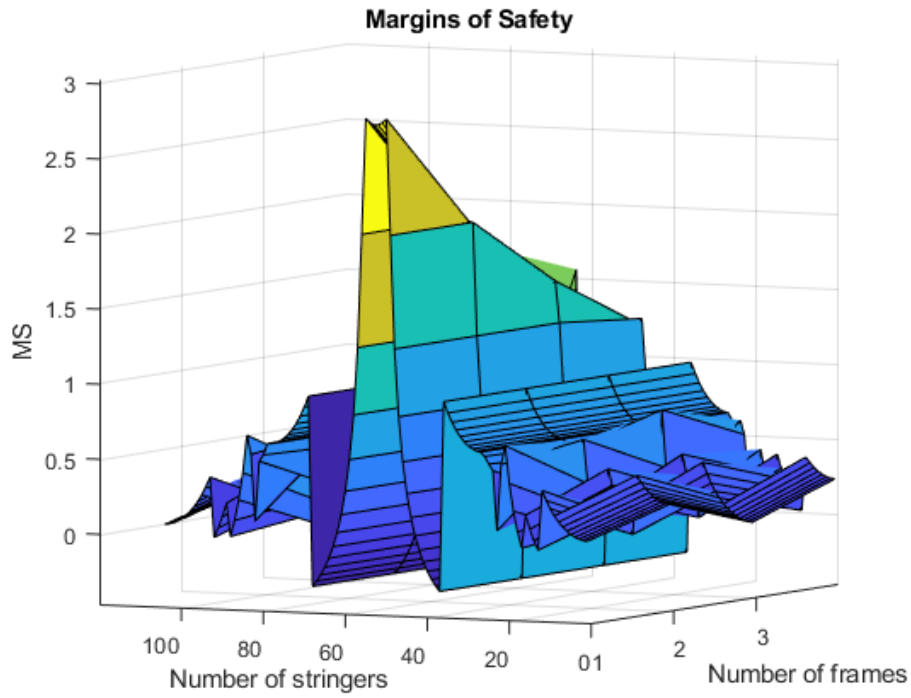


Figure 4.12: Maximum and Minimum margins of safety progression

In the following graph, a design satisfying the constraints and margins of safety range is given. It is clear that the maximum margins are driven to values under one and the minimum ones are kept over zero.

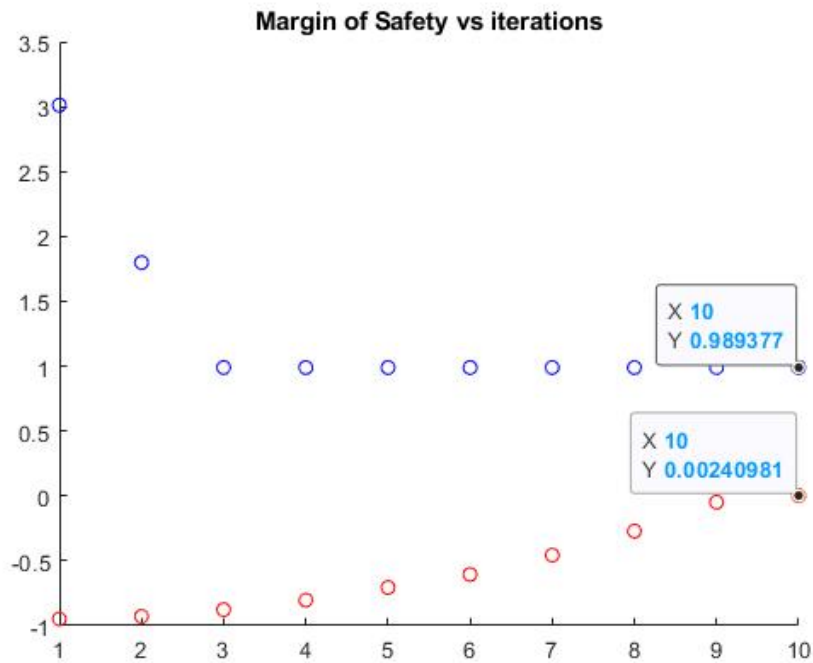


Figure 4.13: Maximum and Minimum margins of safety progression(satisfied)

Trade off studies

In this chapter several trade studies will be done in order to identify the effect of different design choices, using the software developed. The trade study will be based on typical aircraft loads due to the data provided by Fokker with a given diameter of 2 meters and a length of 5 meters. The trade studies will start with the definition of the effect of the number of stringers, following the number of frames for both skin stiffened structure and sandwich structure. An additional comparison will be executed between composite and aluminium designs. The aluminium ones will be checked with the results provided by Fokker and the output data from the developed software.

In order to run the optimization for a batch of files and give the possibility of trade studies the main program `Main_Opt.m` needs to be modified. Thus, a new batch optimization file is created, named `Main_batch_opt.m`. This file runs a number of designs and saves the data in the folder 'saves' that the user can find in the main folder including the source code. The names of the saved files have a specific format. The first component refers to the type of trade off, stringer spacing or frame spacing for example. The second component refers to the radius R and the third to the length L of the design. The next component refers to the fixed variables, either stringer number or frame number. Some extra additions can be found as well. The kind of loadcase is represented by the next component (i.e. `n2`) and the cost lamination method by the next component (i.e. `cost3` refers to automatic ply deposition). The last component refers to the type of configuration, skin-stiffened or sandwich. An example is given below for a variable stringer spacing with a radius of 1 meter, a length of 5 meters, the number of frames is 5, the loadcase is upbending, thus `nloads=2`, the lamination method is AFP and the configuration is a sandwich design:

```
Str_R10_L5_Fr5_nloads_2_cost3_sand
```

5.1. Skin-Stiffened configuration-Composite

In this section, several trade studies for a composite skin-stiffened design take place.

5.1.1. Investigation of the effect of stringer number

First of all, the effect of the stringers number change will be examined for different stringer types. In the following graphs the results in terms of weight and cost for a T,C and J stringer type are presented.

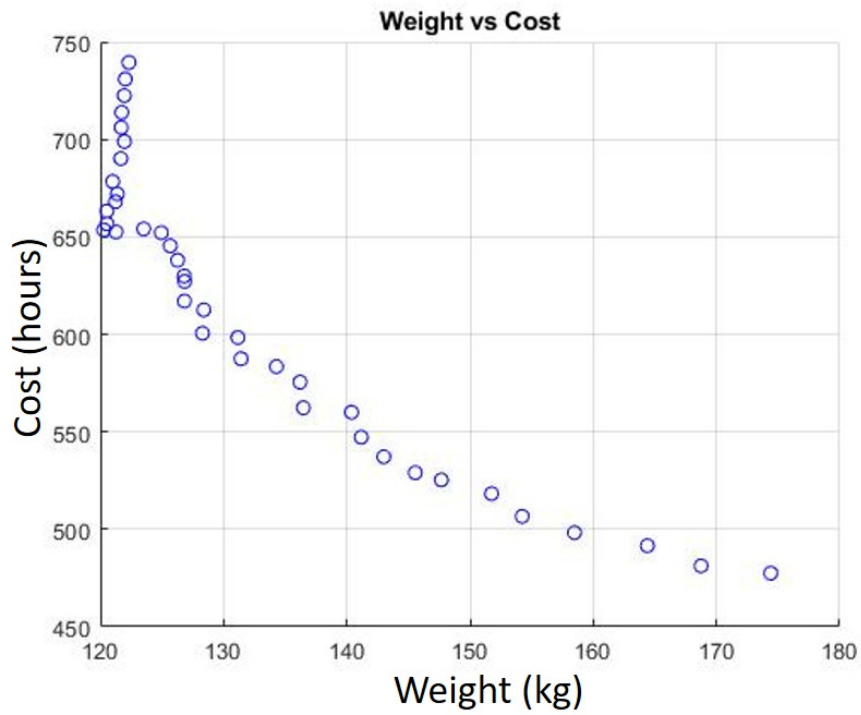


Figure 5.1: Weight versus Cost trade study for stringer spacing (T stringer)

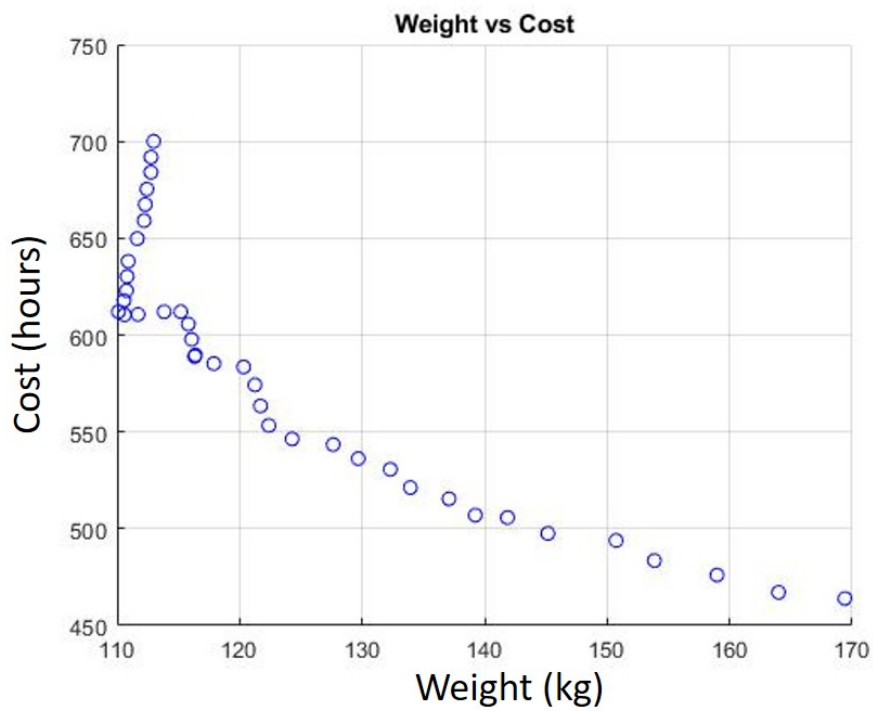


Figure 5.2: Weight versus Cost trade study for stringer spacing (C stringer)

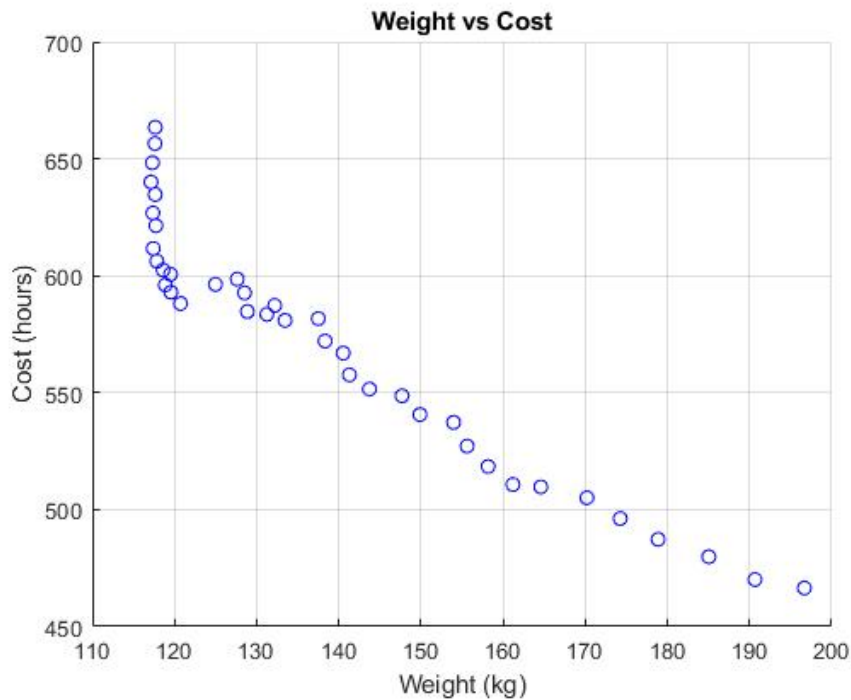


Figure 5.3: Weight versus Cost trade study for stringer spacing (J stringer)

For all the configurations presented we can distinguish some specific characteristics or trends. First of all, the increase of the number of stringers by a number of 2 every time leads to a general decrease in the total weight and an increase in cost. This can be seen until a certain number of stringers. After this number, we see a plateau in the results and then an almost vertical increase in weight and cost. This observation, though strange at first sight, can be explained. Given the manufacturing limitations introduced in the design, the increase of stringers after a certain level cannot reduce the weight because they have reached the minimum dimensions or the skin has reached the minimum thickness constraint. The increase in cost is pretty logical, because the addition of more stringers leads to higher manufacturing times. From the three designs compared, the lower values for both weight and cost are achieved with the second one, the C stringer type. An important observation from the presented graphs, is that an increase in the number of stringers leads to a faster decrease in weight for a low amount of stringers and this trend decreases as the number of stringers increases. For example, based on J stiffeners analysis, in the first iteration, the increase of 2 stringers leads to a decrease of 8 kg, while an increase of two stringers in the 10th iteration leads to a small decrease of around 1 kg in weight. In terms of cost, a linear trend is observed until the point mentioned before. By increasing the amount of stringers the cost keeps increasing, even though the structural weight, thus the amount of plies and flanges geometry, is lowered. This observation can be explained. The addition of two stringers in the fuselage will almost always increase the manufacturing and assembly cost, introducing more parts in the process.

5.2. Skin-Stiffened configuration-Aluminium

5.2.1. Investigation of the effect of stringer number

The same observations found in composite designs were found for aluminium ones as well. Typically, the biggest difference here is in the total weight and cost being at least 40 percent higher and 40 percent lower, respectively, in comparison with the composite designs.

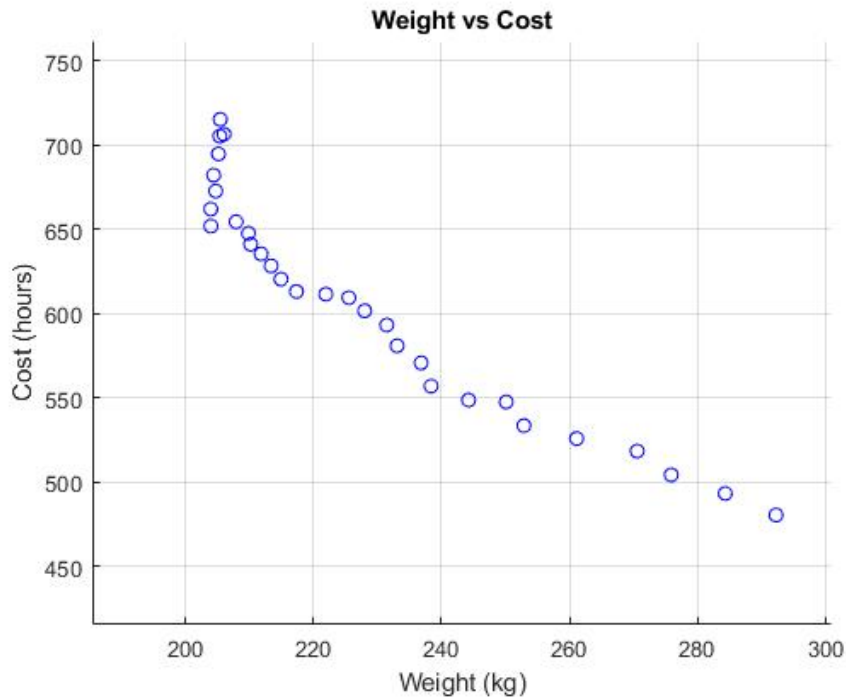


Figure 5.4: Weight versus Cost trade study for stringer spacing (aluminium design)

5.3. Sandwich configuration-Composite

The effect of the change of the number of radial splits in sandwich design is examined here. Even though, the weight is comparable to the skin-stiffened designs the cost is much lower, around 60 percent of the skin-stiffened design. The same trend is observed here, too. It has to be noted that in the case of sandwich, the fuselage is not split in panels according to the stringer number but according to the number of panels chosen by the user referred as radial splits. In the optimization process the same logic as in the skin stiffened design is followed, increasing the number of panels in the radial direction by a number of two. An increase of 2 radial splits leads to a decrease of 1 kg in weight and the increase of 1 hour in cost until a certain level. After that level, The cost continues to increase, but the weight converges to a value of around 103 kg.

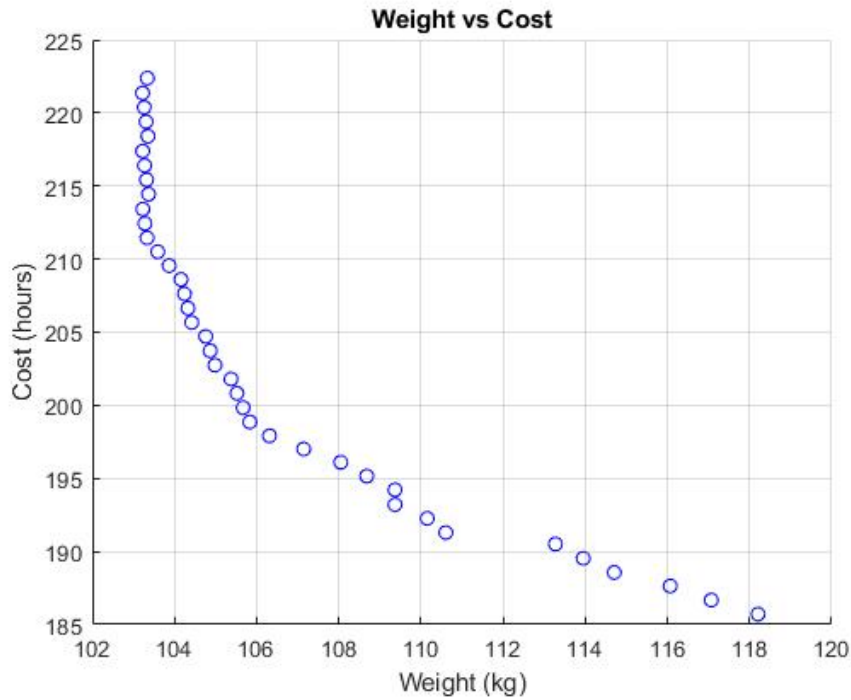


Figure 5.5: Weight versus Cost trade study for splits spacing (sandwich design)

5.4. Comparison of different configurations

In this section, a comparison between the aforementioned configurations takes place. In table 5.1 the resulting values are given for T stringer, C stringer, J stringer, sandwich and aluminium design configurations.

Table 5.1: Comparison of different configurations

| Configuration | T stringer | C stringer | J stringer | Sandwich | Aluminum |
|---------------|------------|------------|------------|----------|----------|
| Weight (kg) | 120 | 110 | 115 | 103 | 202 |
| Cost (hours) | 470 | 460 | 465 | 185 | 288 |

While the different stringer configurations show a small percentage of difference (around 1 percent in weight and 2 percent in cost), the sandwich design and the aluminium skin-stiffened show a larger difference. The sandwich design minimum is lighter in weight in comparison to the skin-stiffened by 2 percent and around 60 percent cheaper to manufacture. On the other hand, the aluminium design is much heavier than the composite designs (both for skin-stiffened and sandwich composite) by 40 percent while the manufacturing cost is approximately lower by 65 percent due to the lower complexity of the metal design.

5.5. Influence of the application of different lamination methods

In the following graph 5.6, the influence of different lamination methods choice is shown. In this trade study two lamination methods were used, hand layup and automatic fiber placement. It is clear that using automation in manufacturing, a decreased cost is achieved.

An average difference of 140 hours occurs between the two curves. The upper curve represents the hand layup method and the lower one, the automatic deposition method. It has to be mentioned, that even though the automated option gives a lower cost in manufacturing hours, it requires a large investment in machinery to use the technology. In some applications, the hand-layup option might lead to lower overall costs and larger flexibility, assuming that the learning curve is almost flat. For large projects, with a vast amount of same parts and assembly methods the automation option will be the most suitable.

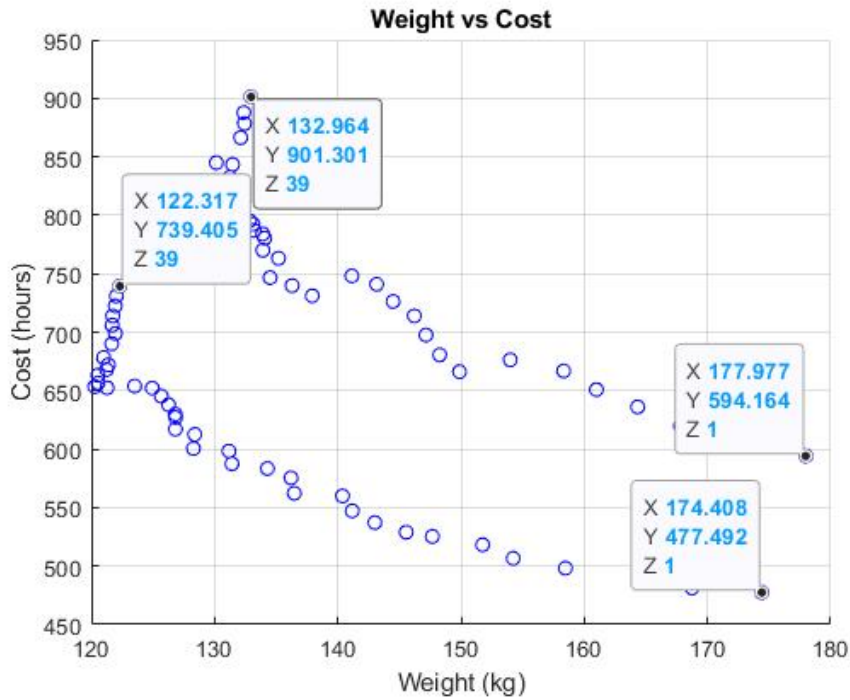


Figure 5.6: Weight versus Cost trade study for stringer spacing under different lamination methods

5.6. Investigation of the effect of frame number

In this section the effect of the frame number on the weight and cost of the fuselage is examined. Setting a standard value for the number of stringers in the middle of the examined range([28-104]) and changing the number of frames starting from a number of five frames the software runs in batch mode to create the desired curves. It has to be mentioned that one frame is added to the design at each iteration. In the following figure 5.7 the results are presented.

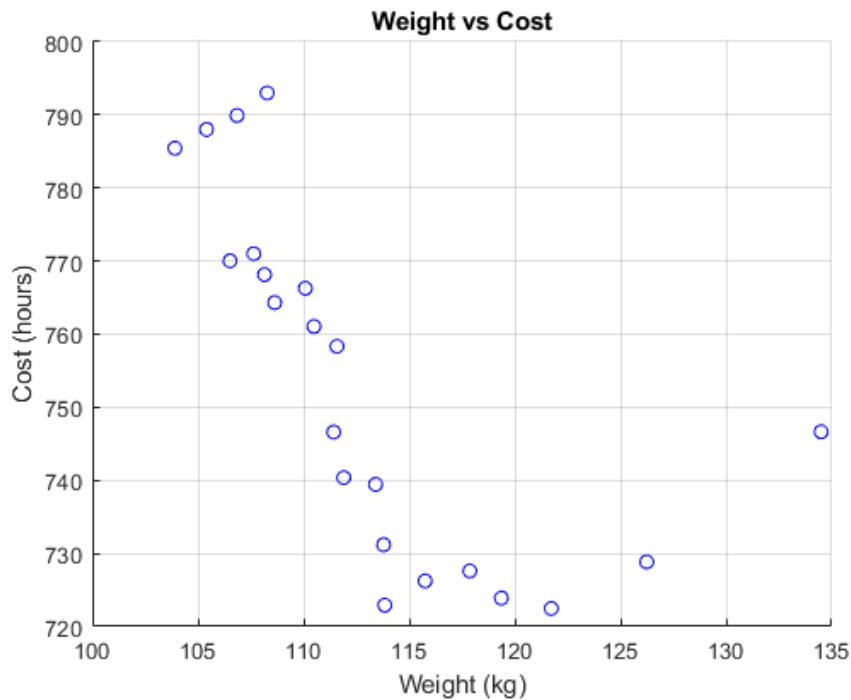


Figure 5.7: Weight versus Cost trade study for frame spacing (T stringer)

A similar trend as the number of stringers examination, is observed here with some differences. In terms of weight, the increase of one frame leads to the decrease in weight until a certain level of frames. After that point an increase in weight is observed. That can be again explained. Increasing the amount of frames leads to an increase in stringers because of the way the software is developed. Thus increasing the stringer number after a certain point only leads to an increase in weight because of the manufacturing constraints applied. In terms of cost, there are areas of different characteristics in the graph. For a small amount of frames the cost shows some oscillations in the range of [720-745] hours. Then a more linear trend is observed, which was more expected. In that area, increasing the frame number leads to an almost steady increase in cost.

5.7. Influence of the application of composite design rules-of-thumb

In this section, the effect of various laminate design rules of thumb in the weight and cost is examined. The options given to the user were four, as mentioned in earlier chapters, symmetrical, balanced, following the 10 percent rule and avoiding the concentration of unidirectional plies of the same orientation over four. The influence of the last two options will not be analysed in the context of this study. The `feed.m` and `jenga.m` functions were modified accordingly to accommodate these additional rules. A comparison between the results of the aforementioned rules is done afterwards and the effect on the final weight and cost is analysed. In the context of this study, the possibilities of this application will be examined for specific scenarios and configurations. Thus, the effect of these rules of thumb will be examined for a T stringer configuration as examined in section 5.1.1. and the comparison will be done according to that. In future steps, the user is capable of producing

trade studies for the desired configurations. It has to be mentioned that the software used a symmetric rule for the already examined case but without examination of odd number of plies. This graph (odd number of plies used) is given below (5.8).

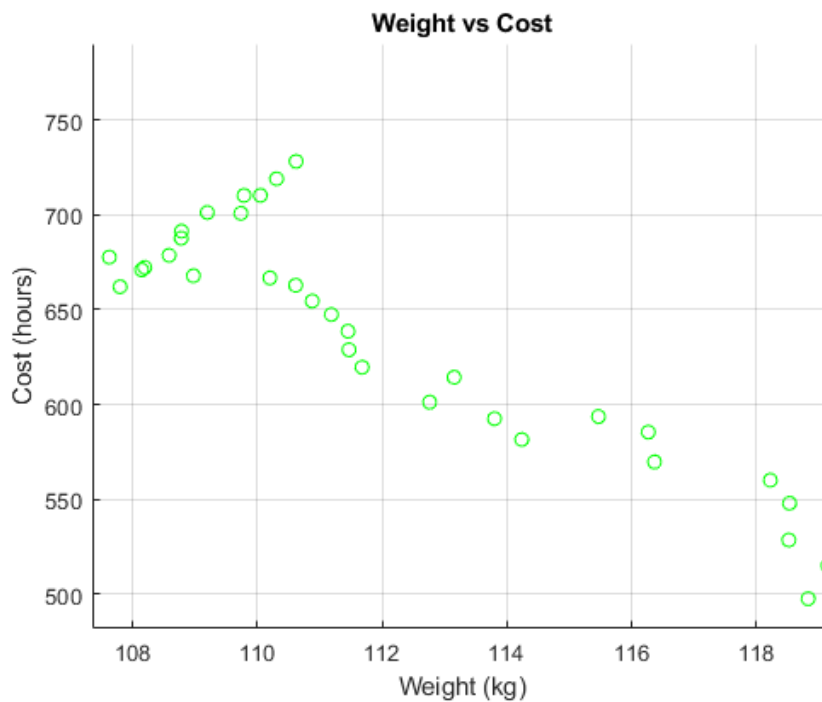


Figure 5.8: Weight versus Cost trade study for stringer spacing under symmetric constraint (T stringer)

The addition of one ply in the middle makes a big difference in the final result. The minimum weight obtained under that design rule is 108 kg while the minimum weight obtained with the standard approach was 120 kg. It is clear, that, adding two layers at a time instead of one leads to an increased weight with almost the same cost. A similar behaviour is observed here in the increase of weight after the addition of a certain amount of stringers. Another design rule to be examined is the balanced laminate constraint. In that case, for every ply of θ degrees a ply of $-\theta$ should be present in the laminate. This constraint is pretty similar to the symmetric constraint used in the standard approach in terms of weight influence because of the number of plies added or removed each time. The result is presented in figure 5.9.

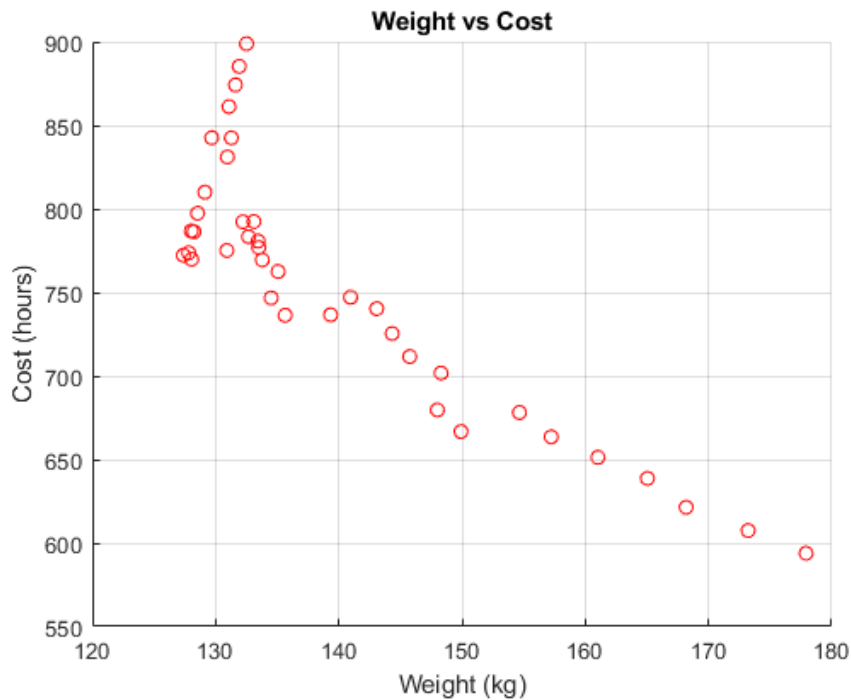


Figure 5.9: Weight versus Cost trade study for stringer spacing under balanced constraint (T stringer)

As mentioned above, a similar trend can be seen for the balanced constraint. The minimum weight is 128 kg and the minimum cost is 590 hours. After reaching the minimum cost an increase in weight is observed while the cost continues to increase to higher levels than that of the symmetric constraint (750 h in the symmetric and 900 h in the balanced constraint). The use of balanced laminates might help in eliminating the stretching/shearing coupling but leads to a higher amount of plies added to the laminate increasing the weight and cost of the design in comparison to the standard one.

The influence of the application of both rules of thumb in one design is shown in figure 5.10. Here a higher increase is observed in weight and cost minimum and maximum values starting from 190 kg in weight and 675 hours in cost (maximum and minimum respectively) and reaching a minimum weight of 132 kg with a cost of 825 hours, while the maximum cost is observed at 958 hours with a weight of 138 kg. The difference from the standard configuration is given in the following table 5.2.

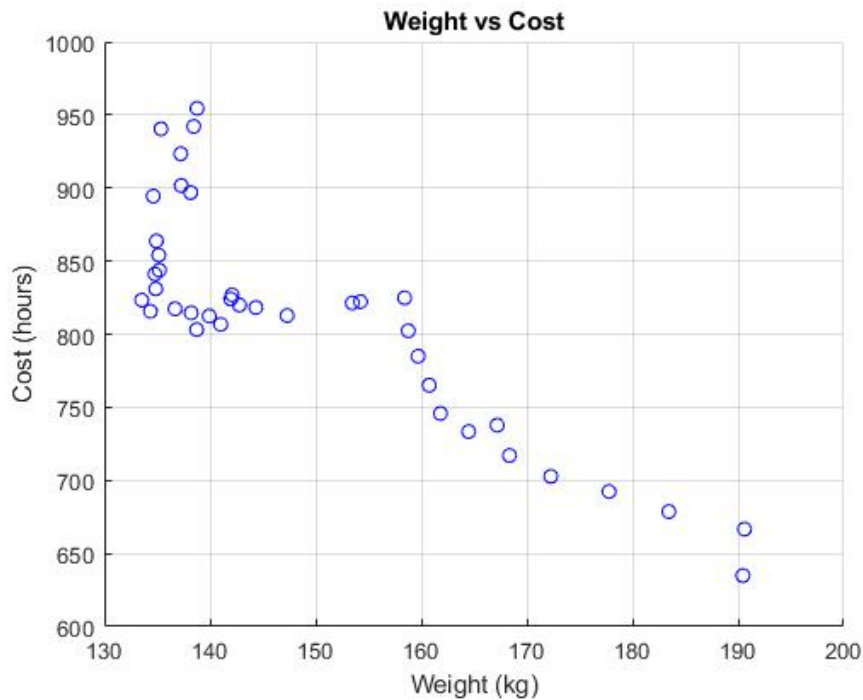


Figure 5.10: Weight versus Cost trade study for stringer spacing under balanced and symmetric constraint (T stringer)

Table 5.2: Comparison of different design rules-of-thumb with the default software's rules

| Configuration | Standard Design (symmetry) | Symmetry (odd numbers) | Balanced | Symmetric and Balanced |
|------------------|----------------------------|------------------------|-----------|------------------------|
| Max Weight (kg) | 175 | 130/-25% | 178/+1.6% | 190/+7.8% |
| Min Weight (kg) | 120 | 106/-11% | 127/+5.5% | 132/+9% |
| Max Cost (hours) | 740 | 735/-0.7% | 900/+17% | 958/+23% |
| Min Cost (hours) | 470 | 490/+4% | 594/+21% | 675/+30% |

From the table 5.2, some important conclusions can be drawn. First of all, it is clear that the way plies are added or removed from the laminate has a great influence on the weight and cost depending on the design rule-of-thumb. The default approach used in the software provides a symmetric composite result. A modification in the software for odd number of plies when symmetry is applied leads to a general decrease in weight and cost. The use of balanced laminates has a similar result with the default, as explained earlier, with slightly higher values in terms of cost and weight but still comparable in weight. The cost results show an average increase of 19 percent, a result showing that the addition of more plies after a certain level only adds to the cost with small weight differences. For the final trade-off, the symmetry and balance rules used, show the biggest increase in weight and cost in comparison to the other rules. Thus, the weight has an average increase of 8 percent and the cost 26.5 percent. The assumption that, the design rules-of-thumb add to the weight and cost of the fuselage can be verified with the aforementioned results. Nevertheless, these rules are used in order to avoid failure under specific/unknown loading scenarios and account for manufacturing defects or curing deformations that might lead to non-predicted

failure, too. A detailed sensitivity analysis of the influence of these rules will be one of the future improvements of this research.

5.8. Case Study: Reference aircraft fuselage station

In this section a comparison between the results of a report from GKN Fokker for a reference aircraft project and the developed software is done. The same dimensions, configurations and materials are used in order to have a good approximation and comparable results.

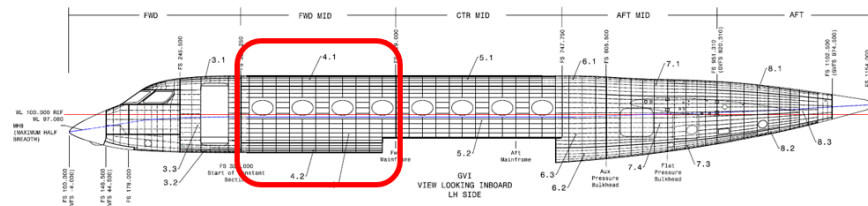


Figure 5.11: Reference aircraft fuselage station (GKN Fokker)

The basic dimensions of the design are given in the report. The fuselage station has a radius of 1.5 meters with a length of 5 meters. The type of stringers used is T and their number in the circumferential direction is 48. The frame number is 12. The study runs an optimization for a combination of loadcases and takes into account the result of all of them in the final result. In the following graph the skin thickness result is given in a 2-D plot for an unraveled fuselage barrel visualization.

Thickness distribution [mm]

| Stringer | Frame → | 1 | 2 | 3 | 4 | 5 | 6 | 7 | 8 | 9 | 10 | 11 |
|----------|---------|-----|-----|-----|-----|-----|-----|-----|-----|-----|-----|-----|
| 1 | | 1.3 | 1.3 | 1.4 | 1.4 | 1.5 | 1.5 | 1.5 | 1.5 | 1.5 | 1.6 | 1.6 |
| 2 | | 1.3 | 1.3 | 1.4 | 1.4 | 1.5 | 1.5 | 1.5 | 1.5 | 1.5 | 1.6 | 1.6 |
| 3 | | 1.3 | 1.3 | 1.4 | 1.4 | 1.4 | 1.5 | 1.5 | 1.5 | 1.5 | 1.5 | 1.6 |
| 4 | | 1.2 | 1.3 | 1.4 | 1.4 | 1.4 | 1.5 | 1.5 | 1.5 | 1.5 | 1.5 | 1.5 |
| 5 | | 1.3 | 1.4 | 1.4 | 1.4 | 1.4 | 1.4 | 1.4 | 1.5 | 1.5 | 1.5 | 1.5 |
| 6 | | 0.9 | 1.0 | 1.0 | 1.0 | 1.0 | 1.0 | 1.0 | 1.0 | 1.0 | 1.1 | 1.1 |
| 7 | | 1.1 | 1.1 | 1.1 | 1.1 | 1.1 | 1.1 | 1.2 | 1.2 | 1.2 | 1.2 | 1.3 |
| 8 | | 1.0 | 1.0 | 1.0 | 1.0 | 1.0 | 1.0 | 1.0 | 1.0 | 1.1 | 1.1 | 1.1 |
| 9 | | 0.9 | 1.0 | 1.0 | 1.0 | 1.0 | 1.1 | 1.0 | 1.1 | 1.1 | 1.1 | 1.2 |
| 10 | | | | | | | | | | | | |
| 11 | | | | | | | | | | | | |
| 12 | | | | | | | | | | | | |
| 13 | | | | | | | | | | | | |
| 14 | | 1.0 | 0.9 | 1.0 | 1.0 | 1.0 | 1.0 | 1.1 | 1.0 | 1.0 | 1.1 | 1.1 |
| 15 | | 1.0 | 1.0 | 1.0 | 1.0 | 1.0 | 1.0 | 1.1 | 1.1 | 1.1 | 1.1 | 1.2 |
| 16 | | 1.0 | 1.1 | 1.1 | 1.1 | 1.2 | 1.2 | 1.2 | 1.2 | 1.3 | 1.3 | 1.4 |
| 17 | | 0.9 | 1.0 | 1.0 | 1.0 | 1.1 | 1.1 | 1.1 | 1.1 | 1.1 | 1.2 | 1.2 |
| 18 | | 1.2 | 1.2 | 1.3 | 1.3 | 1.4 | 1.4 | 1.5 | 1.5 | 1.5 | 1.6 | 1.6 |
| 19 | | 1.2 | 1.3 | 1.3 | 1.4 | 1.4 | 1.5 | 1.5 | 1.6 | 1.6 | 1.6 | 1.6 |
| 20 | | 1.2 | 1.3 | 1.3 | 1.4 | 1.5 | 1.5 | 1.6 | 1.6 | 1.7 | 1.6 | 1.7 |
| 21 | | 1.3 | 1.4 | 1.5 | 1.5 | 1.6 | 1.7 | 1.7 | 1.8 | 1.8 | 1.8 | 1.8 |
| 22 | | 1.0 | 1.1 | 1.1 | 1.2 | 1.2 | 1.3 | 1.3 | 1.4 | 1.4 | 1.5 | 1.5 |
| 23 | | 1.0 | 1.1 | 1.2 | 1.2 | 1.3 | 1.3 | 1.4 | 1.4 | 1.5 | 1.5 | 1.6 |
| 24 | | 1.2 | 1.2 | 1.2 | 1.3 | 1.3 | 1.4 | 1.4 | 1.5 | 1.5 | 1.6 | 1.7 |
| 25 | | 0.9 | 0.9 | 0.9 | 0.9 | 0.9 | 0.9 | 1.0 | 1.0 | 1.0 | 1.1 | 1.3 |
| 26 | | 1.1 | 1.2 | 1.2 | 1.2 | 1.3 | 1.3 | 1.4 | 1.4 | 1.5 | 1.5 | 1.6 |
| 27 | | 1.4 | 1.5 | 1.5 | 1.6 | 1.7 | 1.7 | 1.8 | 1.9 | 1.9 | 2.0 | 2.0 |
| 28 | | 1.2 | 1.4 | 1.4 | 1.5 | 1.6 | 1.6 | 1.7 | 1.7 | 1.8 | 1.8 | 1.8 |
| 29 | | 1.2 | 1.3 | 1.4 | 1.4 | 1.5 | 1.6 | 1.6 | 1.7 | 1.7 | 1.7 | 1.7 |
| 30 | | 1.2 | 1.3 | 1.3 | 1.4 | 1.5 | 1.5 | 1.6 | 1.6 | 1.6 | 1.6 | 1.7 |
| 31 | | 1.0 | 1.0 | 1.1 | 1.1 | 1.1 | 1.2 | 1.2 | 1.2 | 1.3 | 1.3 | 1.3 |
| 32 | | 1.1 | 1.1 | 1.2 | 1.2 | 1.2 | 1.3 | 1.3 | 1.3 | 1.4 | 1.4 | 1.5 |
| 33 | | 1.0 | 1.0 | 1.0 | 1.0 | 1.1 | 1.1 | 1.1 | 1.1 | 1.1 | 1.2 | 1.3 |
| 34 | | 0.9 | 1.0 | 1.0 | 1.0 | 1.0 | 1.1 | 1.1 | 1.1 | 1.1 | 1.2 | 1.2 |
| 35 | | 1.0 | 1.0 | 1.0 | 1.0 | 1.0 | 1.0 | 1.1 | 1.1 | 1.1 | 1.1 | 1.2 |
| 36 | | 1.1 | 1.0 | 1.0 | 1.0 | 1.1 | 1.1 | 1.3 | 1.1 | 1.2 | 1.2 | 1.2 |
| 37 | | | | | | | | | | | | |
| 38 | | | | | | | | | | | | |
| 39 | | | | | | | | | | | | |
| 40 | | | | | | | | | | | | |
| 41 | | 0.9 | 1.0 | 1.0 | 1.0 | 1.0 | 1.0 | 1.0 | 1.0 | 1.1 | 1.0 | 1.1 |
| 42 | | 0.9 | 0.9 | 0.9 | 0.9 | 0.9 | 0.9 | 0.9 | 0.9 | 0.9 | 1.0 | 1.0 |
| 43 | | 1.2 | 1.2 | 1.2 | 1.2 | 1.2 | 1.2 | 1.3 | 1.3 | 1.3 | 1.4 | 1.4 |
| 44 | | 1.2 | 1.3 | 1.3 | 1.3 | 1.3 | 1.4 | 1.4 | 1.4 | 1.4 | 1.4 | 1.5 |
| 45 | | 1.2 | 1.3 | 1.3 | 1.4 | 1.4 | 1.4 | 1.4 | 1.5 | 1.5 | 1.5 | 1.5 |
| 46 | | 1.2 | 1.3 | 1.4 | 1.4 | 1.4 | 1.4 | 1.5 | 1.5 | 1.5 | 1.5 | 1.5 |
| 47 | | 1.3 | 1.3 | 1.4 | 1.4 | 1.4 | 1.5 | 1.5 | 1.5 | 1.5 | 1.5 | 1.6 |
| 48 | | 1.3 | 1.4 | 1.4 | 1.5 | 1.6 | 1.6 | 1.6 | 1.6 | 1.6 | 1.6 | 1.7 |

Figure 5.12: Reference aircraft fuselage station thickness distribution provided by GKN Fokker

The software created for the current study was used to create the following graph for skin thickness. It has to be mentioned that only one loadcase was used for this result.

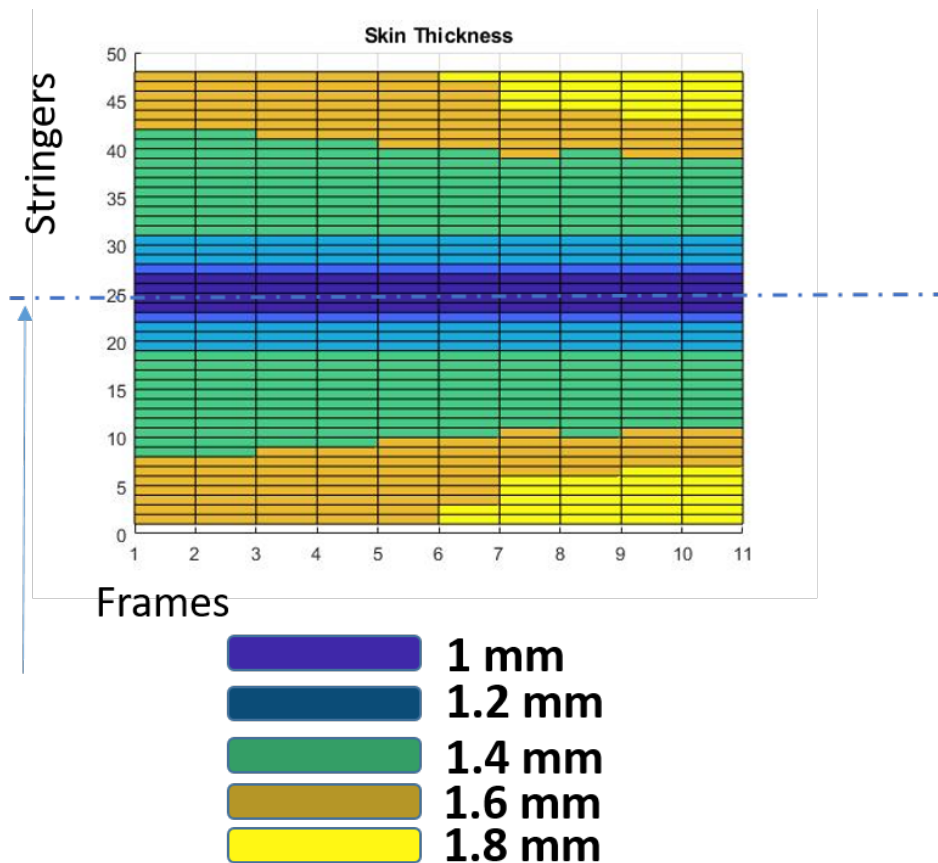


Figure 5.13: Reference aircraft fuselage station thickness distribution using the software

The total weight given in the report for this design was 160 kg for an aluminium design. The result for our software was 218 kg for an aluminium design and 140 kg for a composite one. The results of the software include the part of the window belt, though, something that is excluded from the Fokker study. That is one of the reasons of this divergence in the weight result. It is clear, though, that a composite design of the same characteristics achieves a much lower weight result. Finally, we do not have manufacturing cost in hours data, to compare with the results of our software.

5.9. Run time analysis

One of the goals of the software is to run whole fuselages analyses in a very short time. This means that instead of using high fidelity tools with a large execution time (in the order of magnitude of weeks) the software developed tries to achieve approximately the same result within minutes. In this section the run time will be examined.

It becomes clear that because of the software's nature the run time is increasing by increasing the number of panels. This happens, because the structural analysis runs per panel. A trend observed in the results is that the run time is really low for a low amount of stringers or frames and increases with the increase of them. This has to do with the optimization algorithm as well. Having a large amount of panels leads to more iterations, and consequently, larger iteration times. For a typical analysis of a specific design the software has a running time in the magnitude of minutes (or seconds for smaller configurations) while in

the batch mode it can take up to a couple of hours. A typical progression of the run time through the iterative process is shown in figure 5.14 below.

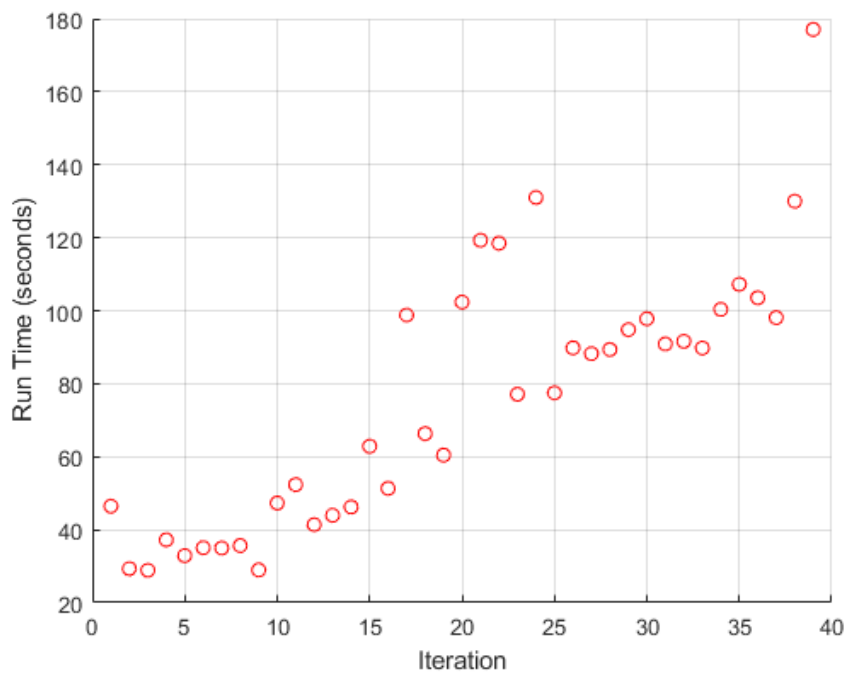


Figure 5.14: Run time versus iteration for the batch optimization process

Conclusions and Future Research Recommendations

6.1. Conclusions

In order to assess to what extent the main research question:

Can a low fidelity, knowledge based preliminary sizing tool, provide realistic weight and cost optimization results, for composite fuselage assemblies, enabling the speed up of the decision making process?

has been answered, a short summary is given on the conclusions.

An approach was presented, in order to determine the weight and cost of various configurations of fuselage structures. The software described, makes use of the theoretical content presented in chapter 3, and an empirical optimization process to achieve the goal of the research. Both weight and cost aspects of the design are examined and estimated through the software to achieve feasible and low weight and cost designs. The software, utilizing the analytical equations for weight and cost, represents a low fidelity tool that can provide sufficient outputs for fuselage structures in a short amount of time. More specifically, in comparison to the high fidelity finite element models, that need weeks to provide a result for a fuselage analysis, the software presented in this thesis tackles this problem in minutes or a few hours for larger structures. Having compared the results with data provided from GKN Fokker, it is clear that the software, though at an early stage, gives comparable results. Therefore, the part of the research question asking for realistic weight and cost optimization results is achieved. Moreover, it gives the freedom to the user, to change the desired variables according to the working project and introduce weight and cost errors that influence the design. This feature, given the application, gives the possibility to 'train' the software using data from past applications to achieve higher accuracy. Taking into account the aforementioned, the study shows that such a low fidelity tool is able to achieve the goal of the research in the preliminary phase, speeding up the decision making process.

The second important goal of the study is to provide trade-offs that will help to set new design guidelines. To achieve that, a number of trade studies was executed, regarding the effect of the number of stringers, frames, configurations (skin-stiffened or sandwich), cost parameters, metal or composite materials. The conclusions resulting from this analysis are given below.

First of all, the study of the change of the number of stringers for a given geometry was examined. For the chosen range, the analysis shows that the increase of number of stringers leads to a general decrease in weight and cost, both for composite, with different stringer

types, and aluminum. This is observed until a certain level, though. After that point, both weight and cost show an increasing trend. This can be explained, taking into account the manufacturing constraints applied. When all the values of the variables reach the lower limits, no excess material can be removed. This leads to an increase in weight, because adding 2 more stringers to the fuselage will not lower the plies and geometrical characteristics of the panels anymore. Changing these ranges, according to the application, can show a different behaviour in the trending lines. As a design guideline, an increase in the number of stringers improves the weight of the structure while increasing the cost. The user must take into consideration, if a penalty in manufacturing hours will be a realistic penalty in working hours, given the lower weight of the structure. Thus, the fuel cost reduction, might balance the scale in the long run.

The same study, but for a sandwich design was examined as well. The composite sandwich configuration shows a similar trend. At first, the increase in stringer number leads to faster decrease in weight and increase in cost. Thus, the starting designs have more potential for weight saving by the addition of more stringers. In terms of weight, the sandwich design gives comparable, with the skin-stiffened design, values. However, in this case, the introduction of more panels in the design does not show an increase in weight but a convergence in the same value. Again, the minimum limits are reached, but there is no addition of parts in the design, only greater manufacturing costs due to the larger amount of panels and joining required. The cost, shows a steady increase as expected.

A comparison of the different configurations, provides interesting results. For the given data and geometry, the composite designs tend to provide lighter solutions, with a lower value observed for the sandwich design and the C stringer in the other configuration as a second lower. The aluminium design, gives the heavier solutions, thus validating the trend for composite solutions.

In the case, of the effect of changing the number of frames, the trend resulting from the analysis follows a similar route. It has to be mentioned, that a change in the frames' number, leads to an increase in stringers. That happens because of the software's geometry definition. Increasing the frame number, leads to a general decrease in structural weight. Again, faster in the start and slower in larger number of frames. The phenomenon of increasing the weight when increasing the frames, after a certain point, is observed here, too. The explanation is based on the same criteria explained above. The cost values are comparable to the ones obtained in the stringer number analysis and so is the weight.

A very important aspect of this software, is the possibility to examine different manufacturing cost parameters. Thus, a trade study, about the influence of the lamination methods provides an example of the software's possibilities and helps draw conclusions. The lamination method, giving the lower cost is the automatic deposition method with an average difference of 140 hours. As mentioned earlier, though, this result is logical, but might not give the most efficient results under certain circumstances. Automatic deposition, needs a larger investment and also more time to flatten the learning curve. In a hand layup factory, and for smaller in number of parts applications, this difference might not be realistic. On the other hand, in mass production with a significantly large amount of parts the automatic deposition would be more beneficial.

The last factor examined, in terms of its influence in weight and cost, was the application of various design rules-of-thumb. In the context of this study, the application of symmetric, balanced and both of them was examined. As mentioned earlier, the default function

for adding and removing plies utilizes the symmetrical constraint for even number of plies. The use of odd number of plies, gives a lower weight and almost similar cost. This means, that by having the same symmetry constraint we can achieve lower results in weight. When applying, the balanced constraint, an increase in weight and cost is observed, smaller percentage for weight values than cost. The same behaviour is observed, when applying both symmetric and balanced constraints, giving higher values in weight and cost. Even though, these rules add to the overall weight and cost, they are used to account for non-predictable scenarios and empirical observations and their usage should be seriously considered by the user for the application required.

6.2. Future Research Recommendations

This thesis, was an attempt to provide a fast and realistic tool for fuselage design in the preliminary phase. The software developed and the trade-offs resulting from it, added a small stone to the body of knowledge in this field, but as always, the word research encapsulates the word improvement. These improvements and recommendations will be discussed in the current section.

First of all, the current software, examines parts of the fuselage (stations) separately. A future step, would be to incorporate whole fuselage structures in the design. Furthermore, non-cylindrical fuselages can be examined by the software with small modifications. This would enable the examination of different types of aircrafts, such as blended wing bodies or delta wings or even more conventional ones with tapered fuselage geometries.

Another improvement, would be the application of an optimization algorithm or the update of the current empirical one. This step, would increase the processing time, but would result in more accurate weight and cost estimations. It has to be mentioned that, a trade-off would be suitable in choosing this update because of the low-fidelity nature of the algorithm. The approach provided by this thesis is followed in order to provided better estimation in the preliminary phase to input in higher fidelity models for validation purposes afterwards. Thus, its goal is not to replace them.

A whole new era of trade-offs can result from this application. For the current study, the possibilities of the software were discovered and a specific amount of trade-offs were carried out, in order to study the effect of different factors. The analysis can be, then, applied to a large amount of configurations and different parameters in order to produce trends about the influence of different fuselage sizes, failure criteria, stringer types and of course, different cost parameters. Another improvement, will be the examination of additional design rules-of-thumb, such as the 10 percent rule, and their influence in weight and cost. This could be the topic of a follow-up thesis.

In terms of structural analysis, the current study follows a conservative approach. The introduction of post-buckling or buckling at lower-than-ultimate-load would give the chance to produce lighter designs, but with the disadvantage of increasing the software's complexity.

The last improvement suggested, is the creation of a more user-friendly interface. In that way, the user input and post-processing would become easier to be applied and help in understanding the outputs of the software.

Bibliography

- [1] Kassapoglou, C. (2010) 'Design and analysis of composite structures' West Sussex: John Wiley and sons Ltd.
- [2] Moors, G. et al. (2019) 'Weight trades in the design of a composite wing box: effect of various design choices', CEAS Aeronautical Journal. Springer Vienna, 10(2), pp. 403–417. doi: 10.1007/s13272-018-0321-4.
- [3] Lusk, J. (2006) 'Wing and Fuselage Structural Optimization Considering Alternative Material Systems'.
- [4] Zabihollah, A. and Ganesan, R. (2010) 'Buckling analysis of tapered composite beams using a higher order finite element formulation', Journal of Reinforced Plastics and Composites, 29(17), pp. 2663–2683. doi: 10.1177/0731684409352124.
- [5] Van Gent, I. and Kassapoglou, C. (2014) 'Cost-weight trades for modular composite structures', Structural and Multidisciplinary Optimization, 49(6), pp. 931–952. doi: 10.1007/s00158-013-1019-1.
- [6] Hodges, D. H. (1990) 'Modeling of Composite Beams and Plates for Static and Dynamic Analysis'.
- [7] Apostolopoulos, P. and Kassapoglou, C. (2008) 'Cost-weight trades for stiffened composite panels under compression', Civil-Comp Proceedings, 88, pp. 1–16. doi: 10.4203/ccp.88.14.
- [8] Kassapoglou, C. (1999) 'Minimum cost and weight design of fuselage frames. Part B: Cost considerations, optimization, and results', Composites Part A: Applied Science and Manufacturing, 30(7), pp. 895–904. doi: 10.1016/S1359-835X(98)00191-2.
- [9] Bruhn, Elmer Franklin. (1965) Analysis and design of flight vehicle structures. Tri-state offset company.
- [10] Sen, I. (2010). Aircraft Fuselage Design Study. Master of Science Thesis, Delft University of Technology.
- [11] Kassapoglou, C. and Dobyns, A. L. (2001) 'Simultaneous cost and weight minimization of postbuckled composite panels under combined compression and shear', Structural and Multidisciplinary Optimization, 21(5), pp. 372–382. doi: 10.1007/s001580100116.
- [12] Kassapoglou, C. and Dobyns, A. L. (2001) 'Simultaneous cost and weight minimization of postbuckled composite panels under combined compression and shear', Structural and Multidisciplinary Optimization, 21(5), pp. 372–382. doi: 10.1007/s001580100116.
- [13] Schwinn, D. B. et al. (2018) 'Structural sizing of a rotorcraft fuselage using an integrated design approach', 31st Congress of the International Council of the Aeronautical Sciences, ICAS 2018. doi: 10.4050/jahs.65.042008.
- [14] Thianwiboon, M. (2019) 'Optimization of a hybrid carbon/glass composites afterbody of the amphibious plane with finite element analysis', Engineering Journal, 23(5).
- [15] Izzi, M. I. et al. (2021) 'Multi-scale optimisation of thin-walled structures by considering a global/local modelling approach', Proceedings of the Institution of Mechanical Engineers, Part G: Journal of Aerospace Engineering, 235(2), pp. 171–188.
- [16] Choi, J. W., Kelly, D. and Raju, J. (2007) 'A knowledge-based engineering tool to estimate cost and weight of composite aerospace structures at the conceptual stage of the design process', Aircraft Engineering and Aerospace Technology, 79(5), pp. 459–468. doi: 10.1108/00022660710780588.

- [17] Klinkert, R. and Klinkert, R. (2012) 'Master of Science Thesis Master of Science Thesis', (August), pp. 1–155.
- [18] Base, W. A. I. R. F. (1976) 'Composite cost estimating manual aircraft division', Northrop Corporation, I.
- [19] Northrop Corporation, (1976) 'Advanced Composite and Estimating Manual'
- [20] L.B. Ilcewicz, P.J. Smith, C.T. Hanson, T.H. Walker, S.L. Metshan, G.E. Mabson, K.S. Willden, B.W. Flynn, D.B. Scholz, D.R. Polland, H.G. Frendrikson, J.T. Olson, B.F. Backman, (1997), 'Advanced Technology Composite Fuselage- Program Overview'
- [21] Collier, C. et al. (2007) 'An approach to preliminary design and analysis', Collection of Technical Papers - AIAA/ASME/ASCE/AHS/ASC Structures, Structural Dynamics and Materials Conference, 6(April), pp. 5642–5655. doi: 10.2514/6.2007-2176.
- [22] Bednarczyk, B. A. et al. (2011) 'Efficient design and analysis of lightweight Reinforced Core Sandwich and PRSEUS structures', Collection of Technical Papers, Structures, Structural Dynamics and Materials Conference, pp. 1–42.
- [23] Collier, C. S. and Jones, S. P. (2020) 'Unified analysis of aerospace structures through implementation of rapid tools into a stress framework', AIAA Scitech 2020 Forum, 1 PartF, pp. 1–26. doi: 10.2514/6.2020-1478.
- [24] Library, E. (2020) 'Analysis of Curved Plates'.
- [25] Führer, T. et al. (2016) 'Automated model generation and sizing of aircraft structures', Aircraft Engineering and Aerospace Technology, 88(2), pp. 268–276. doi: 10.1108/AEAT-02-2015-0054.
- [26] Martins, J. P. et al. (2018) 'Behaviour of thin-walled curved steel plates under generalised in-plane stresses: A review', Journal of Constructional Steel Research. Elsevier Ltd, 140, pp. 191–207. doi: 10.1016/j.jcsr.2017.10.018.
- [27] Grihon, S. et al. (2010) 'Fuselage Structure Optimization', Advances in Collaborative Civil Aeronautical Multidisciplinary Design Optimization, pp. 193–247.
- [28] Abramovich, H. and Weller, T. (2009) 'Buckling and postbuckling behavior of laminated composite stringer stiffened curved panels under axial compression: Experiments and design guidelines', Journal of Mechanics of Materials and Structures, 4(7–8), pp. 1187–1207. doi: 10.2140/jomms.2009.4.1187.
- [29] Ueda, Y., Rashed, S. M. H. and Paik, J. K. (1995) 'Buckling and ultimate strength interaction in plates and stiffened panels under combined inplane biaxial and shearing forces', Marine Structures, 8(1), pp. 1–36. doi: 10.1016/0951-8339(95)90663-E
- [30] Jacques, T., Maquoi, R. and Fonder, G. (1983) 'Buckling of unstiffened compression curved plates', Journal of Constructional Steel Research, 3(1), pp. 28–34. doi: 10.1016/0143-974X(83)90014-7.
- [31] Ainsworth, J. (2015) 'Composite Design and Analysis'.
- [32] Kaufmann, M., Zenkert, D. and Mattei, C. (2008) 'Cost optimization of composite aircraft structures including variable laminate qualities', Composites Science and Technology, 68(13), pp. 2748–2754. doi: 10.1016/j.compscitech.2008.05.024.
- [33] Kaufmann, M., Zenkert, D. and Åkermo, M. (2010) 'Cost/weight optimization of composite prepreg structures for best draping strategy', Composites Part A: Applied Science and Manufacturing. Elsevier Ltd, 41(4), pp. 464–472. doi: 10.1016/j.compositesa.2009.11.012.
- [34] Hernandez, S., Baldomir, A. and Mendz, J. (2008) Size optimization of aircraft structures, ICAS Secretariat - 26th Congress of International Council of the Aeronautical Sciences 2008, ICAS 2008.
- [35] Dähne, S. and Hühne, C. (2018) 'Gradient Based Structural Optimization of a Stringer

Stiffened Composite Wing Box with Variable Stringer Orientation', *Advances in Structural and Multidisciplinary Optimization*, (June), pp. 814–826.

[36] Hiken, A. (2017) *The Evolution of the Composite Fuselage - A Manufacturing Perspective*, *SAE International Journal of Aerospace*, 10(2), pp. 1–30. doi: 10.4271/2017-01-2154.

[37] Díaz, J., Cid Montoya, M. and Hernández, S. (2016) 'Efficient methodologies for reliability-based design optimization of composite panels', *Advances in Engineering Software*, 93, pp. 9–21. doi: 10.1016/j.advengsoft.2015.12.001.

[38] Siggel, M. et al. (2018) 'TiGL - An open source computational geometry library for parametric aircraft design', arXiv.

[39] Denkena, B. et al. (2017) 'Estimation of Production Cost in an Early Design Stage of CFRP Lightweight Structures', *Procedia CIRP. The Author(s)*, 62, pp. 45–50

[40] Mukhopadhyay, M. and Mukherjee, A. (1990) 'Finite element buckling analysis of stiffened plates', *Computers and Structures*, 34(6), pp. 795–803.

[41] Hueber, C., Horejsi, K. and Schledjewski, R. (2016) 'Review of cost estimation: methods and models for aerospace composite manufacturing', *Advanced Manufacturing: Polymer and Composites Science. Taylor and Francis*, 2(1), pp. 1–13.

[42] Creemers, R. J. C. (2010) 'Interlaminar shear strength criteria for composites - An assessment by means of statistical analysis', *Nlr-Tp-2009-262*, (June 2009), pp. 8–9.

[43] Kowalski, M., Goraj, Z. J. and Goliszek, B. (2021) 'The use of FEA and semi-empirical equations for weight estimation of a passenger aircraft', *Aircraft Engineering and Aerospace Technology*, ahead-of-print(ahead-of-print). doi: 10.1108/aeat-12-2020-0287

[44] Kong, C., Kim, J. and Park, H. (2008) 'Preliminary design for the fuselage of a small scale WIG craft using composite materials', *Science and Engineering of Composite Materials*, 15(3), pp. 189–205. doi: 10.1515/secm.2008.15.3.189.

[45] Swanson, G. D. et al. (1990) '5-/3s/', pp. 795–814.

[46] Swanson, G. D. (no date) 'STRUCTURES developed', pp. 601–624.

[47] T. H. G. Megson, (2007), *Aircraft Structures for engineering students Fourth Edition*

[48] Kassapoglou, C. (1999) 'Minimum cost and weight design of fuselage frames. Part A: Design constraints and manufacturing process characteristics', *Composites Part A: Applied Science and Manufacturing*, 30(7), pp. 887–894. doi: 10.1016/S1359-835X(98)00190-0.

[49] Kassapoglou, C. (1999) 'Minimum cost and weight design of fuselage frames. Part B: Cost considerations, optimization, and results', *Composites Part A: Applied Science and Manufacturing*, 30(7), pp. 895–904. doi: 10.1016/S1359-835X(98)00191-2. [50] Lee, M. A. et al. (2012) 'Considerations', pp. 1–16.

[51] Hrinda, G. A. (2008) 'Structural optimization of conceptual aerospace vehicles', *WIT Transactions on the Built Environment*, 97, pp. 411–419 doi: 10.2495/HPSM080421.

[52] Megahed, M., Abo-bakr, R. M. and Mohamed, S. A. (2020) 'Optimization of hybrid natural laminated composite beams for a minimum weight and cost design', *Composite Structures. Elsevier*, 239(January), p. 111984. doi: 10.1016/j.compstruct.2020.111984.

[53] Krakkers, L. A. (2009) 'Parametric Fuselage Design', p. 326.

[54] Kothapalli, A. K. R., Mohanty, A. and Adika, S. R. K. (2012) 'Finite Element Modeling And Analysis Of Fuselage Stiffened Panel Subjected To Cabin Pressurization', *Researchgate.Net*, (January), pp. 678–681.

[55] Noever, A., Collier, C. and Harik, R. (2019) 'Integrated design and manufacturing analysis for automated fiber placement structures', *International SAMPE Technical Conference*, 2019-May. doi: 10.33599/nasampe/s.19.1500.

- [56] Ainsworth, J. et al. (2010) 'Airframe wingbox preliminary design and weight prediction', 69th International Conference on Mass Properties 2010, pp. 155–195.
- [57] D.R Polland, K.H. Griess, J.L. Hafenrichter, C.T. Hanson, L.B. Ilcewicz, S.L. Metschan, P.B. Scholz, P.J. Smith, (1997), 'Global Cost and Weight Evolution of Fuselage Side Panel Design Concepts'.
- [58] Sascha, D. and Werthen, E. (no date) 'Stringer-Concept Evaluations with Multidisciplinary Gradient Based Optimization of Composite Wing Structures'.
- [59] Liu, D. et al. (2018) 'Topology optimization of a novel fuselage structure in the conceptual design phase', *Aircraft Engineering and Aerospace Technology*, 90(9), pp. 1385–1393. doi: 10.1108/AEAT-04-2017-0100.
- [60] Autry, B. A. (2020) 'Verification and refinement of an aircraft structural design and optimization tool, atlass', *AIAA Scitech 2020 Forum*, 1 PartF(January), pp. 1–13.

